Dissertation

submitted to the
Combined Faculties for the Natural Sciences and for Mathematics
of the Ruperto-Carola University of Heidelberg, Germany
for the degree of
Doctor of Natural Sciences

presented by

Aniello Federico, Master of Pharmaceutical, Veterinary and Medical Biotechnologies

born in: Naples, Italy

Oral-examination: 14.05.2019

Molecular and functional characterization of the role of the histone methyltransferase SETDB1 in malignant melanoma

Referees: Prof. Dr. Viktor Umansky

Prof. Dr. Jochen Utikal

Declarations according to § 8 (3) b) and c) of the doctoral degree regulations:

b) I hereby declare that I have written the submitted dissertation myself and in this process have used no other sources or materials than those expressly indicated,

c) I hereby declare that I have not applied to be examined at any other institution, nor have I used the dissertation in this or any other form at any other institution as an examination paper, nor submitted it to any other faculty as a dissertation.

Heidelberg, 11.03.2019

(Aniello Federico)

This Thesis is dedicated to my wife, my parents and my sister.

Parts of this thesis have been published in:

Conferences and workshop presentations:

- **Aniello Federico**, Jochen Utikal
  Summer school presentation: “Molecular and Functional Analysis of SETDB1-downstream targets in malignant melanoma”
  Anglo-German Research Training Initiative, July 2016, London, England

- **Aniello Federico**, Elias Orouji, Lionel Larribere, Daniel Novak, Viktor Umansky, Jochen Utikal
  Poster presentation: “Functional characterization of the histone methyltransferase SETDB1 in melanoma: a potential therapeutic target”
  Hallmarks of Skin Cancer Conference, November 2017, Heidelberg, Germany

- **Aniello Federico**, Jochen Utikal
  Summer school presentation: “Molecular and functional characterization of the role of the histone methyltransferase SETDB1 in malignant melanoma”
  RTG2099: Summer School, June 2018, Mannheim, Germany

- **Aniello Federico**, Elias Orouji, Lionel Larribère, Daniel Novak, Daniel B. Lipka, Yassen Assenov, Sachindra, Laura Hüser, Karol Granados, Christoffer Gebhardt, Christoph Plass, Viktor Umansky, and Jochen Utikal
  Poster presentation: “Molecular and functional characterization of the role of the histone methyltransferase SETDB1 in malignant melanoma”
  International conference “System Epigenetics, towards precision cancer medicine”, November 2018, Amsterdam, the Netherlands

Within the thesis, works from the following publications were included:

Federico A, Orouji E, Larribère L, Novak D, Lipka D, Assenov Y, Sachindra, Hüser L, Granados K, Gebhardt C, Plass C, Umansky V, Utikal J. The histone methyltransferase SETDB1 contributes to melanoma tumorigenesis and serves as a new potential therapeutic target. Manuscript in submission.

Table of Contents

Abstract

Malignant melanoma is the most deadly skin cancer. Clinical studies reported a dramatic increase in the incidence of melanoma over the past few years. A very distinctive feature of melanoma is its high degree of heterogeneity and cellular plasticity. Within the tumor there are different genetically defined subpopulations of melanoma cells, which is one of the reasons for the low efficacy of targeted therapies. Furthermore, most melanomas quickly develop a resistance to these therapies, causing tumor relapse. For all these reasons, gaining an understanding of the molecular and cellular mechanisms driving melanoma progression will be important for developing potent therapeutic approaches. So far, some key regulatory pathways normally activated in melanoma have been well defined, and these pathways are mainly driven by activation of oncogenes like BRAF and NRAS, with a considerable relevance for clinical practice. However, the identification of novel key regulators and pathways is still a challenge and will help to better understand melanoma development and to open up new possibilities to treat therapy resistant tumors.

Recent studies and work previously conducted in our laboratory reported that the histone methyltransferase SETDB1 plays a major role in melanoma pathogenesis. It has been observed that SETDB1 expression, which correlates with its amplification state in melanoma, is also associated with melanoma progression. However, the role of SETDB1 and its mode of action in melanoma are still unclear.

The aim of this project is to clarify the role of SETDB1 in melanoma, through the identification and functional characterization of SETDB1-mediated molecular mechanisms. Here, I report that SETDB1 expression caused deep changes in melanoma transcriptome resulting in the deregulation of pro- and anti-tumorigenic factors. Specifically, SETDB1 induced THBS1 upregulation and suppressed DCT expression. SETDB1 functions are dependent on its catalytic SET domain. During melanoma progression, SETDB1 promoted important epigenetic alterations such as changing the genomic distribution of H3K9me3 and H3K4me1 marks. These histone

modifications impacted the transcription of SETDB1 downstream targets. I could show that melanoma cells were sensitive to treatment with the SETDB1-inhibitor mithramycin A. Mithramycin treatment suppressed SETDB1 expression and tumorigenic properties of melanoma cells. Combinatorial treatment with mithramycin and MAPK inhibitors showed enhanced anti-tumor effects.

Taken together, the findings presented here highlight the crucial functional and mechanistic role of SETDB1 in melanoma. SETDB1 could be considered as a potential future target for the treatment of melanoma.

Zusammenfassung

Das maligne Melanom ist die tödlichste Form von Hautkrebs. Klinische Studien haben einen drastischen Anstieg von Melanomerkrankungen in den letzten Jahren festgestellt. Ein grundlegendes Merkmal des Melanoms ist sein hoher Grad an Heterogenität und zellulärer Plastizität. Innerhalb eines Tumors lassen sich verschiedene genetisch-definierte Subpopulationen von Melanomzellen finden, die eine effiziente zielgerichtete Krebstherapie erschweren. Darüber hinaus führt die schnelle Ausbildung von Resistenzen gegen zielgerichtete Therapien zu Rezidiven. Daher ist es wichtig, die molekularen und zellulären Mechanismen der Melanomprogression genauer zu untersuchen, um einen wirkungsvollen therapeutischen Ansatz zu finden. Es wurden bereits einige wichtige regulatorische Signalwege beschrieben, die in Melanomen aktiviert sind. Diese Signalwege werden hauptsächlich durch die beiden Onkogene BRAF sowie NRAS aktiviert, was von hoher klinischer Relevanz für die Auswahl einer geeigneten Therapiemethode ist. Eine große Herausforderung stellt jedoch die Identifikation von weiteren in der Melanomentstehung wichtigen Schlüsselregulatoren und Signalwegen dar. Dies ist wichtig, um die Entwicklung des Melanoms genauer zu verstehen um so in Zukunft therapieresistente Melanome behandeln zu können.

Kürzlich veröffentlichte Studien und Vorarbeiten aus unserem Labor haben gezeigt, dass die Histon-Methyltransferase SETDB1 eine wichtige Rolle in der Melanompathogenese spielt. Es wurde herausgefunden, dass die Expression von SETDB1, die im Melanom mit dem Amplifikationsstatus korreliert, mit einem Voranschreiten des Melanoms assoziiert ist. Jedoch ist die genaue Rolle und Funktion von SETDB1 bis heute unklar.

Das Ziel dieser Doktorarbeit bestand darin, die Rolle von SETDB1 im Melanom anhand der Identifizierung und funktionellen Charakterisierung der von SETDB1 vermittelten molekularen Mechanismen zu untersuchen. In dieser Arbeit wird gezeigt, dass die Expression von SETDB1 tiefgreifende Veränderungen des Melanomtranskriptoms nach sich zog und damit einen großen Einfluss auf die Regulation von pro- und anti-tumorigenen Faktoren hatte. Im Einzelnen induzierte SETDB1 die Expression von THBS1 und unterdrückte die Expression von DCT. Zudem ging die Expression von SETDB1 mit einer erhöhten Sekretion melanomzellspezifischer Onkoproteine einher. Die Funktionen von SETDB1 waren abhängig von der Aktivität seiner katalytischen SET Domäne. Während der Melanomprogression veranlasste SETDB1 wichtige epigenetische Modifizierungen, wie die Veränderung der genomischen Verteilung von H3K9 Trimethylierungen und H3K4 Monomethylierungen. Diese Histonmodifikationen wirkten sich auf die Transkription von Downstream-Faktoren von SETDB1 aus. Weiterhin konnte ich zeigen, dass Melanomzellen sensitiv gegenüber der Behandlung mit dem SETDB1-Inhibitor Mithramycin A waren. Die Behandlung mit Mithramycin unterdrückte die Expression von SETDB1 und damit dessen krebsfördernde Eigenschaften in Melanomzellen. Eine Kombinationstherapie mit Mithramycin und MAPK-Inhibitoren erzielte einen erhöhten antitumorigene Effekt.

Zusammengefasst zeigen die Ergebnisse dieser Studie, dass SETDB1 eine entscheidende funktionelle und mechanistische Rolle im Melanom spielt. SETDB1 könnte daher als potentieller Angriffspunkt für zukünftige Melanomtherapien in Betracht gezogen werden.

List of Figures

List of Tables

Abbreviations

%	percentage
°C	degree celsius
µM	micromolar
18S	18S ribosomal RNA
1X	working solution
2D	two-dimensional
3D	three-dimensional
Ac	acetylation
AE	adverse effect
AGO2	Argonaute protein 2
AKT	v-akt murine thymoma viral oncogene
ALDOC	aldolase C
AML	acute myeloid leukemia
ANOVA	analysis of variance
ANXA2	Annexin A2
APOE	Apolipoprotein E
ATF	Activating transcription factor
ATF7IP	Activating transcription factor 7-interacting protein 1
BARD	BRCA1-associated RING domain protein
BCA	Bichinonic Acid Protein Assay
BET	Bromodomain and Extra-Terminal motif
bp	base pair
BRAF	B-Raf Proto-Oncogene, Serine/Threonine Kinase
BRAFi	BRAF inhibitor
BSA	Bovine serum albumin
C02	carbon dioxide
CAS	Chemical Abstracts Service
CCL2	CC-chemokine ligand 2
Cdc5	Cell cycle serine/threonine-protein kinase 5

CDKN2A	Cyclin Dependent Kinase Inhibitor 2
CDS	coding region sequence
CH_3	methyl group
ChIP	Chromatin Immunoprecipitation
ChIP-seq	Chromatin Immunoprecipitation-sequencing
cm	centimeter
cMYC	Proto-Oncogene C-Myc
COH_3	acetyl group
CRC	colorectal cancer
CREB	CREB binding protein
Ct	cycle threshold
CTCF	CCCTC-binding factor
CTLA-4	Cytotoxic T lymphocyte antigen 4
CXCL	Chemokine (C-X-C motif) ligand
d	day
DAPI	4’,6-diamidino-2-phenylindole
DAVID	Database for annotation, visualization and integrated discovery
DCT	Dopachrome Tautomerase
DKFZ	Deutsches Krebsforschungszentrum
DMEM	Dulbecco’s modified eagle’s medium
DMSO	dimethylsulfoxide
DNA	deoxyribonucleic acid
DNMT	DNA methyltransferases
DNMT3A	DNA (cytosine-5)-methyltransferase 3A
DZNep	3-Deazaneplanocin A
EDTA	ethylenediaminetetraacetic acid
EGFR	Epidermal Growth Factor Receptor
EMT	Epithelial-to-Mesenchymal Transition
ERK	Extracellular Signal Regulated Kinase
ERV	Endogenous retrovirus

ES	enrichment score
et al.	et alteri
EV	empty vector
EZH2	Enhancer of zeste homolog 2
FC	fold change
FCS	fetal calf serum
FDA	Food and Drug Administration
FDR	false discovery rate
FosB	FBJ Murine Osteosarcoma Viral Oncogene Homolog B
Fz	Frizzled
G9a	Euchromatic Histone Lysine Methyltransferase 2
GAPDH	Glyceraldehyde 3-phosphate dehydrogense
GATA-1	GATA Binding Protein 1
GFP	Green fluorescent protein
GO	gene ontology
gp100	Glycoprotein 100
GSEA	gene set enrichment analysis
GTP	Guanosine triphosphate
h	hour
HAT	Histone acetyl transferase
HCl	chloridric acid
HDAC	Histone deacetylase
HDACi	HDAC inhibitors
HDM	Histone demethylases
hg19	human reference genome 19
HMT	Histone methyltransferase
HMTi	HMT inhibitor
Hox	Homeobox
HP	Heterochromatin protein
HRP	Horseradish peroxidase
IC50	half maximal inhibitory concentration

IF	Immunofluorescence
IGDFB2	IGF-binding protein 2
IGV	Integrative Gene Viewer
IHC	immunohistochemistry
IL	Interleukin
IPA	Ingenuity pathway analysis
JMJD2C	Jumonji Domain-Containing Protein 2C
K	Lysine
KAP1	KRAB-associated protein-1
KD	knockdown
kDa	kiloDalton
KMT	Lysine methyltransferases
KRAB	Krüppel associated box domain
LB	Lysogeny broth
Lmo2	LIM domain only 2
log	logarithm
log2	binary logarithm
LSD1	Lysine-specific demethylase 1
Lys	Lysine
M	molar
MAPK	Mitogen-activated protein kinase
MAPKi	MAPK inhibitor
MART-1	Melan-A
MBD	Methyl-CpG-binding domain
MBD1	Methyl-CpG-binding domain protein 1
MBT	Malignant Brain Tumor
MC1R	Melanocortin 1 receptor
MCAF	Malonyl-CoA-Acyl Carrier Protein Transacylase
me	methylation
MEF	Mouse Embryonic Fibroblasts
MEK	Mitogen Activated Protein Kinase

min	minutes
mit	mythramycin A
MITF	Microphthalmia-Associated Transcription Factor
ml	milliliter
MMP	Matrix-Metalloprotease
mRNA	Messenger Ribonucleic Acid
MSK1/2	Mitogen and stress activated protein kinase 1/2
g	sodium hydroxide
NCT	National Center of Tumor Diseases, Heidelberg, Germany
NEAA	non-essential amino acids
NES	normalized enrichment score
NF1	Neurofibromatosis 1
NFY	Nuclear transcription factor Y
ng	nanogram
NHM	Normal Human Melanocytes
nM	nanomolar
NOD/SCID	Nonobese Diabetic/Severe Combined Immunodeficient
NRAS	Neuroblastoma RAS Viral Oncogene Homolog
NSCL	Non-small cell lung
NSD	Nuclear receptor binding SET domain
ns	non-significant
NT	non-targeting
OE	overexpression
ORF	open reading frame
OS	overall survival
OSCC	Oral squamous cell carcinoma
p	p value
p53	Tumor protein p53
PBS	phosphate buffered saline
PCR	polymerase chain reaction
PD-1	Programmed death 1

PD-L1	PD-ligand 1
PFA	paraformaldehyde
PI3K	Phosphatidylinositol-4,5-bisphospahte 3-kinase
PIP3	Phosphatidylinositol phosphate
PKA	Protein kinase A
PMEL17	Melanosomal matrix protein 17
PML	Promyeolicytic leukaemia
PML-NBs	Promyeolicytic leukaemia- nuclear bodies
PP	Protein phosphatases
PRDM	PR Domain zinc finger protein
PTEN	Phosphatase and tensin homolog
PTMs	post translational modification
PVDF	polyvinylidenfluorid
qPCR	quantitative real-time polymerase chain reaction
r	Spearman correlation
R	Arginine
RAF	Rat fibrosarcoma
RAS	Rat sarcoma
Rb	Retinoblastoma
RFU	relative fluorescence unit
RIPA	radioimmunoprecipitation assay buffer
RNA	ribonucleic acid
RNF	ring finger protein
rpm	revolutions per minute
RSK	Ribosomal S6 kinase
RT	room temperature
S	Serine
S2	Biosafety level 2 laboratory
SAM	S-adenosyl methionine
SCG2	Secretogranin 2
SDS	sodium dodecyl sulfate

SET	Su(var)3-9, Enhancer-of-zeste and Trithorax
SETDB1	SET domain bifurcated histone lysine methyltransferase 1
SETDB2	SET domain bifurcated histone lysine methyltransferase 2
shRNA	short hairpin RNA
SIRT	Sirtuin
SMAD2/3	Small mother against decapentaplegic
SOX	SRY (sex determining region Y)-box
SOX10	SRY-Box 10
Sp1	Specificity protein 1
STAT3	Signal transducer and activator of transcription 3
T	Threonin
TAD	topologically associated domain
TCGA	The Cancer Genome Atlas
TCP	tranylcypromine
TEB	Triton Extraction Buffer
TF	transcription factor
TGFβ-	Transforming growth factor beta
THBS1	Thrombospondin-1
TMA	Tissue Microarray
TNF	Tumor necrosis factor
Tra	trametinib
TRAIL	TNF-related apoptosis-inducing ligand
TRIM28	Tripartite motif-containing 28
TRP1	Tyrosinase-related protein 1
TRP2	Tyrosinase-related protein 2
TSS	transcription start site
TYR	Tyrosinase
USP	Ubiquitin-specific protease
UVR	ultraviolet radiation
Vem	vemurafenib
VS	versus

WB	Western Blot
WNT	Wingless/Integrated
WT	wild type
α-MSH	α-melanocyte stimulating hormone
µg	microgram
µl	microliter

1 Introduction

1.1 Malignant melanoma

1.1.1 Epidemiology and risk factors

Malignant melanoma is the most common and lethal skin neoplasia. According to the worldwide cancer statistics provided by the Global Cancer Observatory (Bray et al, 2018), in 2018 almost 300.000 new cases of melanoma and more than 60.000 deaths were estimated, confirming the remarkable increasing trend observed over the last years (Leiter et al, 2014) (Whiteman et al, 2016). Several main risk factors have been defined for melanoma. The most known and well-characterized is represented by the exposure to UV radiation (UVR), which induces profound genetic and biological changes linked to malignant transformation of cells (Watson et al, 2016). UVR DNA damages mostly occur in light-skinned people and people with a genetic susceptibility (Gloster & Neal, 2006) (Ferguson et al, 2019). While the sporadic cases are the most frequent, familial melanomas represent about 10% of the total cases per year (Soura et al, 2016).

1.1.2 Melanoma development and progression model

Malignant melanomas arise from melanocytes, which are melanin pigment-synthesizing cells found in the skin and in several other anatomical sites, such as eyes, mucosa, inner ear, nervous system, and heart (Cichorek et al, 2013). Melanin produced by melanocytes is delivered to neighboured keratinocytes and serves as skin protection system to UVR.

Melanocytic transformation is accompanied by increased proliferation and morphological changes. Pro-oncogenic processes are triggered by intrinsic (e.g. genetic alterations) and environmental factors (e.g. chronic UVR exposure) (Bandarchi et al, 2013) (Bermudez, 2014). The presence of a singular risk factor is not generally sufficient to induce melanoma development. Mutated BRAF ($BRAF^{V600E}$) expression in melanocytes is associated with limited cell proliferation, resulting in the formation of benign neoplasms (melanocytic nevi), while additional genetic alterations are required for

melanoma initiation (Abildgaard & Guldberg, 2015) (Shtivelman et al, 2014). Most of cutaneous melanomas are classified as *de novo*, meaning that they are not associated with pre-existing nevus lesions (Greene et al, 1985). Melanoma cells are characterized by uncontrolled proliferation and high genetic heterogeneity. Depending on tumor localization and cell behaviour, it's possible to distinguish between melanoma *in situ*, which is the earliest cancer stage where tumor cells are all confined to the epidermis, showing slow progression and better prognosis outcome (Mocellin & Nitti, 2011), and invasive melanoma. In this latter condition, melanoma cells show a widespread distribution within the dermis and closer interactions with the surrounding microenvironment composed of stromal cells (fibroblasts, endothelial cells, infiltrating inflammatory cells) and macromolecules (extracellular matrix and soluble factors). Microenvironment components together with the accumulation of genetic aberrations shape the tumor phenotype towards a more aggressive and invasive one (Villanueva & Herlyn, 2008). During melanoma tumor growth, melanoma cells undergo reversible alterations defined as phenotype-switching, characterized by a loss of cell proliferative potential and acquisition of prominent pro-invasive and pro-metastatic properties, making the tumor more prone to metastasize (Hoek et al, 2008) (Hoek & Goding, 2010). Formation of melanoma metastases is observed when cells leave the primary tumor and reach local and distant regions. The metastatic process is articulated in distinct stages. During stage I/II, melanoma cells start disseminating from the primary tumor and circulating via the vascular and lymphatic system. However, no metastases can be detected at these stages. Stage III is defined by the observation of clear lymph node metastases. Lymph nodes, and the sentinel lymph nodes in particular, are the primary sites where melanoma metastases form (Wong et al, 2018). In the most advanced melanoma phase (stage IV), cells colonize distant sites and re-acquire proliferative capacity. Melanoma metastases are especially found in lungs, bones, brain and liver (Tas, 2012) (**Figure 1**).

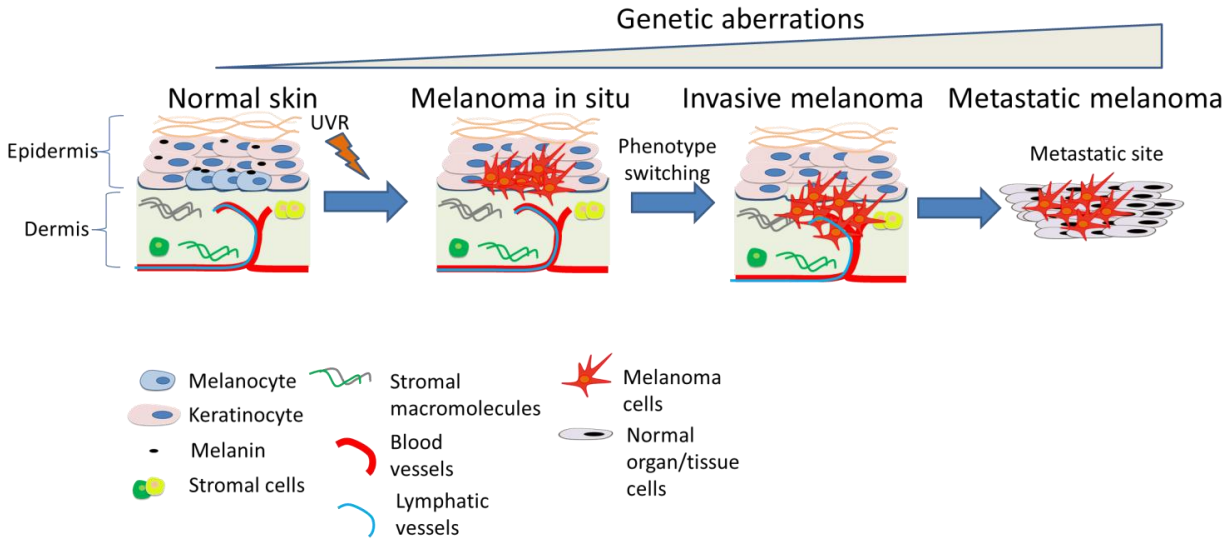

Figure 1: Schematic model of melanoma initiation and progression. In normal skin, melanocytes are located in the basal layer of the epidermis. Melanocytes produce melanin which is then transferred to the surrounding keratinocytes. Combination of genetic alterations and exposure to carcinogenic stimuli (e.g. UVR) determine the malignant transformation of melanocytes to melanoma cells. The accumulation of genetic mutations and the activation of oncogenic signaling pathways result in a more aggressive phenotype of melanoma cells («phenotype switching»), which are now capable to invade the dermis, forming the «pre-metastatic niche», and to interact with the stromal components (invasive melanoma). Chromosomal aberrations and stimulation from the tumor microenvironment are crucial for the metastatic process, where tumor cells leave the primary site and colonize, through extravasation in blood and lymphatic vessels, distant organs and tissues (metastatic melanoma).

1.1.3 Key signalling pathways and oncogenes in melanoma

Melanoma development and progression are defined by the deregulation of molecular and cellular mechanisms. In particular, the activation of signal transduction pathways related to cell proliferation and survival, together with repression of tumor suppressors, greatly contribute to the oncogenic potential of melanoma cells.

Several signalling pathways have been characterized in detail in relation to melanoma progression, including the mitogen-activated protein kinase (MAPK) pathway, which represents the most recurrently deregulated signalling cascade, the phosphoinositide 3-kinase (PI3K) pathway, the MITF pathway and WNT/β-catenin pathway. For each of these processes, oncogenic driver mutations occur in key signalling factors.

MAPK pathway

Activation of MAPK signalling promotes biological processes like cell proliferation, cell survival, differentiation and apoptosis (2015; Obenauf et al, 2015). Cells expose tyrosine

kinase- and cytokine-receptors on their surface, which, when stimulated, communicate the signal to monomeric GTPases belonging to the RAS protein family. RAS activates a serine/threonine kinase cascade, composed of BRAF, MAP2K (MEK) and MAPK (ERK). Active ERK phosphorylates a wide range of substrates, including transcription factors, in this way mediating cell growth and survival effects. In melanoma, the MAPK signalling pathway is mostly found constitutively activated. In almost 50% of melanoma patients, this is due to *BRAF* gene mutations. The most frequent oncogenic BRAF mutation (90% of BRAF mutation cases) is an amino acid substitution (the valine at position 600 is replaced by a glutamic acid; V600E). As a result, the $BRAF^{V600E}$ variant encodes for a constitutively active BRAF protein (Ascierto et al, 2012). Almost 20% of melanoma patients are characterized by activating mutations of the neuroblastoma RAS (NRAS) protein, which is the predominant RAS isoform expressed in melanoma. Q61R and Q61K amino acid substitutions are the most frequent NRAS mutations. NRAS-mutated melanomas are associated with an aggressive phenotype and a worse prognosis compared with non-NRAS mutated melanomas (Jakob et al, 2012) (Lee et al, 2011).

PI3K pathway

Besides MAPK pathway activation, NRAS induces also PI3K signalling. Activated PI3K promotes the phosphorylation of phosphatidylinositol-3, 4, 5-triphosphate (PIP_3), required for the recruitment and activation of the protein kinase B (AKT), a serine/threonine kinase involved in the control of cell survival, motility, angiogenesis and metabolism. PIP_3 is negatively regulated by the tumor suppressor PTEN. Loss of PTEN by gene deletion or by epigenetic interference is highly recurrent in melanomas with the worst clinical outcome (Aguissa-Toure & Li, 2012) (Mirmohammadsadegh et al, 2006).

MITF pathway

Melanocytes normally expose the melanocortin 1 receptor (MC1R) on their surface, which is usually stimulated by the α-melanocyte-stimulating hormone (α-MSH). MC1R activation leads to an increase of microphthalmia-associated transcription factor (MITF) expression. MITF plays a crucial role in melanocyte survival and differentiation by regulating the genes responsible for melanin synthesis, including tyrosinase (TYR),

tyrosinase-related protein 1 (TYRP1), tyrosinase-related protein 2 (TRP2, DCT), Melan-A (MART1) and melanosomal matrix protein 17 (PMEL17) (Goding, 2000) (Du et al, 2003). The role of MITF in melanoma is controversial. The *MITF* gene has been found to be amplified in about 20% of the melanomas and its expression is associated with reduced patient-survival. On the other hand, several studies showed that MITF expression and regulatory activity is impaired in melanoma cells (Wellbrock & Arozarena, 2015).

Wnt/β-catenin pathway

Wnt proteins are involved in pathogenic mechanisms in various cancer types (Zhan et al, 2017). In WNT/β-catenin signalling (also known as the canonical pathway), the WNT ligand binds to Frizzled (Fz) receptors and induces accumulation of β-catenin in the cell. β-catenin enhances the transcription of Wnt target genes that are described as inducers of tumor growth and mediators of drug resistance (Sinnberg et al, 2011).

c-KIT

The oncogene *c-KIT* (*CD177*) encodes for a tyrosine kinase receptor expressed on the surface of stem-like tumor cells (Galli et al, 1993). *c-KIT* mutations are detected in about 1% of all melanomas and mostly observed in non-sun exposed lesions (acral /mucosal melanoma). Mutated c-KIT constitutively stimulates the MAPK and PI3K pathways via RAS activation (Ashida et al, 2009) (Carlino et al, 2014).

CDKN2A

The cyclin-dependent kinase Inhibitor 2A (CDKN2A) is a cell-cycle regulator. The *CDKN2A* gene encodes two different transcript variants, which both function as tumor suppressor proteins. $p16^{INK4A}$ is involved in the regulation of retinoblastoma (RB) signalling related to cell cycle checkpoint control, while $p14^{ARF}$ plays a role in p53-mediated apoptosis. *CDKN2A* mutations abrogate these tumor suppressor mechanisms (Freedberg et al, 2008). *CDKN2A* is frequently mutated in cases of familial melanoma (Goldstein, 2004).

NF1

The tumor suppressor neurofibromatosis 1 (NF1) is expressed in many cell types. It inhibits RAS activity. *NF1* mutations impair its tumor suppressor activity and are frequently detected in melanoma lesions on chronically sun-exposed skin (Kiuru & Busam, 2017).

1.1.4 Melanoma treatment options

Malignant melanoma is characterized by high complexity and genetic heterogeneity. For this reason, a great number of therapeutic approaches has been developed in the past decades, clinically tested and approved by the US Food and Drug Administration (FDA), with the aim to treat and cure melanoma. Depending on tumor histopathological parameters, the presence of metastases and the genetic profile of a melanoma, the most suitable therapeutic options are chosen among: surgical resection, chemotherapy, radiotherapy, immunotherapy and targeted therapy.

Surgical treatment

For patients in the earliest stages of melanoma disease before the occurrence of metastases, surgical excision of the tumor mass represents the principal therapeutic option. The overall survival rate after surgical resection is 92% (Torre et al, 2015). However, the presence of unresectable tumors and disseminated metastases required the development of alternative and effective treatment options.

Chemotherapy

The use of chemotherapeutic agents is a standard approach for the treatment of cancer. However, chemotherapeutic treatment of melanoma patients does not really increase their overall survival (OS). For this reason, chemotherapeutic drugs (dacarbazine, temozolomide) are mainly used for palliative treatment of patients with advanced melanoma (Wilson & Schuchter, 2016).

Radiotherapy

For many cancer types, radiation therapy is solely applied as a complement to surgical treatment or alternatively as a palliative cure in late-stage melanoma associated with painful conditions (i.e. unresectable brain metastases) (Mahadevan et al, 2015).

Immunotherapy

Innovative therapeutic approaches developed in the last few years focused on the interactions between tumor cells and the immune system. In particular, efforts have been made to stimulate and enhance the mechanisms by which cytotoxic T cells, which play a central role in pathogen-specific immune response, undergo activation and clonal amplification once tumor cells expose specific antigens on their surface. As a consequence, activated T cells specifically kill tumor cells (Lanitis et al, 2017). It has been shown that during tumor progression and metastases formation, various immunosuppressive mechanisms are activated. Current immunotherapy strategies aim at circumventing the immunosuppressive effects and inducing a prompt and effective immune response. First FDA-approved immunotherapies for melanoma were based on the use of cytokines (Interferon α-2b, FDA-approved in 1995; interleukin 2, approved in 1998; peginterferon α-2b, approved in 2011) (ClinicalTrials.gov). These cytokines mediate immunomodulative and antitumor effects via stimulating the activation of immune cells (Rafique et al, 2015) (Kirkwood et al, 2001) (Eggermont et al, 2008) (Krieg et al, 2010). Despite the poor patient response, cytokine-based immunotherapies are still used in combinatorial treatment studies. Different immunotherapy-based approaches were developed to specifically interfere with immunosuppressive mechanisms. One of the most promising and widely used immunotherapeutic agent, ipilimumab (anti- CTLA-4 antibody), efficiently reverses the drug tolerance induced by the cytotoxic T lymphocyte-associated antigen 4 (CTLA-4). Ipilimumab treatment, approved by the FDA in 2011, reverses CTLA-4-mediated T cell dormancy (Grosso & Jure-Kunkel, 2013). Melanoma patients treated with ipilimumab showed promising drug responses, although accompanied by modest to severe adverse effects (AEs) (Hodi et al, 2010) (Wolchok et al, 2010). A new immunotherapy strategy was developed to prohibit immunosuppressive effects resulting from the binding of the programmed cell death protein 1 (PD-1)

receptor, present on the surface of T cells, with the PD-1 ligand (PD-L1), exposed by several cancer cell types. The PD-1/PD-L1 interaction promotes T cell suppression. Anti-PD-L1 antibodies (nivolumab, FDA-approved in 2014; pembrolizumab, approved in 2015) represent a valid immunotherapeutical option to reverse tumor-mediated T cell suppression and to positively modulate immune response, with relatively modest AEs (Tsai et al, 2014) (Jazirehi et al, 2016). Additional immunotherapy options include the development of vaccines (g100 peptide, Toll like receptor agonists) (Yuan et al, 2009a) (Kanzler et al, 2007), the use of oncolytic viruses or the administration of melanoma-specific mature T cells (Pol et al, 2016) (Dudley et al, 2008).

Targeted therapy

The identification of activating mutations driving melanoma progression permitted to develop new therapeutic strategies, based on small molecules able to specifically target and inhibit the mutated protein variants. $BRAF^{V600E}$, the most common mutation in melanoma and responsible for aberrant MAPK pathway activation, is effectively inhibited by vemurafenib (PLX4032, FDA-approved in 2011) and dabrafenib (approved in 2013). Selective BRAF inhibition resulted in remarkable clinical responses, namely a strong tumor regression in melanoma patients harbouring the BRAF mutation. Trametinib, the inhibitor of MEK (approved in 2013), also achieves beneficial effects in terms of patient response and overall survival rates. Alternative molecular targets for drug inhibition include the tyrosine kinase receptor c-KIT (imatinib) and the PI3K-AKT pathway (PI-103; rapamycin) (Livingstone et al, 2014) (Li et al, 2013). An increasing number of novel targets has been included in clinical trials in order to further optimize targeted therapy approaches and to face the huge molecular complexity observed in melanoma. FDA-approved therapies are currently used for treating unresectable advanced melanoma, as monotherapy or in combinatorial treatments (Gazze, 2018). Despite the promising beneficial effects of targeted therapy observed in patients with malignant melanoma, dramatic tumor relapses occur in most of the cases, together with an acquired resistance to the previously used drug (Kalal et al, 2017). Several mechanisms may contribute to the development of resistance: i) the presence and/or accumulation of additional genetic aberrations affecting components of the MAPK and PI3K signalling

pathways, such as NRAS mutation, aberrant splicing variants of BRAF or loss of NF1 or PTEN tumor suppressors; ii) alterations in cellular processes, like cell cycle control or apoptotic program; iii) cellular effects mediated by the close interactions with tumor microenvironment components; iv) high degree of intra-tumor heterogeneity. Novel targeted strategies aim at overcoming resistance via the identifying novel oncogenic drivers of melanoma and by the use of combinatorial treatments.

1.2 Epigenetics in melanoma

1.2.1 Epigenetics overview

The term “epigenetics” was first used by Conrad Waddington in 1942 to indicate the influence of the interactions between genes and microenvironment during development and embryogenesis (Noble, 2015). Improved knowledge of molecular mechanisms allowed to identify peculiar phenotypic traits which are induced or repressed by alterations of the chromatin structure. Interestingly, chromatin changes were not found as related to modification of DNA sequence, but attributed to reversible, dynamic and heritable variations occurring on chromatin structure components.

Chromatin is a macromolecule composed of genomic DNA, RNA and proteins. The basic chromatin unit is the nucleosome, which is constituted of 147 base pairs (bp) of DNA assembled with an octamer core of alkaline proteins, known as histones (H3, H4, H2A, H2B) (McGinty & Tan, 2015). The C- and N- terminal amino acid chains (tails) of histones are subjected to a wide range of posttranslational modifications (PTMs). Histone modifications induce drastic changes of the structural conformation of chromatin, which are directly linked with the alteration of molecular mechanisms: depending on the local level of chromatin compaction (high-condensed form, termed heterochromatin; low-condensed form, referred to as euchromatin), genomic sites may be more or less accessible for the gene regulatory machinery.

Transition from heterochromatin to euchromatin (and *vice versa*) is strictly modulated by DNA methylation and histone modifications. DNA methylation is the addition of hydrophobic methyl groups (chemical formula: $-CH_3$) to specific genomic DNA bases

(cytosine) located at important regulatory sites defined as CpG islands. DNA methylation prevents these regions from binding transcription factors (TFs), resulting in the repression of the corresponding gene (Newell-Price et al, 2000). Epigenetic changes are regulated by various enzymes that, depending on their specific functions, can be defined as: i) “writers”, responsible for the insertion of chemical structures (epigenetic marks) to histones and DNA; ii) “readers”, enzymes capable of recognizing and interacting with epigenetic traits; iii) “erasers” enzymes mediating the removal of epigenetic marks(Gillette & Hill, 2015) (**Figure 2**).

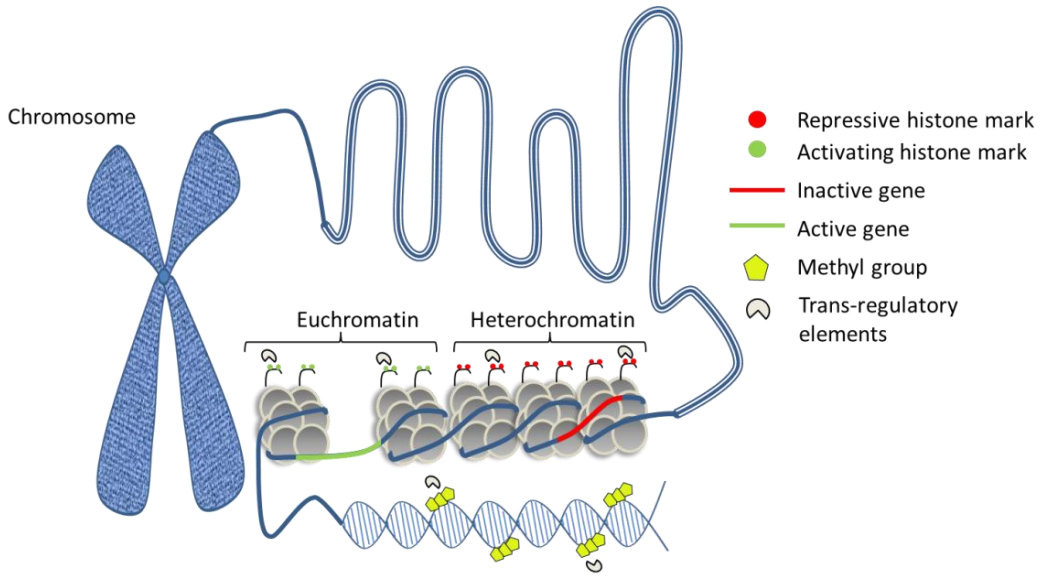

Figure 2: Landscape of epigenetic mechanisms. Human chromosomes are physically organized in complex of DNA, RNA and protein which form the chromatin. Chromatin is in turn composed by nucleosomes, in which DNA segments are wrapped around octamers of histone proteins. Chromatin structure can undergo reversible modifications which lead to alterations in gene expression. Epigenetic changes comprise the methylation of specific DNA nucleotides (DNA methylation) and chemical alterations of amino acid residues protruded from the N terminal tails of histones (histone modifications). Each histone exhibits a wide range of histone modifications which generally impact on the chromatin condensation state and, therefore, on the gene expression. Based on this, histone marks can be categorized as repressive (mostly found in the highly condensed chromatin state, heterochromatin) or as activating (enriched in the euchromatin, which is less compacted). Epigenetics marks mediate transcriptional effects also by recruiting trans-regulatory factors.

1.2.2 Histone modifications

PTMs of histones have been reported to greatly contribute to regulatory mechanisms by directly inducing structural changes in the chromatin structure or by recruiting transcription factors and other trans-elements (Bannister & Kouzarides, 2011). Each histone protein possesses a great number of modification sites, mostly located at the terminal tails. Multiple histone modifications can co-occur on the same histone. Although several histone marks are generally associated either with enhancing (H3Ac, H3K4, H3K36, H3K9me1) or repressing (H3K9me2/me3, H3K27) transcription (Dong & Weng, 2013), the final impact of histone modifications on gene expression is defined by multiple variables, like the histone type and amino acid residues involved in PTMs, as well as the interplay with other histone marks in the surrounding area ("histone cross-talk"). The highly complex scenario of the interactions and combinatorial effects of PTMs is also called histone code (Lee et al, 2010). Gene regulation-related histone modifications can be generally classified as: acetylation, methylation, phosphorylation and ubiquitination (**Figure 3**). Other PTMs (sumoylation, citrullination, glycosylation, carbonylation, ADP-ribosylation, formation of histone variants) are much less frequent.

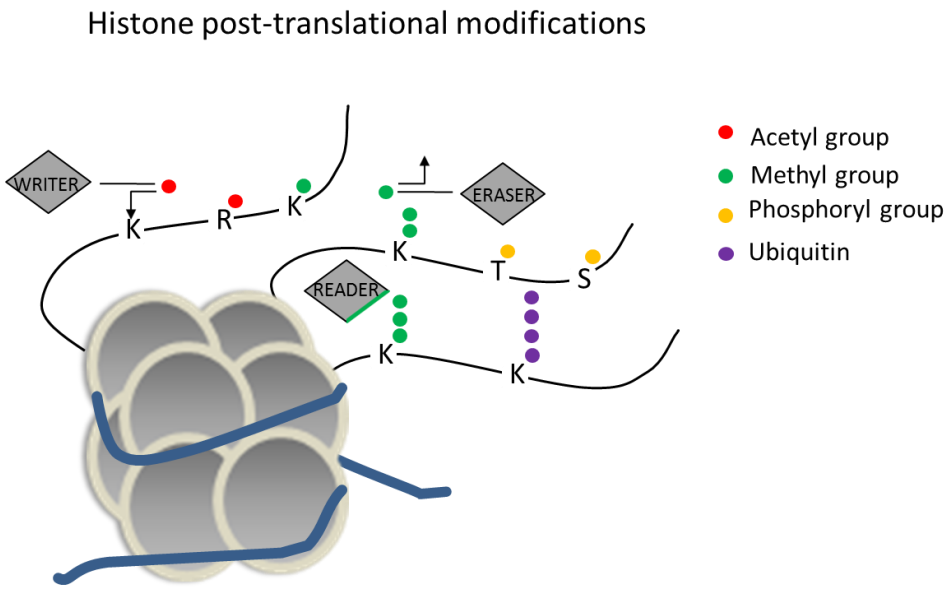

Figure 3: Overview of histone modifications. Histone proteins exhibit side chains subjected to specific post-translational modifications. Lysine (K) residues can be acetylated, methylated and ubiquitinated. Arginine (R) is mostly found acetylated, while histone phosphorylation occurs on serine (S) and threonine (T) residues. Histone modifications are modulated by different classes of enzymes responsible for the adding («writers»), removal («erasers») or recognition («readers») oh histone PTMs.

Histone acetylation

Acetylated histones carry functional acetyl groups (chemical formula: $-CO-CH_3$) at their N-terminal tails. Depending on the histone type, acetylation is restricted to specific lysine (Lys) residues. The introduction and removal of an acetyl group are mediated by histone acetyl transferases (HATs) and histone deacetylases (HDACs), respectively. Several HAT/HDAC variants have been identified which can be distinguished by their structural conformations and by cell type distribution. HAT-mediated histone acetylation induces critical molecular effects. First, introduction of acetyl groups mediated by the CREB-binding protein (CBP) destabilizes the histone-DNA interactions, rendering the chromatin more accessible for TFs (Verdone et al, 2005). Moreover, histone acetylation marks are recognized and bound by bromodomain-containing proteins. Several factors contain multiple bromodomains, which increases the complexity of histone acetylation-related regulatory effects (Josling et al, 2012).

Histone methylation

Histone methylation is the addition of methyl groups to specific basic residues (lysine, arginine) protruding from the terminal tails. In contrast to acetylation, a particular amino acid residue can incorporate one (monomethylation), two (dimethylation) or three (trimethylation) methyl groups (Greer & Shi, 2012). Histone methyltransferases (HMTs) represent the key writer enzymes for this histone mark. Each HMT shows methylation site-specificity: in particular, the EZH2 enzyme specifically methylates Lys 27 of histone H3 (H3K27), resulting in gene silencing (Yoo & Hennighausen, 2012). MLL1 catalyses the methylation of H3K4, mostly associated with gene activation (Guenther et al, 2005), while SUV39H and members of the SET-domain protein family, like SETDB1 and G9a, regulate the H3K9 methylation status, often linked with transcriptional repression (Stewart et al, 2005). Histone demethylases (HDMs) act as eraser factors, removing methyl groups from histone residues. Lysine-specific demethylase 1 (LSD1) is the most well characterized histone demethylase (Chen et al, 2012). Methylation tags are specifically recognized by proteins containing chromodomains, Tudor domains or MBT domains (Yap & Zhou, 2011). Functional effects induced by histone methylation are very complex and depend on the localization of the histone tag, number of added methyl

groups (mono- , di-, trimethylated status) and, finally, concomitant epigenetic marks for that particular genomic region.

Histone phosphorylation

Histone proteins contain various serine and threonine residues which can be phosphorylated under physiological and pathological conditions. Histone phosphorylation and dephosphorylation mechanisms are mediated by histone-specific enzymes, such as H2BS32ph, RSK2 and MSK1/2 kinases, and by less specific components of signalling cascades, like ERK and protein phosphatases (PP) 1 and 2 (Rossetto et al, 2012). Of note, it has been shown that histone phosphorylation marks together with histone acetylation marks synergistically contribute to gene regulation (Cheung et al, 2000).

Histone ubiquitination

The functional role of histone ubiquitination is still subject of debate. Ubiquitination is predominantly observed at lysine residues of histone H2A and H2B. In the first case, the histone mark is associated with gene activation, while monoubiquitinated H2B is mostly found in silenced gene regions. Ring finger proteins RING1A/B, BMI1, BARD1, RNF20 and RNF40 strongly enhance E3 ubiquitin ligase activity towards histone proteins. Deubiquitinating factors, in particular ubiquitin-specific proteases (USPs), revert this catalytic reaction (Cao & Yan, 2012).

1.2.3 Histone modifications in cancer and therapeutic options

During malignant transformations, a wide range of oncogenic driver mutations affects epigenetic regulators, leading to alterations of chromatin structure and histone modification pattern. Epigenetic aberrations, in turn, drastically change gene regulatory mechanisms leading to an increase of oncogene expression, or tumor suppressor gene silencing. For all these reasons, epigenetic alterations strongly contribute to tumor development and progression. Moreover, the global landscape of epigenetic changes, especially of histone modifications, may represent a valuable predictive indicator of clinical outcome in cancer. The identification of the main dysregulated epigenetic

components in the last few years allowed to develop epigenetic targeted therapies and to test them against various solid cancers. Histone acetylation and methylation are the most deregulated epigenetic pathways in cancer (Muntean & Hess, 2009). Histone acetylation patterns are defined by the activity of HAT and HDAC enzymes. The histone acetylase CBP has been found mutated or aberrantly expressed in solid tumors and leukemias (Gao et al, 2014) (Giotopoulos et al, 2016). In the same way, HDACs are highly expressed in cancer and participate in tumorigenic mechanisms (Yang et al, 2014). To counteract HDAC activity in malignancies, unselective and selective HDAC inhibitors (HDACi) are currently used as therapeutic options. It has been reported that HDACi, such as vorinostat (unselective) and romidepsin (selective for HDAC1/2 inhibition), induce tumor cell cycle arrest and are included in clinical trials on cutaneous and peripheral T cell lymphomas (Olsen et al, 2007) (Piekarz et al, 2011). Epigenetic regulators related to histone methylation and frequently deregulated in cancer belong to both the HMT and HDM family. EZH2 is overexpressed in breast and prostate cancer (Pourakbar et al, 2017) (Melling et al, 2015). In contrast, various hematopoietic malignancies exhibit inactivating mutations of EZH2 (Herviou et al, 2016), suggesting that the role of EZH2 in cancer is cell context- and mutation-dependent. EZH2 inhibition approaches rely on competitive binding using analogues of the EZH2 cofactor, S-adenosyl methionine (SAM). DZNep, EI1 and GSK126 specifically target EZH2-positive tumor cells, inducing growth arrest and apoptosis (Kim & Roberts, 2016). The H3K9 HMTs G9a and SUV39H are targeted by the small molecule inhibitors BIX01294 and chaetocin, respectively (Chiba et al, 2015) (Chang et al, 2009). The histone demethylase LSD1 plays a crucial role in acute myeloid leukemia (AML). Tranylcypromine (TCP) was indicated to effectively target LSD1 in tumor cells (Sun et al, 2016).

Besides epigenetic writers and erasers, reader enzymes are also important for the regulation of molecular mechanisms in normal or tumor-related conditions. Approaches utilizing small molecule inhibitors against bromodomain proteins belonging to the BET family or chromodomain HP1 represent innovative and promising therapeutic options for the treatment of cancer (Yu et al, 2015) (Castonguay et al, 2015).

1.2.4 Histone modifications in malignant melanoma

Recently, novel molecular mechanisms linked with melanoma have been described, further implementing the complex landscape of melanoma pathogenesis. In addition to genetic abnormalities and cell signalling dysregulations, several epigenetic alterations have been identified and characterized. Melanomas have one of the highest mutation rates among solid tumors (Hodis et al, 2012), and several of these mutations affecting epigenetic factors. Recent studies indicate how changes in the expression and/or activity of epigenetic regulators lead to critical consequences in melanoma progression, and that approaches that selectively target epigenetic factors represent an innovative and promising therapeutic strategy for the treatment of melanomas. Regulation of melanoma-related factors like the SRY-Box 10 (SOX10) and the signal transducer and activator of transcription 3 (STAT3) proteins is directly modulated by histone H3K27Ac levels and by HDAC6 inhibition, respectively (Verfaillie et al, 2015) (Lienlafa et al, 2016). Moreover, HDACi treatment impairs the activation of the MAPK pathway (Hornig et al, 2016). In contrast to these anti-tumorigenic effects, a recent work showed that melanoma cells exposed to HDACi possess a more aggressive and invasive phenotype (Diaz-Nunez et al, 2016). The EZH2 protein is overexpressed in metastatic melanoma. In primary melanomas, EZH2 expression correlates with the expression of $BRAF^{V600E}$ and with melanoma proliferation (Yu et al, 2017). Functionally, EZH2 induces alterations of genome-wide H3K27me3 enrichment and distribution. H3K27me3 modulates CDKN2A oncogenic splicing mechanisms (Souroullas et al, 2016). The EZH2 inhibitor GSK126 impairs melanoma cell invasiveness (Tiffen et al, 2015). The histone demethylases LSD1 and JMJD2C induce oncogenic transformation of senescent melanocytes by reducing H3K9me3 marks. Loss of H3K9me3 promotes E2F target gene expression, resulting in melanocytes overcoming the cell cycle block. Treatment with LSD1 inhibitors reverts tumorigenic transformation and restores senescence (Yu et al, 2018). The epigenetic reader protein BRD4, which belongs to the BET family, is overexpressed in melanoma. BRD4 inhibition leads to reduced cell proliferation rates (Segura et al, 2013).

Targeting therapies aiming at epigenetic factors are being included in clinical trials to treat melanoma and are especially used in combinatorial treatments. To date, the most

promising epigenetic-based therapeutic option is given by the combination of HDACi and TRAIL, able to stimulate tumor cell apoptosis (Jazirehi & Arle, 2013).

Improved targeted therapies against epigenetic factors may serve as alternative therapeutic approach to overcome melanoma chemoresistance. Recently, it has been reported that treatment of MAPKi-resistant melanoma patients with the HDACi panobinostat and the HMTi decitobine in combination with chemotherapy yields encouraging responses in patients (Ibrahim et al, 2016) (Alcazar et al, 2012). In a different study, the histone deacetylase SIRT6 was shown to modulate melanoma chemosensitivity to MAPKi via the regulation of IGF-binding protein 2 (IGDFB2) (Ming et al, 2014) (**Figure 4**).

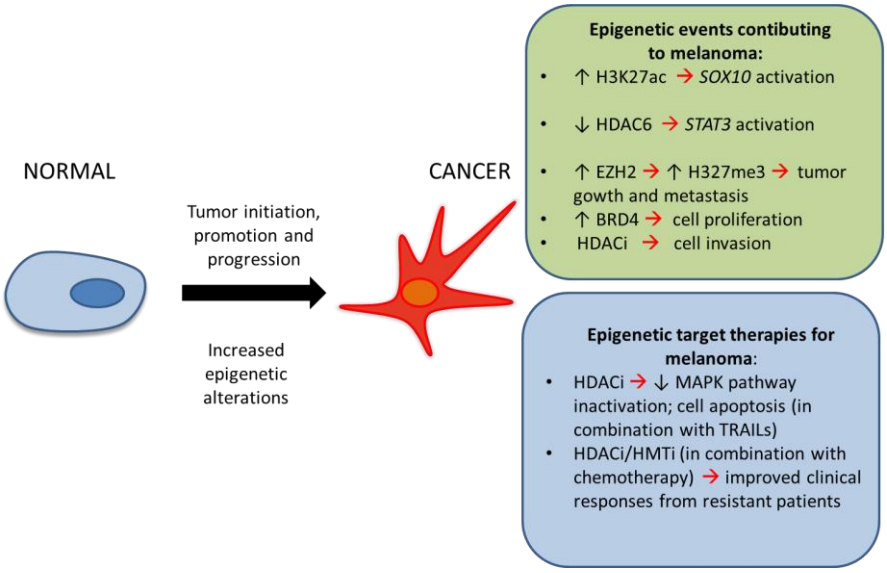

Figure 4: Epigenetic mechanisms in melanoma.Melanoma cell malignant transformation is determined by the presence and accumulation of chromatin modifications. Several studies have reported that the development of melanoma-specific properties is triggered by epigenetic events and that, moreover, targeting epigenetic regulators might represent a promising therapeutic strategy for melanoma treatment.

1.3 SETDB1

SETDB1 encodes for a protein of 1307 amino acids termed as SET-domain protein, bifurcated 1 (SETDB1; ESET; KMT1E), belonging to the SET-domain containing protein superfamily.

1.3.1 SET-domain protein superfamily

The SET (acronym of Su(var)3-9, Enhancer-of-zeste and Trithorax) domain is a protein structure of 130 amino acids initially identified in several Drosophila species (Tschiersch et al, 1994). A large number of human proteins are characterized by the presence of an active SET domain, such as members of the SUV39 family (SUV39H, G9a, SETDB1 and SETDB2), SET 1 family (MLL1, MLL2, MLL4), SET 2 family (NSD2, NSD3), RIZ family (PRDM1, PRDM2), SMYD family (SMYD1, SMYD 3), EZ family (EZH1, EZH2), SUV 4-20 family (SUV 4-20H1, SUV 4-20H2) and SET7/9 and SET 8 proteins (Dillon et al, 2005). Almost all the identified SET-domain proteins function as lysine methyltransferases (KMTs). Crystallographic studies on SET-domain containing proteins showed that the SET domain is generally assembled in a well-conserved multi-motif structure located at the C-terminus, enclosed by the pre-SET and post-SET domains. The pre-SET domain is particularly rich in cysteine residues conjugated with zinc ions, required for protein scaffolding. The post-SET domain contains three conserved cysteines which play a crucial role during HMT activity by physically interacting with the terminal tails of the histone and by supporting the binding of the cofactor SAM. The specificity of a HMT for a particular histone is guaranteed by invariant residues present in SET domain sequence (Rea et al, 2000).

1.3.2 SETDB1 gene mapping and expression

The SETDB1 coding sequence is highly conserved among different species. The human *SETDB1* gene is located on chromosome 1 (cytogenetic band: 1q21.3, plus-strand orientation) and comprises about 37 kilobases with 23 exons. Three different isoforms are known for SETDB1: the first transcript variant encodes for the full-length protein,

constituted of 1291 amino acids, while the other alterative splicing isoforms produce truncated forms of SETDB1. The *SETDB1* promoter contains binding sites for TFs, such as GATA-1, NFY, ATF6, Cdc5, Lmo2 and Sp1. SETDB1 is ubiquitously expressed in human organs and tissue under normal conditions (Human Protein Atlas).

1.3.3 SETDB1 protein structure and localization

In addition to SET, pre-SET and post-SET domains, SETDB1 also possesses a methyl-CpG-binding domain (MBD), involved in DNA binding and protein-protein interaction processes (Bird, 2001), and three tudor domains (**Figure 5**). Recently, it has been shown that tudor domains have the capacity to read and bind methylated and acetylated residues on histone tails, and in that way contribute to the epigenetic functionality of SETDB1 (Jurkowska et al, 2017). Despite SETDB1's HMT and DNA-binding activities SETDB1 is thought to also have a function in the nucleus. Recent studies showed that SETDB1 is mostly enriched in the cytoplasm and that nucleo-cytoplasmatic shuttling may represent a relevant aspect of the role of SETDB1 in human cells (Tachibana et al, 2015). In the nucleus, SETDB1 is often found embedded in promyelocytic leukemia nuclear bodies (PML-NBs), large nuclear structures involved in transcriptional regulation, control of genomic stability and response to DNA damage (Bernardi & Pandolfi, 2003).

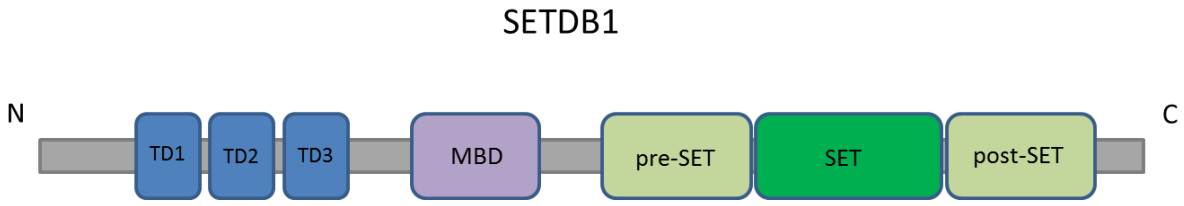

Figure 5: SETDB1 protein structure.SETDB1 protein is 1307 amino acids in length and is organized in multiple functional domains, including 3 tudor domains (TD) located at the N terminus, a central methyl-CpG-binding domain (MBD), while the C terminus exhibits the pre-SET, SET and post-SET motifs.

1.3.4 SETDB1 functions and interactions

The main role of SETDB1 is to trimethylate histone H3 at lysine 9 (H3K9me3) (Schultz et al, 2002), an epigenetic mark generally associated with gene repression (Yang et al, 2002). In the presence of SAM, SETDB1 targets the terminal tails of histones H3 present

in euchromatin regions and catalyses H3K9 trimethylation. SETDB1-mediated transition from euchromatin to heterochromatin occurs when the heterochromatin protein 1 alpha (HP1α) recognizes and binds the trimethylated K9 at histone H3 via its chromodomain. HP1α then recruits KRAB-associated protein-1 (KAP1; Trim28) which, in turn, interacts with the repressor factor KRAB (Sripathy et al, 2006). The SETDB1-HP1α-KAP1-KRAB axis is one of the established SETDB1-centered repressive mechanisms, which include interactions of SETDB1 with several proteins, such as HDAC1/2 in the presence of mSin3A/3B corepressors (Yang et al, 2003), MBD1 assembled with MCAF cofactor (Hammond et al, 2006), ATF7IP (Basavapathruni et al, 2016), Argonaute protein 2 (AGO2) (Cho et al, 2014), DNMT3A (Li et al, 2006) and PML (Kang, 2015). SETDB1 protein interactions sustain the catalytic activity and substrate specificity of SETDB1. Transcriptional silencing occurs via direct promoter binding or through the incorporation into transcriptional repressor complexes.

SETDB1 is involved in various physiological processes during mammalian embryonic development. Several studies indicate an involvement of SETDB1 in X-chromosome inactivation (Minkovsky et al, 2014). Oscillatory SETDB1 gene expression is observed during the early developmental stages of mouse embryos (Cho et al, 2012). Moreover, SETDB1 controls the expression of mesendoderm and ectoderm lineage-specific genes in mouse embryonic stem cells (Yuan et al, 2009b).

1.3.5 SETDB1 in cancer

SETDB1 plays an oncogenic role in a wide range of malignancies, in which it is aberrantly expressed and/or mutated (**Figure 6**).

In breast cancer, SETDB1 is recurrently amplified and overexpressed. Mechanistically, Regina et al. observed that SETDB1 binds delta Np63 (ΔNp63), an oncogenic isoform of p63. SETDB1 sustains ΔNp63 activity during breast tumorigenesis (Regina et al, 2016). Another study showed that SETDB1 expression in mouse xenograft models is impaired by miR-7, inducing tumor regression and anti-metastatic effects (Fang et al, 2012). High levels of SETDB1 were also detected in colorectal cancer (CRC) cell lines a large group

of tissue samples derived from patients with CRC, correlating with the worst clinical outcome. SETDB1 dysregulation impacts the proliferation rate of CRC cells and thereby the tumor growth. Moreover, SETDB1 expression co-occurs with transcriptional silencing of p53 at the promoter level (Olcina et al, 2016); a similar SETDB1-mediated regulatory mechanisms affecting the expression of TP53 was also shown in liver (Fei et al, 2015) and non-small cell lung (NSCL) (Sun et al, 2015) cancer cells, resulting in enhanced tumor growth. In NSCL cells, SETDB1 stimulates the WNT/β-catenin signalling pathway (Sun et al, 2015). A promoting effect of SETDB1 on the invasive potential is observed in prostate (Saraon et al, 2013), as well as in lung cancer, where the *SETDB1* gene is amplified (Rodriguez-Paredes et al, 2014). In contrast to these findings, recent works indicate anti-metastatic roles for SETDB1 in lung cancer. Functionally, SETDB1 inhibits the expression of ANXA2 (via TGFβ-SMAD2/3 signalling) (Wu et al, 2014) and FosB (mediated by ERK2 activation) (Na et al, 2016) factors involved in metastasis formation and cell survival, respectively. SETDB1 inhibits interferon γ response-mediated apoptosis in AML cells by blocking the transcription of endogenous retroviruses (ERVs) (Cuellar et al, 2017).

The role of SETDB1 in melanoma has been studied by Ceol et al. in a zebrafish melanoma model, who observed a recurrent amplification of the 1q21 genomic region, corresponding to the *SETDB1* locus. Additional *SETDB1* copies correlate to SETDB1 expression and enhance tumor growth and aggressiveness in zebrafish, especially if the $BRAF^{V600E}$ mutation is also present (Ceol et al, 2011). At the transcriptomic level, SETDB1 overexpression induces the repression of *Hox* genes that are involved in developmental processes (Taniguchi, 2014). The critical role of SETDB1 in melanoma was further confirmed in a more recent study showing high levels of SETDB1 in patients with metastatic melanoma (Miura et al, 2014). On the other hand, Shi et al. observed that SETDB1-silencing impairs the invasiveness and metastatic potential of human melanoma cells *in vivo* (Shi et al, 2017).

In our laboratory, the contribution of SETDB1 to melanoma pathogenesis was further elucidated. The *SETDB1* gene was found highly amplified and overexpressed in tissue samples from primary melanomas and melanoma metastases. The deregulation of

SETDB1 expression in melanoma cell lines had drastic effects on melanoma proliferation, migration, invasion and *in vivo* tumor growth. Pharmacological silencing of SETDB1 with the small molecule inhibitor CAS 935693-62-2 strongly impacted melanoma cell viability (unpublished data; (Orouji, 2016)).

Although the current knowledge about SETDB1 strongly supports its role as an oncogene in several cancer types including melanoma, little is still known about the underlying mechanisms of action.

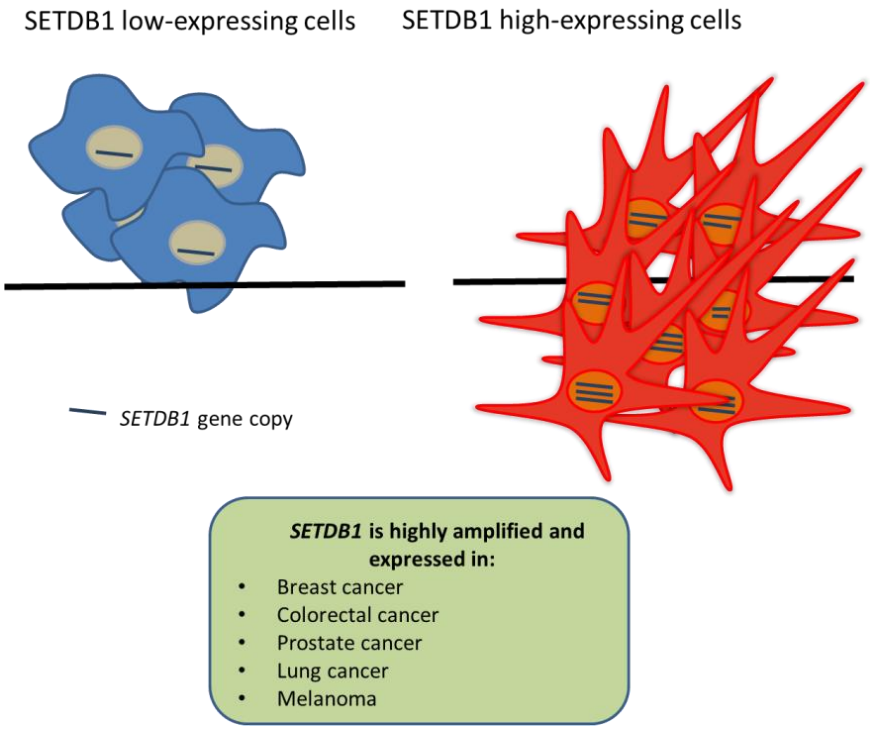

Figure 6: SETDB1 involvement in cancer.A variegated group of cancer types is characterized by high *SETDB1* amplification and expression levels. Based on these parameters, tumor cells show different properties: SETDB1 overexpression is generally associated with increased tumor proliferation, migration and invasion.

2 Aim of the thesis

Different studies and previous work conducted in our laboratory highlighted the involvement of the histone methyltransferase SETDB1 in melanoma progression. This project intended to extensively characterize SETDB1 features and functions which determine its oncogenic potential.

This study firstly aimed at gaining insights into the mechanisms by which SETDB1 mediates its pro-tumorigenic effects. For this reason, transcriptomic, molecular and cellular alterations following SETDB1 gain or loss should be investigated.

Secondly, in this study I wanted to examine the SETDB1-induced epigenetic alterations associated with malignant transformation of melanoma cells.

Lastly, drug-response experiments were performed to investigate whether SETDB1 inhibition might affect the viability of cancer cells and therefore representing a promising therapeutic approach.

3 Materials and Methods

3.1 Materials

3.1.1 Reagents and Kits

Product	Company	Catalog No.
Adhesive Clear qPCR seals	Biozyme	600238
Agarose NEEO Ultra Qualität	Carl Roth	2267,4
Alamar Blue®	Invitrogen	DAL1100
Ampicillin	Carl Roth	HP62.1
BioCoat™ Tumor Cell Invasion Systems	Corning	354165
BSA-Powder, Albumin Fraction V	Carl Roth	8076.2
Complete Mini Protease Inhibitor Cocktail	Roche Diagnostics	4693159001
DAPI	Roche	10236276001
DH5α Competent Cells	Thermo Fisher Scientific	18265017
EcoRI (10 U/L)	Thermo Fisher Scientific	ER0271
EcoRV (10 U/µL)	Thermo Fisher Scientific	ER0301
Endofree Plasmid Maxi Kit	Qiagen	12362
EZ-ChIP™	Merck Millipore	17-371
Fluorescence Mounting Medium	Dako	S3023
High Performance Chemiluminescence Film	GE healthcare	28906836
HumanHT-12 v4 Expression BeadChip Kit	Illumina	BD-103-0204
Immobilon PVDF membrane, 0.45µM	Merck Millipore	IPVH00010
Luminata Forte Western HRP Substrate	Merck Millipore	WBLUF0500
MicroAmp Optical 96well Plate qPCR	Thermo Fisher Scientific	N8010560
microtube afa fiber snap-cap	Covaris	520045

Midori Green Advance	Nippon Genetics	mg-04
NEB Next Ultra DNA Library kit	New England Biolabs	E7370S
NEBNext® Multiplex Oligos for Illumina® (Index Primers Set 1)	New England Biolabs	E7335S
NuPAGE™ Novex™ 4-12% Bis-Tris Protein Gels	Thermo Fisher Scientific	NP0335BOX
NuPAGE™ LDS Sample Buffer (4X)	Thermo Fisher Scientific	NP0008
NuPAGE™ Reducing Agent (10X)	Thermo Fisher Scientific	NP0004
O'GeneRuler 1 kb DNA Ladder	Thermo Fisher Scientific	SM1163
O'GeneRuler 100bp DNA-Ladder	Thermo Fisher Scientific	SM1143
PageRuler Plus Prestained Protein Ladder	Life Technologies	26619
Paraformaldehyd	Sigma Aldrich	P6148-1KG
Pierce BCA Protein Assay Kit	Thermo Fisher Scientific	23225
Platinum Taq Polymerase	Thermo Fisher Scientific	10966034
Proteome Profiler Human Angiogenesis Array Kit	R&D Systems	ARY007
Qiaprep Spin Miniprep Kit	Qiagen	27106
RevertAid First strand cDNA Synthesis Kit	Thermo Fisher Scientific	K1622
Rnase-Free Dnase Set	Qiagen	79254
RNeasy Plus Mini Kit	Qiagen	74136
Rotilabo®-syringe filters, 0,22 µm	Carl Roth	KH54.1
Rotilabo®-syringe filters, 0,45 µm	Carl Roth	P667.1
Skim milk powder	Gerbu Biotechnik	16021000
Sodium hydroxide	Carl Roth	6771.1
SYBR Green PCR Master Mix	Applied Biosystems	4309155
TEMED	Carl Roth	2367,3
TritonX-100	Carl Roth	3051,4
Tween® 20	Applichem	A13890500

Venor Gem Classic Myco PCR Kit	Minerva Biolabs	11-1100
XhoI (10 U/L)	Thermo Fisher Scientific	ER0691
X-treme GENE® 9 DNA Transfection Reagent	Roche Diagnostics	6365787001

3.1.2 Reagents for cell culture

Product	Company	Catalog No.
2-Mercaptoethanol	Gibco®Life Technologies	31350010
Blasticidine	Sigma Aldrich	15205
Calcein AM Fluorescent Dye	Corning	354217
DMSO	Carl Roth	A994.2
Fetal Calf Serum (FCS)	Biochrom	S0115
Non-essential amino acids	Sigma-Aldrich	M7145
PBS	Sigma-Aldrich	D8537
Penicillin/Streptomycin	Sigma-Aldrich	P4333
Polybrene Infection / Transfection Reagent	Sigma Aldrich	TR-1003-G
Puromycin	Carl Roth	240,1
Trypan blue solution	Sigma-Aldrich	93595
Trypsin -EDTA solution	Sigma-Aldrich	T3924

3.1.3 Human cell lines

Cell Line	Source	Cell type	Mutation
A375	ATCC	Melanoma cell line	BRAF V600E
HT144	ATCC	Melanoma cell line	BRAF V600E
SK Mel 28	ATCC	Melanoma cell line	BRAF V600E
C32	ATCC	Melanoma cell line	BRAF V600E
HEK293T	ATCC	embryonic kidney cells	WT

3.1.4 Antibodies

Specificity	Source	Company	Catalog No.
SETDB1	Mouse	Biorad	VMA00243 KT
THBS1	Mouse	Thermo Fisher	MA5-13398

		Scientific	
DCT	Mouse	Santa Cruz Biotechnology	sc-74439
β-Actin	Rabbit	Cell signalling	5125S
Anti-rabbit IgG, HRP-linked	Goat	Cell signalling	7074S
H3K9me3	Rabbit	Abcam	ab8898
α-actinin	Mouse	Santa Cruz	sc-17829
Goat Anti-Rabbit IgG H&L Alexa Fluor® 488	rabbit	Abcam	ab150077
H3K4me1	rabbit	Abcam	ab8895
Anti-mouse IgG, HRP-linked	Horse	Cell signalling	7076

3.1.5 Inhibitor drugs

Product	Company	Catalog No.
Aphidicolin	Sigma Aldrich	A0781-1MG
Mithramycin A	Bio Trend	10-2085-5mg
Trametinib (GSK1120212)	Selleckchem	S2673
Vemurafenib (PLX4032)	Selleckchem	S1267

3.1.6 Plasmids

Name	Source
non-targeting shRNA	Addgene #1864
pCMV-dR8.91 (Packaging)	Konrad Hochedlinger (Harvard, Bosten, USA)
pCMV-VSV-G (Packaging)	Addgene #8454
pLEX980-empty vector	derived from pLEX980-SETDB1
pLEX980-SETDB1	obtained from Craig Ceol (Children's Hospital Boston, USA)
pLEX-980-SETDB1 1224K 1226A	derived from pLEX980-SETDB1 by site-mutagenesis
SETDB1 shRNA	TRCN0000147130
THBS1 shRNA	TRCN0000226403
TRP2-pLenti	derived from Addgene #17448

3.1.7 Primers

Amplification target	Forward Sequence	Reverse Sequence
h18S_qPCR	GAGGATGAGGTGGAACGTGT	TCTTCAGTCGCTCCAGGTCT
hSETDB1_qPCR	CATCCAGGGCAGTGACTAATTG	CGGAGCTTCTGGTCTTTTGG
hTHBS1_qPCR	GCCATCCGCACTAACTACATT	TCCGTTGTGATAGCATAGGGG
hDCT_qPCR	CCACAGTTCTGACGCTGACA	ACAAGCAAGCAAAGCGGAAA
hSCG2_qPCR	CCAGGTCACTGGGGAGTCTGCT	TGAGCATCAACAATGCCA
hTYRP1_qPCR	AAACTTTGGAGAGGGAAAATCT	CACAGGCAATATCCATTGTTG
hAPOE_qPCR	GTTGCTGGTCACATTCCTGG	GCAGGTAATCCCAAAAGCGAC
hALDOC_qPCR	GCCAAATTGGGGTGGAAAACA	TTCACACGGTCATCAGCACTG
hIL6_qPCR	ACAACCACGGCCTTCCCTACTT	CACGATTTCCCAGAGAACATGTG
hCCL2_qPCR	CCTTCATTCCCCAAGGGCTC	GGTTTGCTTGTCCAGGTGGT
hMMP3_qPCR	CGGTTCCGCCTGTCTCAAG	CGCCAAAAGTGCCTGTCTT
HC/KA-SETDB1 mutagenesis	GGCCGCTACCTCAACAAGAGTTGCAGCCCCAAC	TTGGGGCTGCAACTCTTGTTGAGGTAGCGGCC
hTHBS1 promoter_ChIP qPCR	GGAAGGGCTTTGTGTTTGA	CCTATACGGTGGCAGGAAAG
hGAPDH promoter_ChIP qPCR	TACTAGCGGTTTTACGGGCG-	TCGAACAGGAGGAGCAGAGAGCGA

3.1.8 Solutions and Buffers

Transfer buffer (pH 8.3) 25mM Glycine 190mM Tris 20% SDS 20% Methanol dH_2O	**Running buffer (pH8.3)** 25mM Glycine 190mM Tris 0.1% SDS dH2O
TBS 10X (pH 7.6) 150mM NaCl 50mM Tris dH_2O	**Washing buffer (TBST)** 0.02% Tween® 20 1X TBS
Blocking buffer (milk) 5% Skim milk powder 1x TBS	**Blocking buffer (BSA)** 5% BSA 1x TBS

RIPA buffer 4M NaCl 1% IGEPAL (Sigma-Aldrich) 10% Sodim dehocycholate 10% SDS 1M Tris, pH 8 dH2O	**TEB buffer** 0.5% Triton X 100 2mM phenylmethylsulfonyl fluoride 0.02% Sodium Azide dH_2O
SOC Outgrowth Medium New England BioLabs (B9020S)	**LB Medium** 20g LB-Medium (Carl Roth, X964.2) 1l H_2O
Cell freezing medium 80% FCS 20% DMSO	

3.1.9 Devices

Product	Company
12 Well Multiwell Plates	Grenier Bio-One
2100 Bioanalyzer Instrument	Agilent
6 Well Multiwell Plates	Grenier Bio-One
8-well Culture Slide	Falcon
AB 7500 Real-Time PCR Machine	Applied Biosytems
CELLSTAR® Cell Culture Flasks	Grenier Bio-One
ChemiDoc™ Touch Imaging System	Bio-Rad
Haemocytometry	Neubauer
Hi-Seq 2000 system	Ilumina
Leica DM LS light microscope	Leica
MicroAmp Optical 96well Plate qPCR	Thermo Fisher Scientific
Microplates 24-well	Falcon
Microplates 96-well	Falcon
Nanodrop Spectophotometer ND-1000	Peqlab Biotechnologie GmbH
Nikon Eclipse Ti Fluorescence Microscope	Nikon
Nunc™ Cell Culture Cryogenic Tubes	Thermo Fisher Scientific
S220 focused ultrasonicator	Covaris
Tecan Infinite F200 PRO	Tecan
Veriti™ 96-Well Thermal Cycler	Thermo Fisher Scientific

3.1.10 Software tools

Software name	Source
7500 Software v2.0.5	Applied Biosystems
Chipster	Chipster Open source
DAVID tool	https://david.ncifcrf.gov/
Galaxy software	https://usegalaxy.org
GraphPad PRISM	GraphPad software
HLImage++	Western Vision
Image J	NIH
Image Lab 6.0.1	Bio-Rad
Ingenuity® Pathway Analysis (IPA®)	QIAGEN Bioinformatics
Integrative Gene Viewer	Broad Institute
javaGSEA	Broad Institute
NDP. view 2	Hamamatsu Photonics
NIS-Element	Nikon
Primer-BLAST	https://www.ncbi.nlm.nih.gov/tools/primer-blast/
TScratch	CSElab

3.2 Methods

3.2.1 Cell culture

Human melanoma cells, normal human melanocytes (NHM) and dermal fibroblasts isolated from healthy patient's foreskin were cultured in MEF medium, composed by Dulbecco's Modified Eagle medium (DMEM; Gibco, Life Technologies),10% heat-inactivated FCS (Biochrom), 0.1 mM β-mercaptoethanol (Gibco, Life Technologies), 1% non-essential amino acids (NEAA; Sigma-Aldrich) and 1% penicillin/streptomycin (Sigma-Aldrich), and stably kept at 37°C and 5% $C0_2$ in a humidified incubator. Experiments were conducted when the cells reached subclonfluency (around 80% confluence). Briefly, cells were washed with PBS (Sigma-Aldrich) to remove dead cells and debris, followed by trypsinization with trypsin-EDTA solution (Sigma-Aldrich). Once dissociated, viable cells stained with trypan blue solution (Sigma-Aldrich) were counted with a hemocytometer counting chamber and subsequently seeded at defined densities, according to the planned experiments. For long term storage cells were frozen by suspending them in freezing medium and keeping them at -80°C or in liquid nitrogen. Once thawed, cell lines were sub-cultured at least once before every experiment to allow them to recover after the freeze-thaw cycle. Identity of melanoma cells used for this study was authenticated by cell line authentication test (Multiplexion). Cells were routinely tested for mycoplasma contamination with the Venor®GeM Classic Mycoplasma detection kit (Minerva Biolabs).

3.2.2 RNA isolation

Total RNA from cultured cells was isolated using RNeasy Mini Kit (Qiagen), following manufacturer's instructions. To avoid genomic DNA contaminations, RNA samples were incubated with RNase-Free DNase (Qiagen) for 15 min at RT. RNA concentration and quality were evaluated with a NanoDrop ND1000 spectrophotometer.

3.2.3 cDNA synthesis and quantitative PCR

cDNA was generated by reverse transcription of 500 ng of total RNA using the Revert Aid First Strand cDNA synthesis kit (Thermo scientific) according to the manufacturer's protocol. cDNA was then diluted 1:10 in nuclease-free water before quantitative PCR experiments. Gene expression was assessed by real time (quantitative) PCR reaction. Briefly, cDNA was mixed with SYBR Green Master Mix (Applied Biosystems, Life technologies) and with specific primers able to amplify a defined mRNA. Primers were designed using PrimerBlast or obtained from a Primer Bank database (Spandidos et al, 2008); primer efficiency was calculated by amplification of the target from serial fold dilutions. The full list of used primers is provided in section 3.1.7. Each PCR reaction was run in triplicates on 7500 Real-Time PCR System device (Applied Biosystems, Life Technologies) and the results analysed following the delta-delta Ct value method. 18s ribosomal RNA expression was used as endogenous control for all the experiments.

3.2.4 Microarray data analysis

Whole genome expression profiles from cells were obtained by using BeadChip HumanHT-12 v4 technologies (Illumina). RNA quality control, labelling and probe hybridization for sequencing were performed by the Genomics and Proteomics Core Facility at DKFZ. Raw expression data for each cell type and/or condition was quartile normalized and, by comparing two groups (each of them composed by at least two biological replicates), a Bayes statistical test was applied to obtain a set of differentially expressed genes, based on their fold change (FC, expressed as log2 of expression values). In order to predict any correlation between transcriptomic profiles and phenotypic states, gene expression data were further analysed by using gene set enrichment analysis (GSEA) (Subramanian et al, 2005) and Ingenuity Pathway analysis (IPA) tools.

3.2.5 Protein extraction and Western blot

Whole-cell lysate from cultured cells was obtained as follow: first, harvested cells were washed once in PBS and then resuspended in 100 µl RIPA buffer and vigorously

vortexed. Cells were lysed on ice for 30 min and then centrifuged at 15000 rpm, 20 min 4°C. Supernatant containing protein lysate was finally collected and stored at -20°C. In order to isolate histone proteins, cell pellets were washed twice with PBS and then lysed by adding TEB buffer. After 10 min incubation on ice, cells were centrifuged at 10000 rpm 10' 4°C and the supernatant was discarded. Pellet was again resuspended in TEB and centrifuged as above. Histone-enriched protein lysates were then precipitated by adding 0.2M HCl solution, followed by an overnight incubation at 4°C. Samples were centrifuged ad 10000 rpm at 4°C 10 min and supernatant collected, neutralized with 1/10 2M NaOH and stored at -20 °C. All the lysates' protein concentrations were assessed with the Pierce BCA Protein Assay Kit (Thermo Fisher Scientific), following the manufacturer's instructions. Depending on the cell type and the predetermined immunoblotting, around 15-50 µg of whole cell lysates or 10-20 µg histones-enriched protein samples were loaded and run on NuPAGETM NovexTM 4-12% Bis-Tris Protein gels (Thermo Fisher Scientific). Proteins were then transferred onto PVDF membranes (Merck Millipore). Membranes were first incubated 1h at RT with a blocking solution to avoid any unspecific antibody-protein binding, and then probed with specific antibodies, diluted in the same blocking buffer, during the overnight incubation at 4°C on a shaker. The following day, membranes were washed three times in 1X TBST buffer to remove the excess of primary antibody and then incubated with HRP-conjugated secondary antibodies for 1h at 4°C. After three additional washing steps, membranes were shortly exposed to Luminata Forte western HRP substrate (Merck Millipore) before developing. Acquired images were then analysed by ImageJ software (NIH). The full list of primary and secondary antibodies used in this study is described in section 3.1.4.

3.2.6 ELISA Proteome Profiler

Cells were seeded and cultured until they reached around 80% confluence. Then, cell supernatant was collected and tested with the Proteome Profiler Human Angiogenesis array kit (R&D System), following the manufacturer's instructions. Protein signals were quantified by HLImage++ image analysis software (Western Vision).

3.2.7 Mice xenografts

In vivo experiments were conducted in the animal facility of German Cancer Research Center, in accordance with national guidelines and regulations. 1-2x10^6 melanoma cells were subcutaneously injected in NOD-SCID mice. Vital parameters of the mice and tumor growth were routinely monitored and mice were sacrificed once the tumor reached the size of 1,5 cm. Tumors were excised, fixed in 4% paraformaldehyde (PFA) and finally embedded in paraffin sections for further investigations.

3.2.8 Immunohistochemistry and Tissue Microarray (TMA)

Paraffin embedded tissues were stained with antibodies specific against SETDB1 and THBS1. Images were acquired with Nikon NIS Element software.

Human tissue samples derived from healthy donors or patients with melanoma were assembled in TMA samples. TMA sample preparation was previously described (Wagner et al, 2015). Following immunostaining, TMAs were scanned by the NCT-Gewebebank facility at the pathology unit, University of Heidelberg. Informed consent was obtained from each patient included in this study, which was performed in accordance to the ethical vote 2010-318N-MA (ethics committee II of Heidelberg University).

3.2.9 Bacterial transformation and isolation of expression vectors

pLEX980-SETDB1 vector was kindly provided by Dr. Craig Ceol. pLEX980-empty vector control was generated by cutting the SETDB1-coding sequence from pLEX980-SETDB1. pLEX-980-SETDB1 1224K 1226A plasmid was produced by performing site-directed mutagenesis. SETDB1 ORF was amplified with specific primers that introduced point mutations to the SETDB1 ORF. Mutated SETDB1 ORF was then introduced into pLEX980. SETDB1 and THBS1 gene knockdown was performed by using shRNA against SETDB1 (TRCN0000147130) and THBS1 (TRCN0000226403) (RNAi Consortium shRNA library, Broad Institute; Sigma-Aldrich), while a non-targeting shRNA (Addgene, No. 1864) was used as control. Constitutive GFP and constitutive TOMATO plasmids were used for 2D invasion assay. The TRP2-pLenti reporter construct used in

this study contains the ORF of GFP under the control of the DCT (TRP2) promoter. In order to obtain amplified plasmid DNA, competent E. coli bacteria were transformed. Briefly, competent bacterial cells (DH5α, Sigma-Aldrich) from E.coli were first thawed on ice and then mixed with up to 100 ng of plasmid DNA and incubated for 40 min on ice. Next, bacteria were subjected to heat-shock for 3 min at 42°C followed by 1 min cool down on ice. Next, LB medium was added to the bacteria-DNA mixture, followed by 1h incubation at 37°C and constant shaking. Finally, the bacteria were plated on agar plates containing antibiotic (100 µg/mL ampicillin), so that transformed cells could be selected, and incubated overnight at 37°C. Growing colonies on agar plates were randomly picked and allowed to grow in LB medium containing ampicillin. To validate the correct vector sequence, plasmid DNA was isolated with Qiaprep Spin Miniprep Kit (Qiagen), following the manufacturer's instructions, and analysed by restriction enzyme digestion and gel electrophoresis. High quantity of pure plasmid DNA was purified with Endofree Plasmid Maxi Kit (Qiagen) and eluted in nuclease-free water. DNA plasmid sequence was finally confirmed by DNA sequencing (LGC Genomics).

3.2.10 Generation of lentiviral vectors and cell transduction

Lentiviruses containing genes of interest were produced in human HEK293T cells. Shortly, 11 µg of each expression construct were mixed with 8.25 µg of pCMV-dR8.91 and 5.5 µg of pCMV-VSV-G lentiviral packaging constructs and with 50 µl of X-tremeGENE™ 9 DNA transfection reagent (Sigma-Aldrich). This mixture was added to subconfluent HEK293T cells after 30 min incubations. Cell medium was discarded after 12h, and collected after 24, 36 and 48h. Cell supernatant containing lentivirus was filtered through a 0.45 µm PVDF filter (Carl Roth) and either immediately used for cell transduction or aliquoted and stored at -80°C. The day before lentiviral infection (day 0), cells were seeded in 6-well plates. On day 1, cell medium was aspired and transduction medium, composed of 25% MEF medium and 75% lentivirus supernatant, was added to each well. Furthermore, 2-8 µg/mL polybrene (Sigma-Aldrich) were added to increase the transduction efficiency. At day 2, cells were re-infected with fresh transduction medium without polybrene. At day 4, cells were washed twice with PBS solution and

then exposed to culture medium supplemented with antibiotic (1-3 µg/mL Puromycin, Carl Roth; or 10-15 µg/mL Blasticidin, Sigma-Aldrich), accordingly with the used lentivirus. Cells were selected for about 3-5 d or until the un-transduced cells, exposed to the same selection antibiotic, completely died. Lentivirus production, collection, storage and cell infection procedures were all performed in a biosafety level II ("S2") laboratory, according to the safety instructions.

3.2.11 Cell proliferation and viability assay

For proliferation assay, cells were seeded in 96-well plates at a density of 2.5-5x10^3 cells/well, depending on the cell type and on the defined end-points of the experiments. 24h after seeding, 10% of alamarBlue reagent (Invitrogen) was added to each well and after 4h incubation, fluorescence at the excitation wavelength of 560 nm and emission of 590 nm was measured with a Tecan Infinite 200 spectrophotometer. To determine the cell proliferation rate, the same process was repeated every day until the 96h end-point.

Cell viability upon drug treatment was assessed with a similar procedure. Again, cells were seeded in 96-well plates; the following day, cells were exposed to defined drugs (vemurafenib, Selleckchem; trametinib, Selleckchem; mithramycin A, Biotrend) alone or in combination treatments, at different concentrations, depending on cell type and exposure time. DMSO (Carl Roth) was used as control at 0.1% final concentration. 24 or 48h after incubation, alamarBlue was added to cultured medium and fluorescence was detected.

3.2.12 Migration assay

Cells were trypsinized and then counted. 3.5x10^4 cells were seeded in both fields of culture-insert 2 well (Ibidi). The following day, inserts were removed to allow the cells to migrate towards the gap. 1 µg/mL aphidicolin (Sigma-Aldrich), a cell proliferation inhibitor, was added to the culture medium to avoid that gap closure speed was biased by cell proliferation. Cell migration was monitored at defined time points, until the gap

was fully closed, and images acquired with Nikon Eclipse Ti TIRF microscope and NIS-Elements software. Migration rate was analysed with TScratch software (CSElab).

3.2.13 Invasion assay

Cell invasion was assessed with the Tumor Invasion System (Corning), following the manufacturer's guidelines, with some modifications: cells were diluted to $5x10^4$ cells/mL in 0.5% FCS-MEF medium and 500 µl of cell suspension was seeded in each top chamber. 20%FCS-MEF medium was added to the lower chamber to stimulate cell invasion. After 24h, invading cells were stained with 4 µg/mL calcein AM (Corning) in PBS solution for 1h. Then, images were acquired and fluorescence read. Cell invasive rate was quantified as relative fluorescence units (RFUs).

Tumor cell invasive properties were also evaluated by establishing a 2D invasion system. Culture 2 well inserts were filled with about $3x10^4$ melanoma cells on one side and $3x10^4$ fibroblasts on the other. The following day, inserts were removed to allow the two cell types (both labelled with a different fluorochrome) to interact. Once the gap was fully closed, cells were exposed to inhibitor treatment. Images were acquired before and after treatment to define the amount of tumor cells which invaded the fibroblast layer under different conditions.

3.2.14 Chromatin Immunoprecipitation (ChIP) and ChIP sequencing

Chromatin immunoprecipitation was performed with the EZ ChIP kit (Merck Millipore), following the manufacturer's protocol. Briefly, $1\text{-}2x10^6$ cells were crosslinked with 3.6% formaldehyde for each chromatin immunoprecipitation, and then lysed on ice. Chromatin was sonicated using the Covaris S220 focused ultrasonicator and the so obtained sheared DNA was incubated overnight at 4°C with agarose bead-coupled antibodies. Next, immunoprecipitated chromatin was repeatedly washed and the crosslinks were released. DNA fragments were purified and amplified by quantitative PCR. Results were analysed by using the "% input" method.

For ChIP-seq experiments, about 10 ng of ChIP DNA fragments were used for library preparation by using NEB Next Ultra DNA Library kit (New England Biolabs) according to the manufacturer's instructions. DKFZ Genomics and Proteomics Core Facility performed the library sequencing by using the Illumina Hiseq 2000 system, in 50-bp single-end mode.

Sequence reads were aligned against the human reference genome (hg19), using the Bowtie mapping tool, allowing one mismatch and only unique reads in the analysis. Peak calling was conducted using MACS2 with a q-value cut-off of 0.05. Identification of differential binding sites was performed with Bedtools and Galaxy. Input-subtracted, whole-genome coverage tracks of aligned reads were generated and then visualized on Integrative Gene Viewer (IGV).

3.2.15 Immunofluorescence

$3x10^4$ cells were seeded in 8-chamber culture slides (Falcon). Once they reached subconfluency, cells were fixed in 4% PFA for 5 min on ice and additional 10 min at RT. Next, cells were washed with ice-cold PBA and permeabilized with 0.1 % Triton X-100 (Carl Roth) for 10 min. To avoid unspecific signals, cells were pre-incubated with IF blocking solution before primary antibody incubation, overnight at 4°C. The following day, cells were washed and incubated with fluorescent dye-conjugated secondary antibodies for 2h at RT in the dark. Next, cells were stained with DAPI (Roche) and washed. Slide mounting was performed with fluorescence mounting medium (Dako). Images were acquired with a Nikon Eclipse Ti TIRF microscope using NIS-Elements software.

3.2.16 Statistical analysis

Experiments were run in triplicates, unless otherwise stated. Statistical analysis, performed using Prism 5.0 software (Graphpad), included the two-tailed Student's t test to compare two conditions, one-way ANOVA to compare multiple conditions and data sets, spearman correlation to define the association of two parameters and Kaplan-

Meier method for survival analysis. Data are represented as mean ± SEM and statistical significance is indicated with the p-value scale ("*" refers to a p- value <0.05; "**" for p-value <0.01; "***" for p-value <0.001; "ns" refers to a p-value >0.5).

4 Results

4.1 Gene expression analysis reveals putative downstream targets of SETDB1

SETDB1 is a histone methyltransferase which modulates the trymethilation of lysine residue present on the N-terminal tail of histone H3. It has been reported that SETDB1 is widely expressed and contribute to the development of several cancer type, including melanoma. Previous work from our group demonstrated that SETDB1 was heterogeneously expressed in melanoma (Orouji, 2016). SETDB1 expression was assessed in a panel of human melanoma cell lines and they were categorized based on SETDB1 mRNA and protein levels as SETDB1 high- or low-expressing cells. In order to study the role of SETDB1 in melanoma, ectopic expression of SETDB1 was induced in low-expressing melanoma cells (HT144 and C32), by lentiviral transduction with a SETDB1-expressing construct (pLEX980-SETDB1). Following the establishment of stable cell lines overexpressing SETDB1 (hereafter named as SETDB1 OE cells), SETDB1 RNA and protein levels were evaluated in these cells in comparison to control cells transduced with the pLEX980-empty vector (EV) (**Figure 7A**). Next, gene expression profiling of SETDB1 EV (n=3 replicates) and SETDB1 OE (n=2) HT144 melanoma cells was performed. Quantile-normalized microarray data showed that expression values of HT144 EV and SETDB1 OE cells clustered separately, defining two distinct profiles. Differential expression analysis (empirical Bayes two-group t test, $\log_2$ fold change threshold set as > 1, p-value 0.05) suggested that SETDB1 overexpression led to profound changes in melanoma transcriptome (**Figure 7B**). Interpretation of microarray data was further implemented using a web tool based on the Gene Set Enrichment Analysis method (GSEA). GSEA allows the integration of expression data obtained by microarray experiments with phenotypic annotations referring to defined biological states. Genes upregulated in SETDB1 OE cells emerged as enriched in several gene sets which define conditions frequently linked to tumor development and progression, like cell proliferation (Gene ontology term GO:0042127; normalized enrichment score NES = 2.8, nominal p-value < 0.01, FDR < 0.01), cell

motility (GO:0048870; NES = 1.8, p-value = 0.01, FDR = 0.17), epithelial-to-mesenchymal transition (GO:0001837; NES = 2.38, p-value < 0.01, FDR = 0.05) (**Figure 7C**). This analysis suggested that SETDB1 overexpression induced a deregulation of factors which play crucial roles in cancer. This hypothesis was further supported by using the Ingenuity pathway analysis (IPA) tool, which compares molecular data with disease-associated and functional annotations. A wide range of cancer-related functions were predicted to be activated upon SETDB1 upregulation (**Figure 7D**; IPA functional annotation's details are described in **Table 1**). Therefore, expression data of SETDB1-overexpressing melanoma cells gave the first hints that SETDB1 might act as a gene regulator.

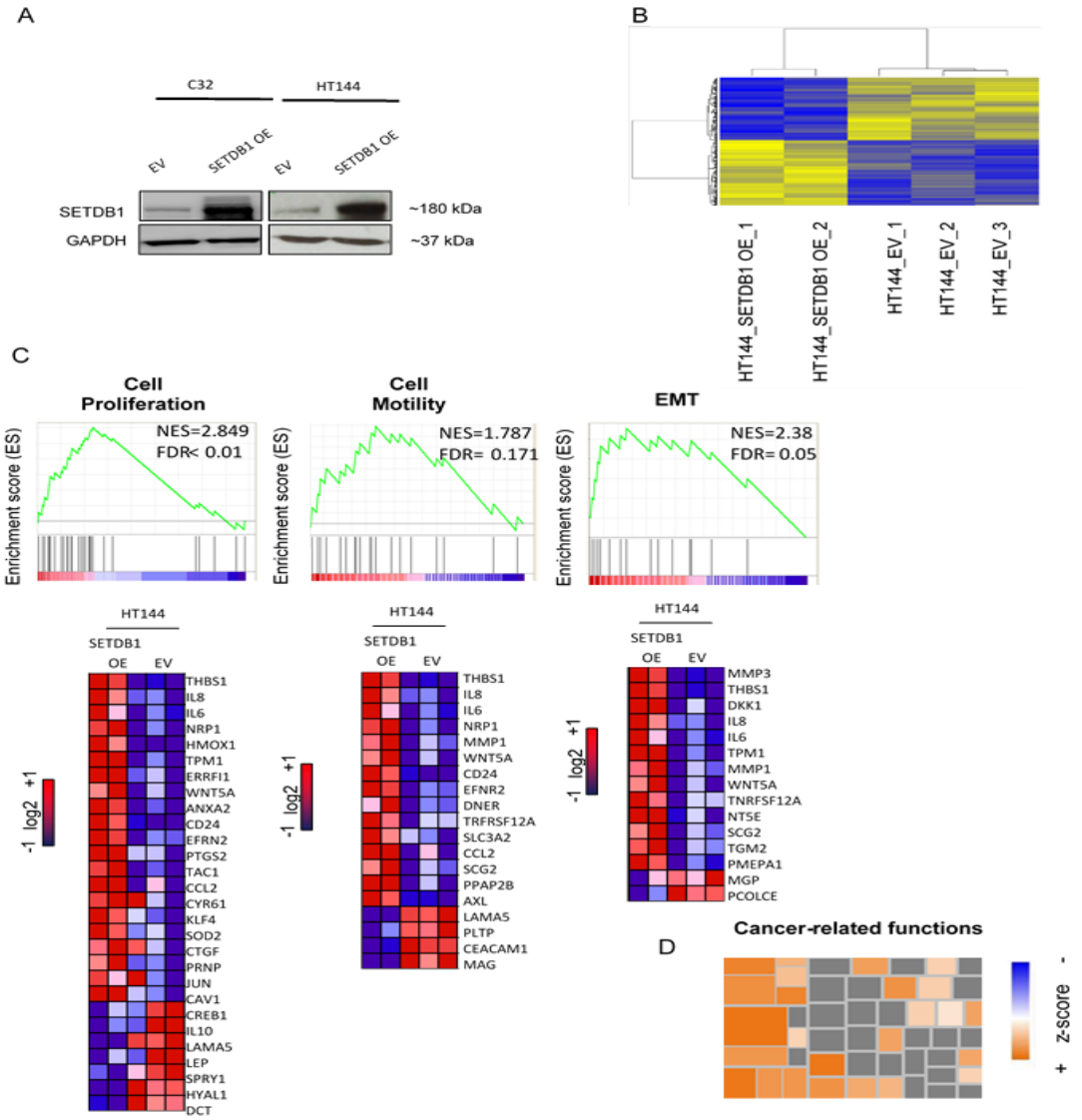

Figure 7: SETDB1 upregulation led to drastic transcriptome changes in melanoma cell lines. A) Validation of SETDB1 overexpression in C32 and HT144 melanoma cell lines by western blot (WB) analysis. Immunoblotting showed an increase of SETDB1 protein signal. GAPDH was used in this experiment as internal control. B) Heat map of microarray data showing differentially expressed genes between HT144 empty vector (EV) and HT144 SETDB1-overexpressing (SETDB1 OE) cells. C) GSEA analysis of significantly deregulated genes found in HT144 SETDB1 OE cells. Top panel showing the enriched GSEA plots related to cell proliferation, cell motility and epithelial-to-mesenchymal transition mechanisms, together with enrichment scores (ES) and false discovery rate (FDR) values. Positive enrichment scores indicate a concordance between the microarray gene expression values and the gene set-related biological state. In this case, top-upregulated genes in SETDB1 OE cells were predicted to promote cell proliferation, motility and EMT. Bottom panel, representation of the top-deregulated genes linked to the above mentioned enriched gene sets. D) IPA biological pathway analysis of deregulated genes in SETDB1 OE cells. Several biological functions related to cancer were found activated (showing a positive Z score) upon SETDB1 upregulation. More details about the top-ranked enriched annotated terms are included in Table 1.

4.2 THBS1, a known marker of melanoma progression, is regulated by SETDB1 in melanoma cell lines

As shown in the previous paragraph, several pro-tumorigenic and pro-metastatic factors were upregulated following SETDB1 overexpression, suggesting that these factors may act as SETDB1-downstream targets. Further analysis of the expression profiles of SETDB1-overexpressing melanoma cells indicated that among the upregulated genes the ones encoding for pro-tumorigenic secreted factors, including thrombospondin 1 (THBS1), secretogranin 2 (SCG2), metalloproteinases 1 and 3 (MMP1, MMP3), interleukin 6 and 8 (IL6, IL8), wnt family member 5a (WNT5A) and C-C Motif Chemokine Ligand 2 (CCL2) were particularly enriched (**Figure 8A**). Amongst the top-ranked candidate genes identified by microarray and gene enrichment analysis was the THBS1 gene (FC = 2.31 in SETDB1 OE vs EV). THBS1 is a glycoprotein involved in the progression of several cancer types. In melanoma, THBS1 strongly contributes to promote cell invasiveness and metastasis formation (Jayachandran et al, 2014). Because of the particular role of THBS1 in melanoma and the observed upregulation in melanoma cells with high levels of SETDB1, which has been also linked to an aggressive phenotype, I hypothesized that there might be a possible regulatory axis between SETDB1, as master regulator, and THBS1, as effector. For this reason, a comprehensive approach was adopted to further confirm and characterize the

relationship between these factors. Besides the establishment of stable melanoma cell lines with ectopic SETDB1 expression, loss-of- function studies based on SETDB1 gene expression silencing were also conducted. In our laboratory the SK-HI-SETDB1 melanoma isogenic cell line was previously established from SKMEL 28 melanoma cells. This cell line is characterized by multiple amplifications of the SETDB1 gene locus and high endogenous SETDB1 expression level (Orouji, 2016). SK-HI-SETDB1 cells were infected with lentivirus carrying a SETDB1-specific shRNA construct (referred to as “SETDB1 KD”). In parallel, cells were also transduced with a non-targeting lentiviral shRNA construct (“NT”), as control (**Figure 8B and 8C**). Established overexpressing and knockdown melanoma cell lines were tested for THBS1 expression. The THBS1 levels was altered by SETDB1 deregulation, observing a prominent increase in SETDB1 OE and a reduction in SETDB1 KD cells, compared with the respective controls (**Figure 8D and 8E**). As a further confirmation, SETDB1 EV and OE C32 cells were subcutaneously injected into immunodeficient NOD-SCID mice to allow tumor formation and growth. Next, tumors were excised; sliced and paraffin-embedded sections were then stained for SETDB1 and THBS1. Interestingly, SETDB1 expression co-localized with THBS1 expression, showing an intense signal in xenograft tissue derived from SETDB1 OE C32 cell lines (**Figure 8F**).

Finally, to ascertain the role of THBS1 as a SETDB1 target and as an effector in melanoma progression, functional properties of SETDB1 OE HT144 melanoma cells with a THBS1 knockdown (“THBS1 KD”) (**Figure 9A and 9B**) was evaluated. THBS1 knockdown in these cells severely impaired the migratory capacity (**Figure 9C**), implying that THBS1 is required for SETDB1-driven migration mechanisms and, therefore, that SETDB1 exerts its pro-tumorigenic role by regulating downstream targets like THBS1.

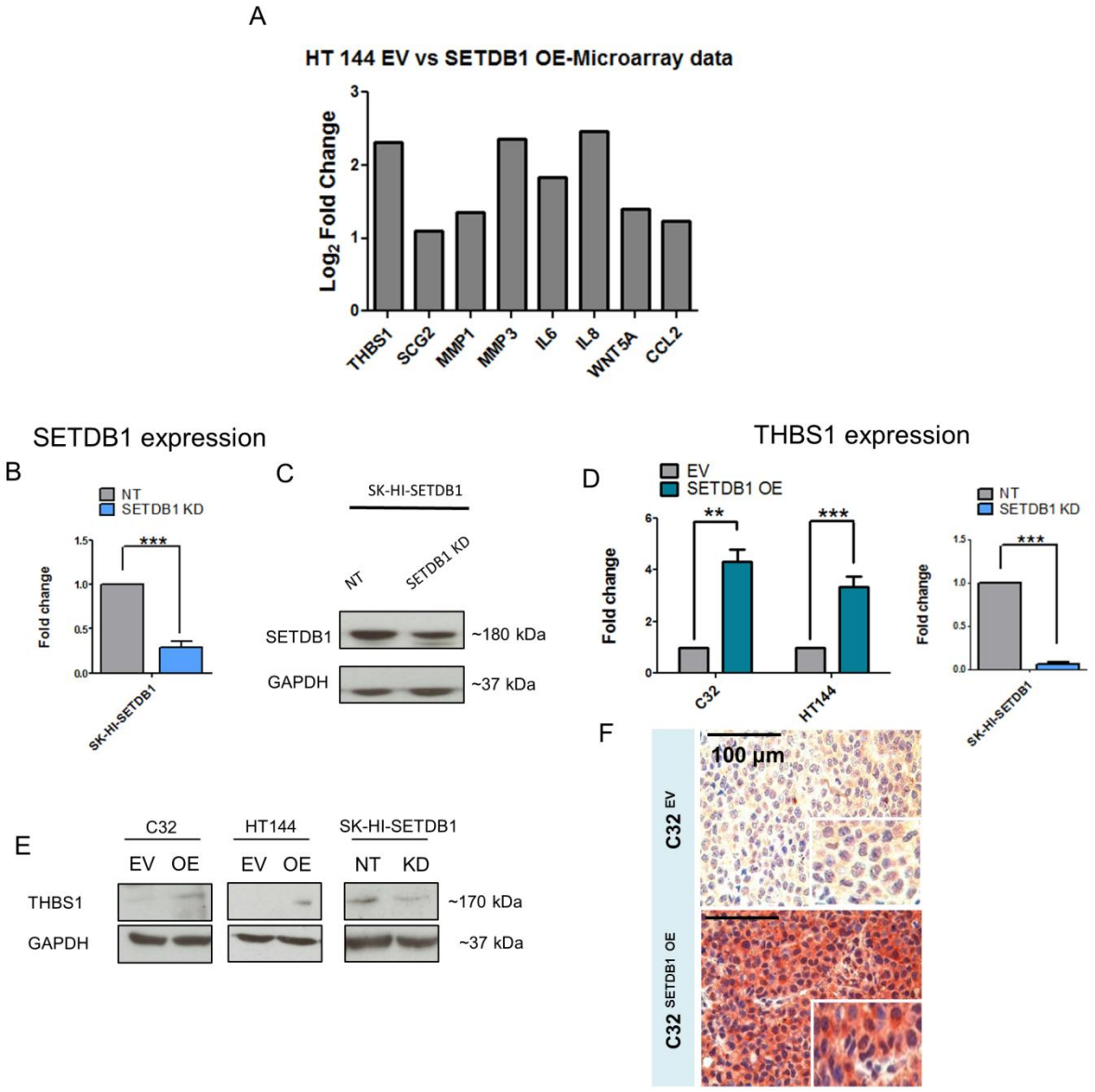

Figure 8: SETDB1 regulated the expression of THBS1 in melanoma cell lines.A) Histogram plot showing microarray expression data (expressed as Log2 fold change) of genes encoding for THBS1, SCG2, MMP1, MMP3, IL6, IL8, WNT5A and CCL2 in HT144 SETDB1 OE cells compared with EV cells. Presented genes were sorted by protein family/ biological functions. B) Real time quantitative PCR (RT-qPCR) showing SETDB1 transcript levels in SK-HI-SETDB1 cells following lentiviral transduction with shRNA against SETDB1 (SETDB1 KD) or with a non-targeting shRNA (NT). Fold change indicates the relative expression change for SETDB1 in knockdown cells compared with the control condition, whose relative expression was set as 1. C) Representative western blot of SETDB1 and GAPDH (used as control) in NT and SETDB1 KD cells. D) qPCR Analysis of THBS1 expression in SETDB1 OE and KD melanoma cells, in comparison to the respective controls. E) Western blot analysis of THBS1 expression in SETDB1-dysregulated melanoma cells. F) Immunohistochemical (IHC) staining of SETDB1 and THBS1 in paraffin-embedded tumor sections derived from NOD/SCID null mice xenografts obtained after injection of C32 EV or SETDB1 OE cells. Scale bar: 100 µm. The bottom-right frames show zoomed-in acquisitions.

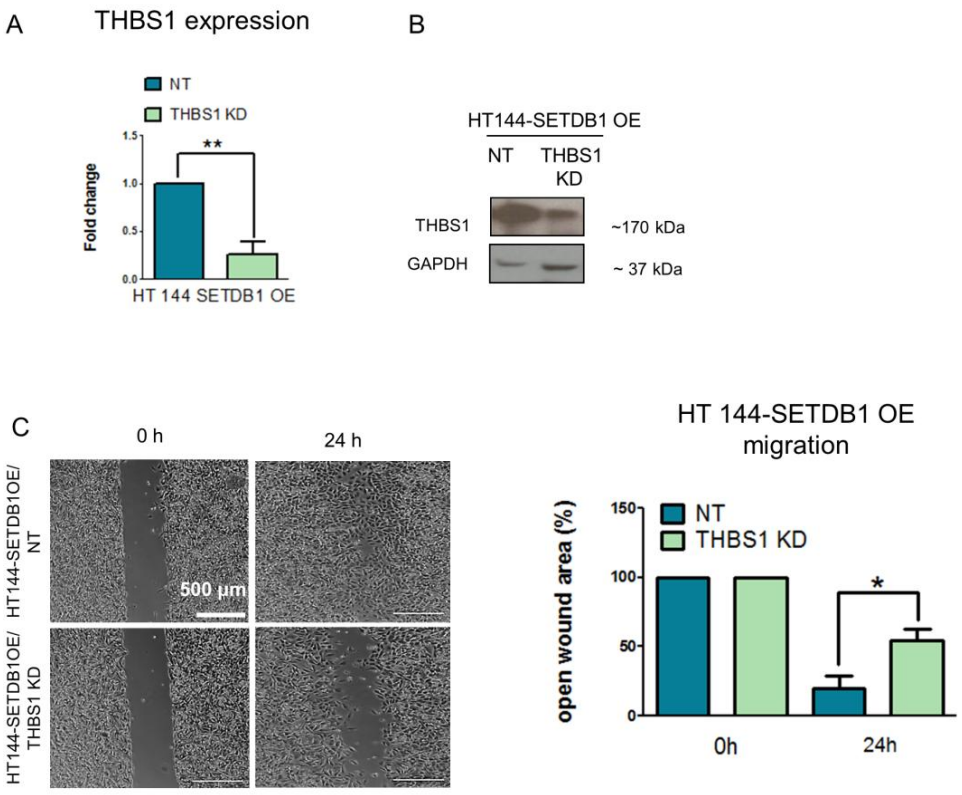

Figure 9: Knockdown of THBS1 in SETDB1 high-expressing melanoma cells impaired the tumor cell migration properties.A) and B) Validation of THBS1 knockdown (THBS1 KD) efficiency in SETDB1 OE (HT144) melanoma cells using quantitative PCR and western blot. C) Wound healing assay performed with HT144 SETDB1 OE cells following THBS1 silencing. The top-panel shows representative images acquired after 0 and 24 hours, indicating the impaired migratory capacity after knockdown of THBS1. The bottom panel depicts the quantification of the wound healing assay.

4.3 THBS1 positively correlates with SETDB1 expression in melanoma clinical samples

The association between SETDB1 and THBS1 was also investigated in melanoma patients' tumor biopsies. Tissue microarray analysis (TMA) allowed us to screen a large number of patients' biopsies. This study included 41 biopsies derived from primary melanomas and 54 metastatic melanoma samples. SETDB1 and THBS1 signals were scored according to the immunohistochemistry (IHC) score system (Wagner et al, 2015). This test takes into account the signal intensity (scored in a range from 1-3) and

abundancy (i.e. percentage of positive cells; score range: 0-4) for each sample. The final IHC score obtained by multiplying the scores for the two parameters indicates the protein expression levels in tumor tissues. I aimed at observing correlations between SETDB1 and THBS1 expression in patients' biopsies and, strikingly, it was possible to observe a positive correlation of their expressions in primary (Spearman correlation r = 0.39, p value = 0.0106) and metastatic melanoma (r = 0.5234, p <0.01) cohorts (**Figure 10A and 10B**). Of note, SETDB1 and THBS1 signals mostly co-localized at the outer regions of the lesions, corresponding to the tumor invasive front (**Figure 10C**). Taken together, THBS1 expression was linked with SETDB1 expression also in clinical samples derived from malignant melanoma patients, adding a prominent prognostic value to this newly established axis.

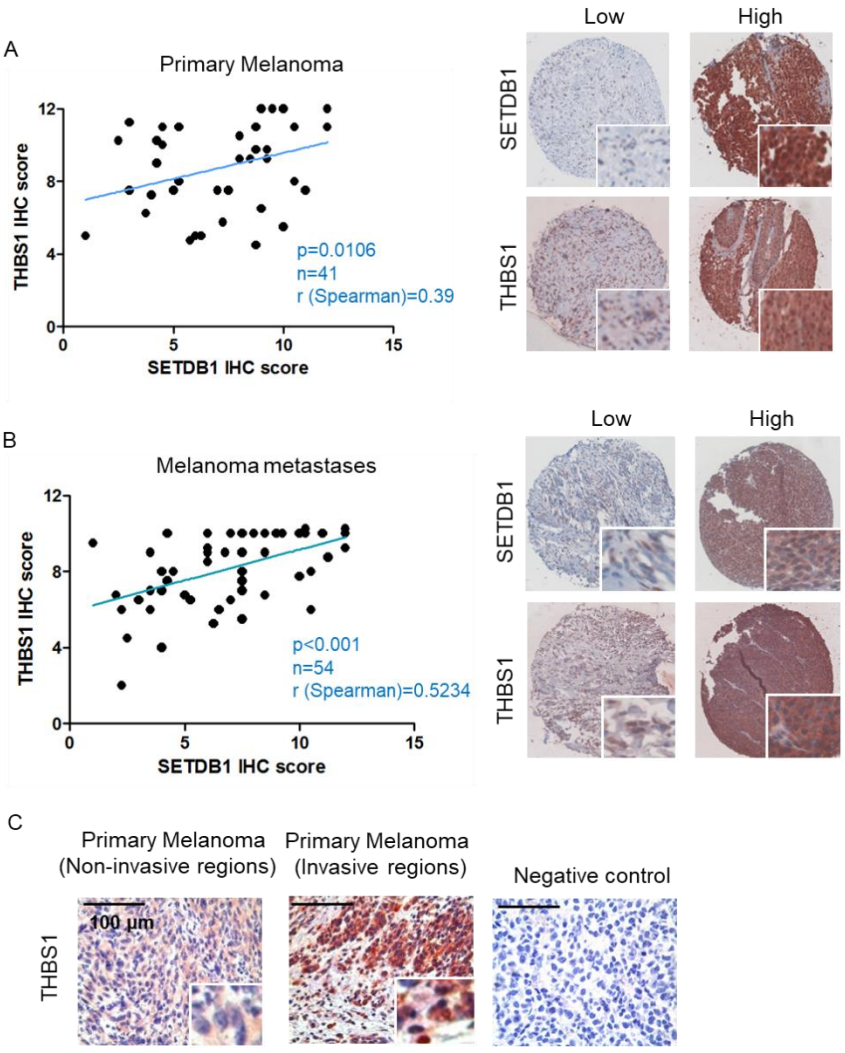

Figure 10: Analysis of SETDB1 and THBS1 expression and localization in patient-derived tumor biopsies. A) Tissue microarray analysis (TMA) of a cohort of melanoma patients showed that SETDB1 expression positively correlated with THBS1 expression in tumor tissue samples derived from A) primary melanomas (n = 41), and B) melanoma metastases (n = 54). On the left panel, the SETDB1 and THBS1 correlation plot is shown. Number of analysed samples (n), Spearman correlation coefficient (r) and p value are reported. On the right side, representative images of patient-derived tissue biopsies stained for SETDB1 and THBS1 are depicted. Tumors characterized by intense SETDB1 staining showed also a high THBS1 signal. Conversely, primary melanoma and metastases specimen exhibiting a weak signal for SETDB1 also showed a weak staining for THBS1. C) THBS1 IHC staining of primary melanoma-derived tissue. As previously observed for SETDB1 (Orouji, 2016), THBS1 expression is particularly enhanced in the external regions (also described as “invasive” tumor front), compared to the internal regions (“non-invasive” front). Negative staining validated the specificity of the THBS1 antibody. Scale bar: 100 µm.

4.4 SETDB1 limits the expression of melanocytic lineage-differentiation and anti-metastatic genes

Gene expression data showed that several factors were downregulated in melanoma cells upon SETDB1 induction (**Figure 11A**). Functional annotation of these gene was performed by using the web tool DAVID and the analysis showed that the top-enriched DAVID annotation terms were mostly associated with melanocytic differentiation and metabolism, like melanin biosynthesis (GO: 0042438), melanosome formation (GO: 0033162) and developmental pigmentation (GO: 0048066) (Detailed list of biological functions downregulated in SETDB1 OE cells is given in **Table 2**). During the transition from melanocytes to melanoma, a loss of differentiation properties occurs towards a more undifferentiated status (Lekmine et al, 2007; Pinner et al, 2009). This process goes along with the downregulation of the differentiation markers, most of which act as tumor suppressors and anti-metastatic factors. Following SETDB1 overexpression, a reduction of melanogenesis-related and metabolic proteins, involved in anti-tumorigenic and anti-metastatic processes, was observed. In particular, DCT showed a negative correlation with SETDB1 in melanoma cell lines (**Figure 11B and 11C**). The obtained data indicate that SETDB1 might interfere with the expression of pro-differentiation and tumor suppressor factors.

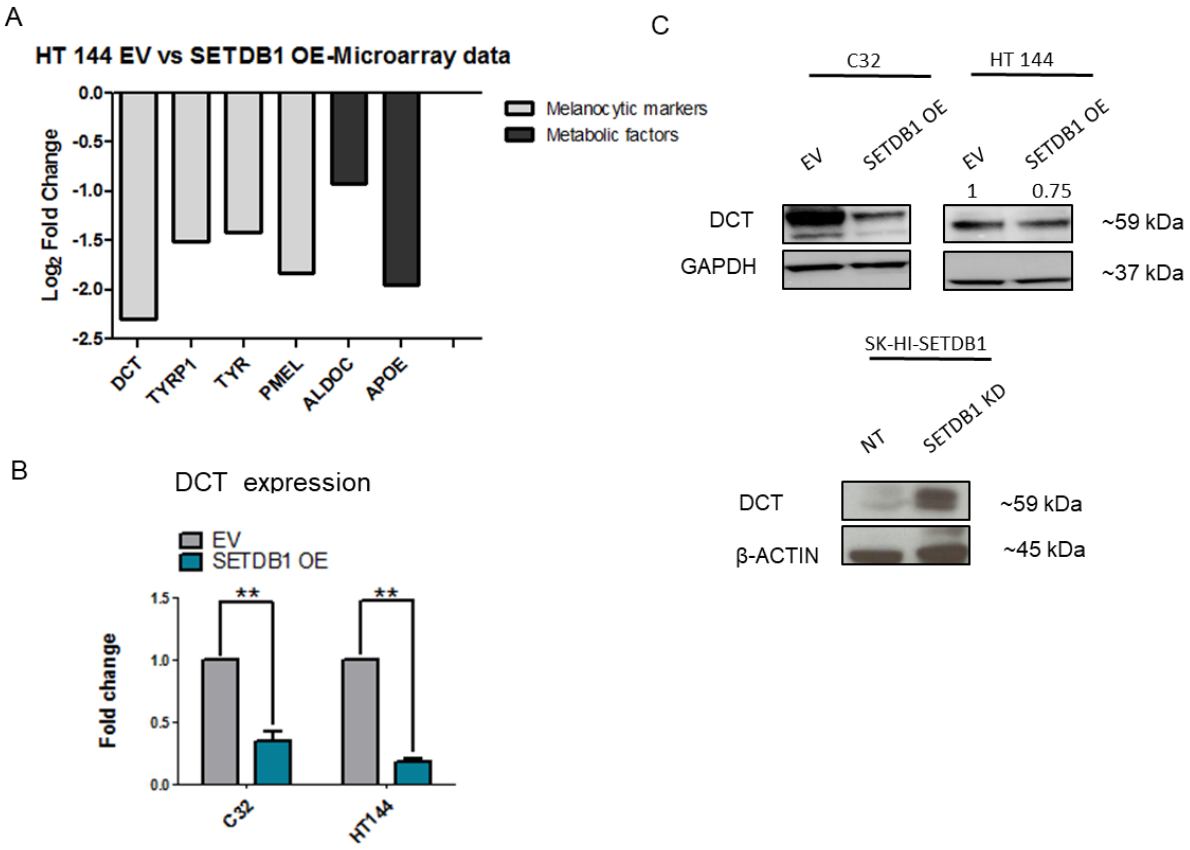

Figure 11: Increasing levels of SETDB1 reduced the expression of melanocytic and metabolic markers.A) Expression data (obtained from the microarray analysis of EV vs SETDB1 OE cells) of the pro-differentiation genes DCT, TYRP1, TYR, PMEL17 genes (grey bars) and of metabolic factor-encoding ALDOC and APOE genes (black bars), following SETDB1 induction. B) Validation of DCT mRNA levels in in SETDB1-overexpressing (C32 and HT144) cell lines. C) DCT western blots of SETDB1 OE and knockdown (SK-HI-SETDB1) cells, with respective controls. Detected DCT band size at ~59 kDa. Beta actin was used as loading control.

4.5 Methyltransferase-deficient SETDB1 impairs the expression of its downstream targets

Although SETDB1 has already been described to be involved in tumor progression in several cancer types, little is still known about how this protein mechanistically acts. As already mentioned, the SETDB1 protein is structurally divided into distinct domains,

each of which responsible for specific activities. In particular, the SET domain is essential for the histone methyltransferase (HMT) function. To determine whether the influence of SETDB1 on melanoma progression is HMT activity-dependent, a loss-of-function approach based on SET domain inactivation was carried out: two specific SET domain amino acids were substituted by site-direct mutagenesis. As indicated by Ceol et al. (PMC3348545), the H1224A and C1226K mutations completely inactivate SET domain activity. The mutated SETDB1 coding sequence (**Figure 12A**) was inserted into pLEX980 lentiviral expression vector and the construct was used for the transduction of melanoma cells. Mutated SETDB1 (HC/KA SETDB1 OE) was overexpressed in C32 and HT144 melanoma cells. In contrast to overexpression of wild-type SETDB1, total levels of trimethylated histone H3 at lysine 9 (H3K9me3) did not increase upon overexpression of HC/KA (**Figure 12B and 12C**). With this methyltransferase-deficient variant of SETDB1, molecular and biological perturbations caused by SETDB1 expression in melanoma were investigated. A whole-genome expression profiling was performed for SETDB1 OE (number or replicates=2) and HC/KA SETDB1 OE (n=3) HT144 cells. Gene expression data obtained by this microarray analysis (empirical Bayes two-group t test, $\log_2$ fold change filtering threshold > 1, p-value 0.05) showed different transcriptome profiles accordingly with SETDB1 mutational status. Interestingly, the most significantly differentially expressed genes between the two groups were the same that have been shown to be differentially expressed between melanoma cells transduced with wild-type SETDB1 and EV (**Figure 12D**). To validate these findings, the expression of SETDB1 target genes was examined. Remarkably, HC/KA SETDB1 did not induce THBS1 expression. In contrast, expression of the pro-differentiation gene DCT was not decreased in cells overexpressing HC/KA SETDB1 compared to cells overexpressing wild-type SETDB1 (**Figure 12E and 12F**). These data indicate that the role of SETDB1 as a master regulator is greatly dependent on SET domain integrity and functionality.

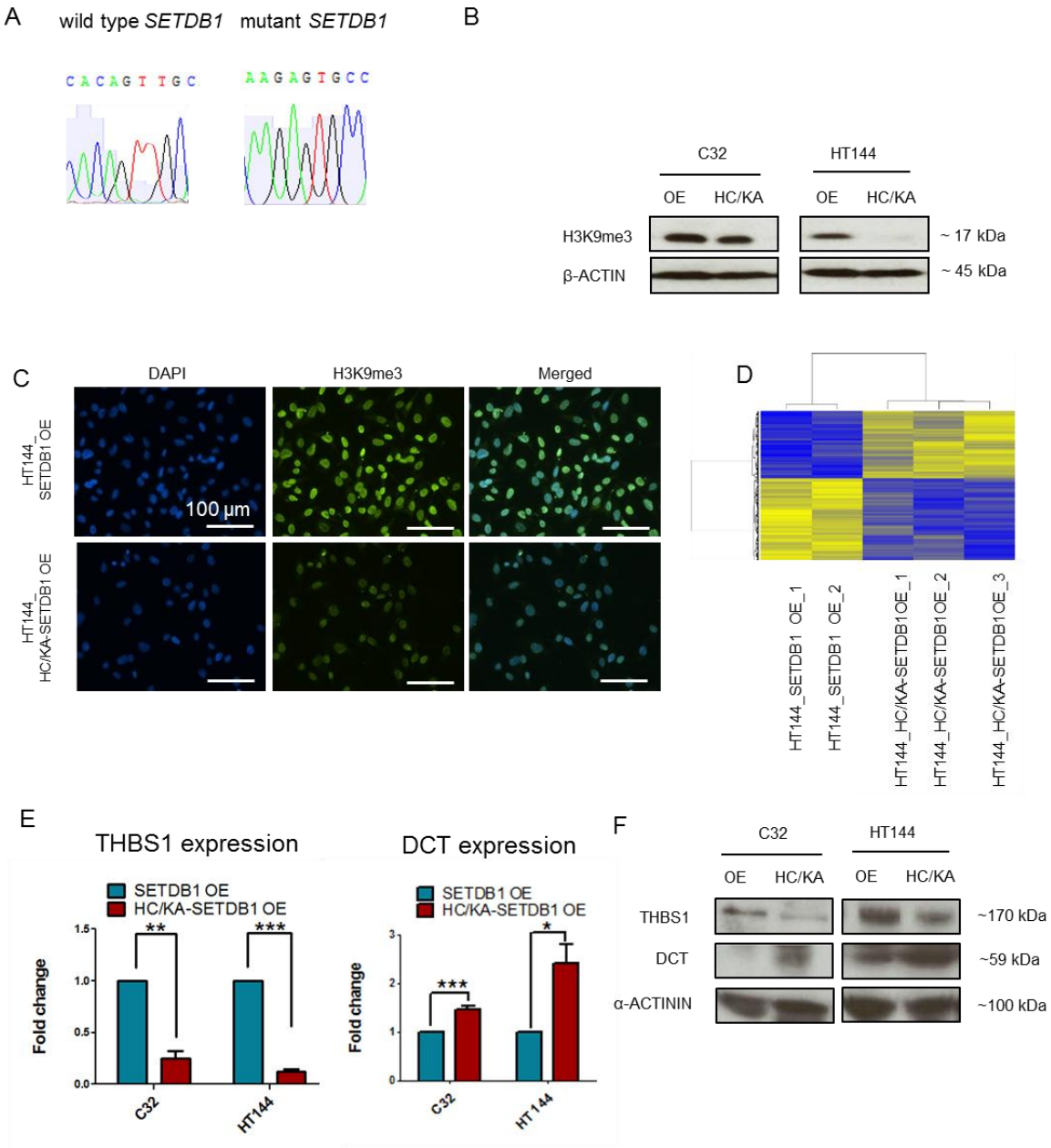

Figure 12: SET domain inactivation restrained as the capacity of SETDB1 to regulate the expression of its downstream targets. A) Sequence comparison between wild-type and methyltransferase-deficient variant of SETDB1 showing the nucleotide substitutions which resulted in SET domain inactivation. B) Western blot assessment of SETDB1 and H3K9me3 expression in C32 and HT144 melanoma cell lines infected with EV-, SETDB1 OE and HC/KA SETDB1 OE lentiviral constructs. GAPDH and beta actin were used as loading controls, respectively. C) Immunofluorescent detection of H3K9me3 in SETDB1 OE and HC/KA SETDB1 OE cells. DAPI was used for nuclear staining. Scale bar: 100 µm. D) Heat map image of a microarray analysis comparing the transcriptomic profiles of melanoma cells overexpressing wild-type vs mutated SETDB1. Microarray expression data were confirmed by measuring THBS1 and DCT mRNA E) and F) protein expression, respectively, in C32 and HT144 SETDB1 OE cells in comparison to HC/KA SETDB1 OE cells. Western blot loading control: α-actinin.

4.6 SETDB1 HMT inactivation results in a less aggressive phenotype of melanoma cells

Differentially expressed genes between melanoma cells expressing HC/KA SETDB1 or wild-type SETDB1 are strictly linked with cancer-related phenotypic states. By using GSEA tool, gene sets related to cell motility (GO: 0048870) and activation (GO: 0050865) were found to be overrepresented, showing in this case a negative enrichment score (NES) in HC/KA SETDB1 OE cells vs SETDB1 OE cells (NES = -2.19, p-value <0.01, FDR = 0.004 for cell motility gene set; NES = -2.35, p-value <0.01, FDR = 0.002 for cell activation annotation term). This means that genes known to promote tumor cell motility and tumor activation were not upregulated in melanoma cells expressing mutated SETDB1 in contrast to cells expressing wild-type SETDB1 (**Figure 13A**). Ingenuity pathway analysis (IPA) provided further hints supporting the hypothesis that eliminating the methyltransferase activity of SETDB1 contributed to the reduction of SETDB1-mediated pro-invasive and pro-metastatic properties and an increase of melanocyte-specific differentiation (**Figure 13B**; IPA functional annotation's details are described in **Table 3**). To confirm these observations, *in vitro* cell-based functional assays with HC/KA SETDB1 OE C32 and HT144 cells were performed. SETDB1 OE cells were used as a control for the following experiments. We could not observe any drastic differences in melanoma cell proliferation between the two cell populations after 24-96h of observation (**Figure 14A**). Next, the migration capacity was evaluated with the scratch assay, which indicated a slower migratory capacity of HC/KA SETDB1 OE cells compared with the control (**Figure 14B**). Additionally, the transwell cell invasion assay showed how the inactivation of the SET domain strongly affected the invasive properties of melanoma cells (**Figure 14C**). Taken together, abrogating the methyltransferase activity of SETDB1 by introducing specific point mutations in its SET domain led to a reduction of progression-related functional features of melanoma cells, which might be the likely due to the dysregulation of SETDB1 target genes involved in pro-migratory and pro-invasive mechanisms.

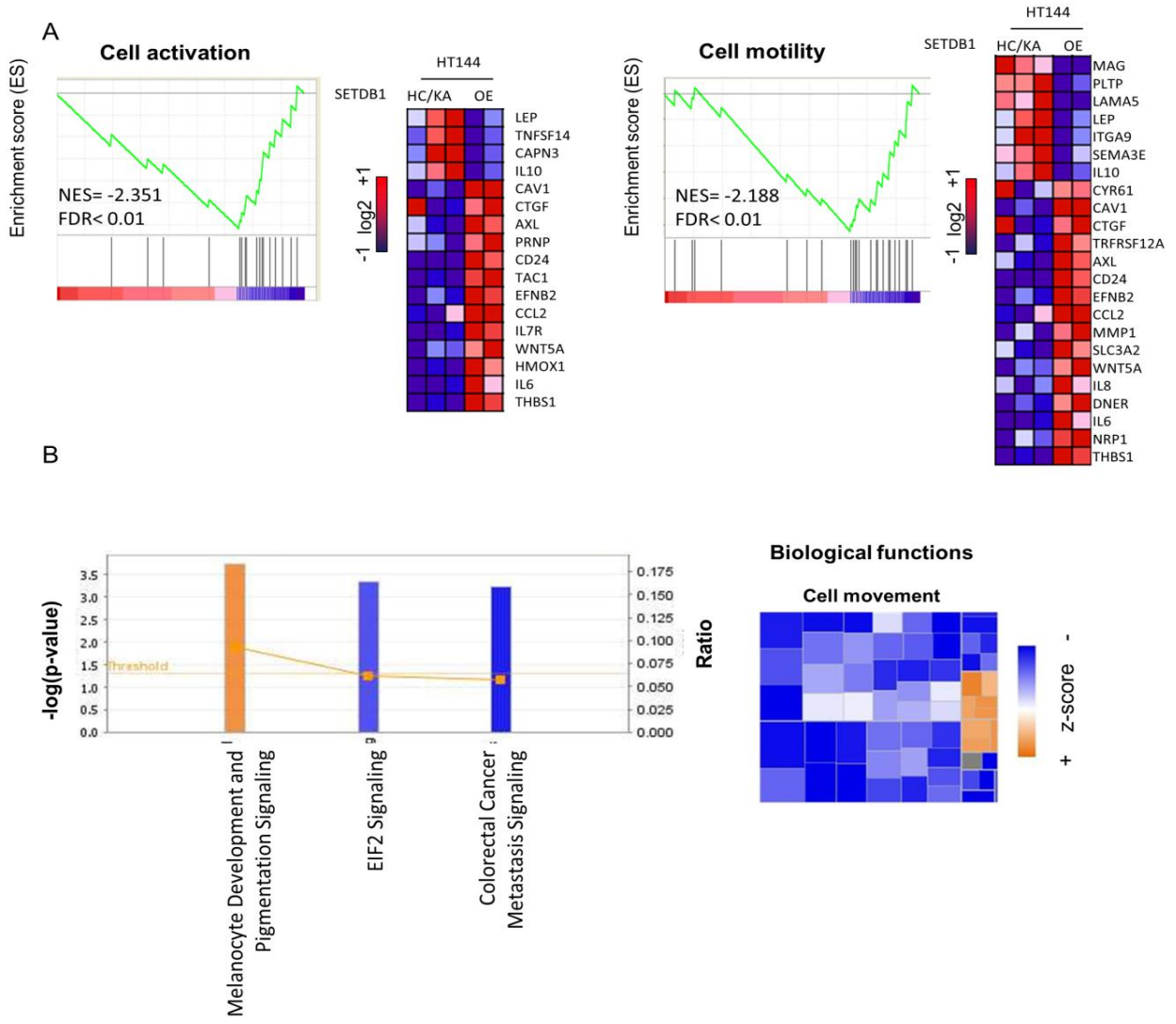

Figure 13: *In silico* prediction of SETDB1's HMT inactivation functional effects.A) GSEA plots and corresponding gene set lists, describing a negative enrichment score obtained by integrating gene expression data (HC/KA SETDB1 OE vs SETDB1 OE cells) with cancer-related gene set annotations. Negative ES indicates that genes which are normally involved in tumor cell activation and motility were found to be downregulated in HC/KA SETDB1 OE cells compared with cells overexpressing wild-type SETDB1. B) IPA pathway and biological feature analysis, predicting an activation (positive Z score) of melanocyte-specific biological processes (i.e. melanocyte development and pigmentation signalling), in concomitance with a strong reduction (negative Z score) of tumor-related features, like cell movement (including migration, invasion, extravasation, metastases formation). More details about the top-ranked enriched annotated terms related to cell movement are included in Table 3.

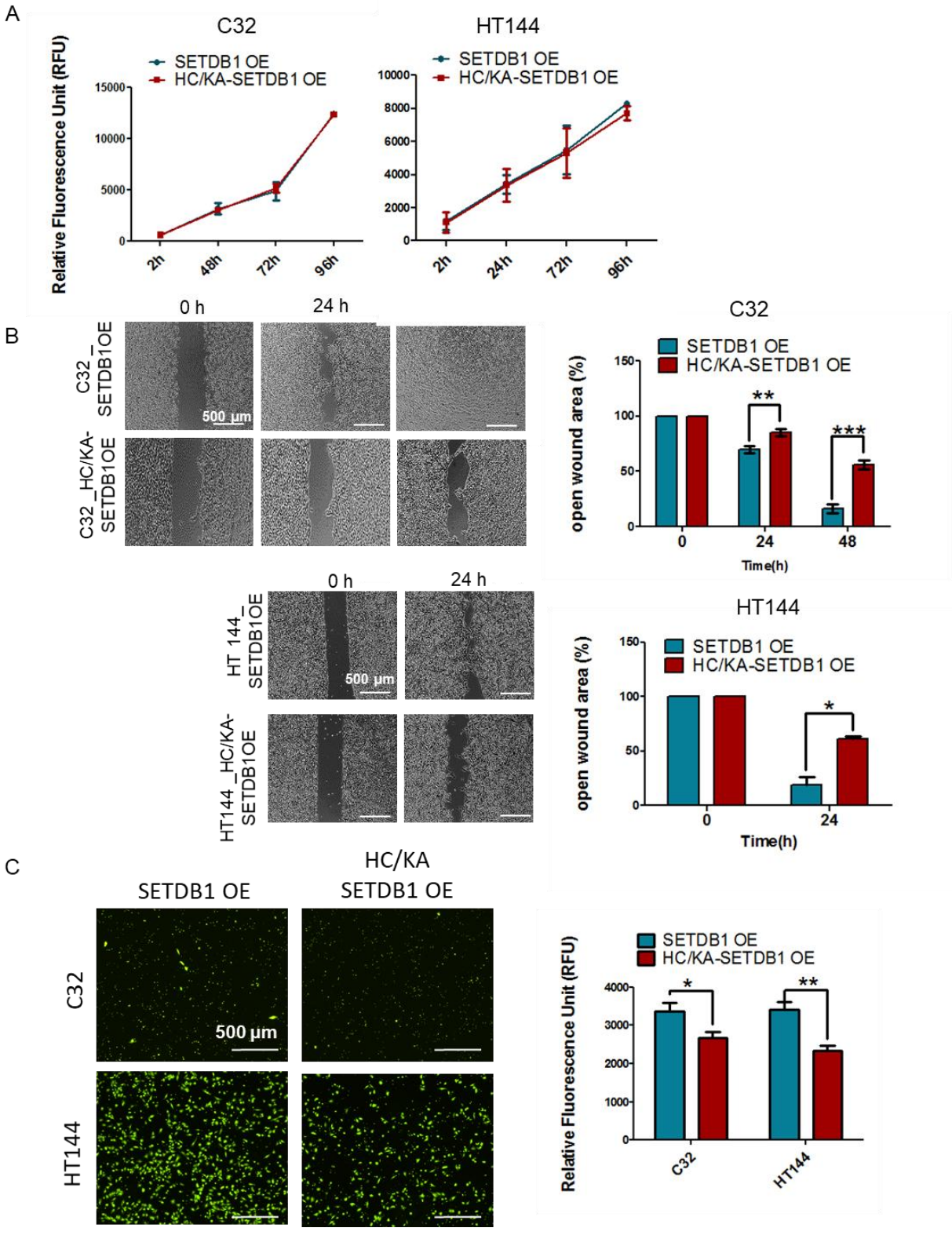
A
C32
HT144
SETDB1 OE
HC/KA-SETDB1 OE
Relative Fluorescence Unit (RFU)
2h
48h
72h
96h
24h
B
0 h
24 h
C32 _SETDB1OE
C32 _HC/KA-SETDB1OE
HT 144_SETDB1OE
HT144 _HC/KA-SETDB1OE
500 µm
open wound area (%)
Time(h)
C
SETDB1 OE
HC/KA SETDB1 OE
C32
HT144
500 µm

Figure 14: HC/KA SETDB1 OE melanoma cells exhibited a remarked impairment of proliferative and migrative capacity. A) Alamarblue assay performed with HC/KA SETDB1 OE and SETDB1 OE cells. Cell proliferation was observed from day 1 to day 5. Proliferative rate was measured as quantity of fluorescence emission following Alamarblue substrate exposure. B) Migration scratch assay performed with melanoma cells (C32 and HT144), transduced with either SETDB1 OE or HC/KA SETDB1 OE lentiviral construct. Migratory capacity of the cells was quantified by measuring the percentage of open gap area observed at each time point compared to 0h. In the case of C32 (slowly migrating cells), the experiment was extended until the 48h-time point. Images scale bar: 500 µm. C) Melanoma cell invasion rate was assessed with the transwell invasion system. 24-48h after seeding the invading cells were exposed to calcein AM fluorescent dye. Fluorescence emission was observed (top panel) and quantified (bottom panel) as relative fluorescence units (RFUs). Invasion plate wells with no seeded cells were used as background control.

4.7 SETDB1 regulates THBS1 via alterations in histone methylation patterns

The data presented here support a crucial role for SETDB1 in regulating the expression of important pro- and anti-tumorigenic factors during melanoma development. Next, I aimed at elucidating the molecular mechanisms of SETDB1 by which it exerts its functions. As a histone methyltransferase SETDB1 contributes to the modification of chromatin structure. Alterations of chromatin structure and chromatin-associated components have been found to directly mediate drastic changes at the molecular level, i.e. gene expression (Bilodeau et al, 2009). For that reason, I wanted to identify altered chromatin states that were linked with SETDB1 expression during melanoma progression. In particular, the investigations focused on histone methylation patterns which were directly involved in regulating gene expression. By performing chromatin immunoprecipitation (ChIP) and ChIP-sequencing (ChIP-seq), I analyzed the global distribution and local enrichment of specific histone marks: trimethylated histone H3 at lysine 9 (H3K9me3), a histone modification directly mediated by SETDB1 and monomethylated H3 at lysine 4 (H3K4me1). The H3K4me1 histone modification is found particularly enriched at active gene enhancer sites and plays a pivotal role in determining chromatin state-based gene expression alterations (Heintzman et al, 2007). Furthermore, an inverse correlation between SETDB1-induced H3K9me3 and the K4 methylation status (Binda et al, 2010) as well as between SETDB1 expression and

H3K4me1 distribution have been recently described (Perner et al, 2014). Chromatin obtained from SETDB1 OE (C32) and SETDB1 KD (SK-HI-SETDB1) cells and from the corresponding controls was immunoprecipitated with antibodies against H3K9me3 and H3K4me1. Immunoprecipitated chromatin was then de-crosslinked and resulting DNA fragments were amplified and assembled in DNA libraries, before multiplex sequencing (n = 2 sequencing experiments conducted). ChIP-seq raw reads were mapped to human genome (hg19 used as reference), and regions enriched for the investigated histone marks were marked by peaks. Large-scale histone methylation profiling included the analysis of global number of enriched areas and of the peak regions surrounding the regulatory sites of SETDB1 targets. First, following the alteration of SETDB1 expression, profound changes of genome-wide H3K9me3 abundancy occurred. SETDB1 overexpression induced a massive increase of detected H3K9me3-binding sites (unique peaks observed in C32 EV cells: 3.528; unique peaks in C32 SETDB1 OE cells: 19.510), while SETDB1 silencing severely affected the global H3K9me3 levels (H3K9me3 ChIP-seq performed on SK-HI-SETDB1 NT cells resulted in 52.203 unique peaks, whereas only 13.877 enriched regions were exclusively found in SETDB1 KD cells) (**Figure 15A**). These data suggest that SETDB1 might be particularly relevant in melanoma for determining and regulating the trimethylated histone H3 at lysine 9 status. Local H3K9me3 enrichment analysis did not show any differential H3K9me3 enrichment patterns in genomic regions corresponding to the genes previously shown to be regulated by SETDB1. However, by exploring the genome distributions of the H3K4me1 mark, it was possible to observe that H3K4me1 enrichment profiles were altered, in correspondence with SETDB1 expression levels, at specific regulatory sites of the THBS1 gene. Strikingly, in melanoma cells overexpressing SETDB1, low levels of H3K4me1 surrounding *THBS1* regulatory regions were observed, whereas in cells exhibiting low amounts of SETDB1, H3K4me1 marks were significantly enriched around the THBS1 gene locus (**Figure 15B**). ChIP-qPCR experiments further confirmed these observations: H3K4me1 ChIP DNA samples, together with relative input samples (containing the pre-immunoprecipitation DNA), were amplified with specifically designed primers annealing to H3K4me1-enriched regions nearby the THBS1 transcription start site (chr15:39,870,657-39,871,729). Results showed that SETDB1 repression increased

the amount of H3K4me1 marks. No differences were detected for the GAPDH promoter region which was used as control in this experiment (**Figure 15C**). These results support the role of SETDB1 as a regulator of THBS1. Mechanistically, SETDB1 expression resulted in drastic epigenetic alterations in melanoma cells. Regarding the histone modifications associated with altered gene expression, my experiments suggest that SETDB1 specifically altered the expression of its target by affecting the H3K4me1 distribution and enrichment patterns.

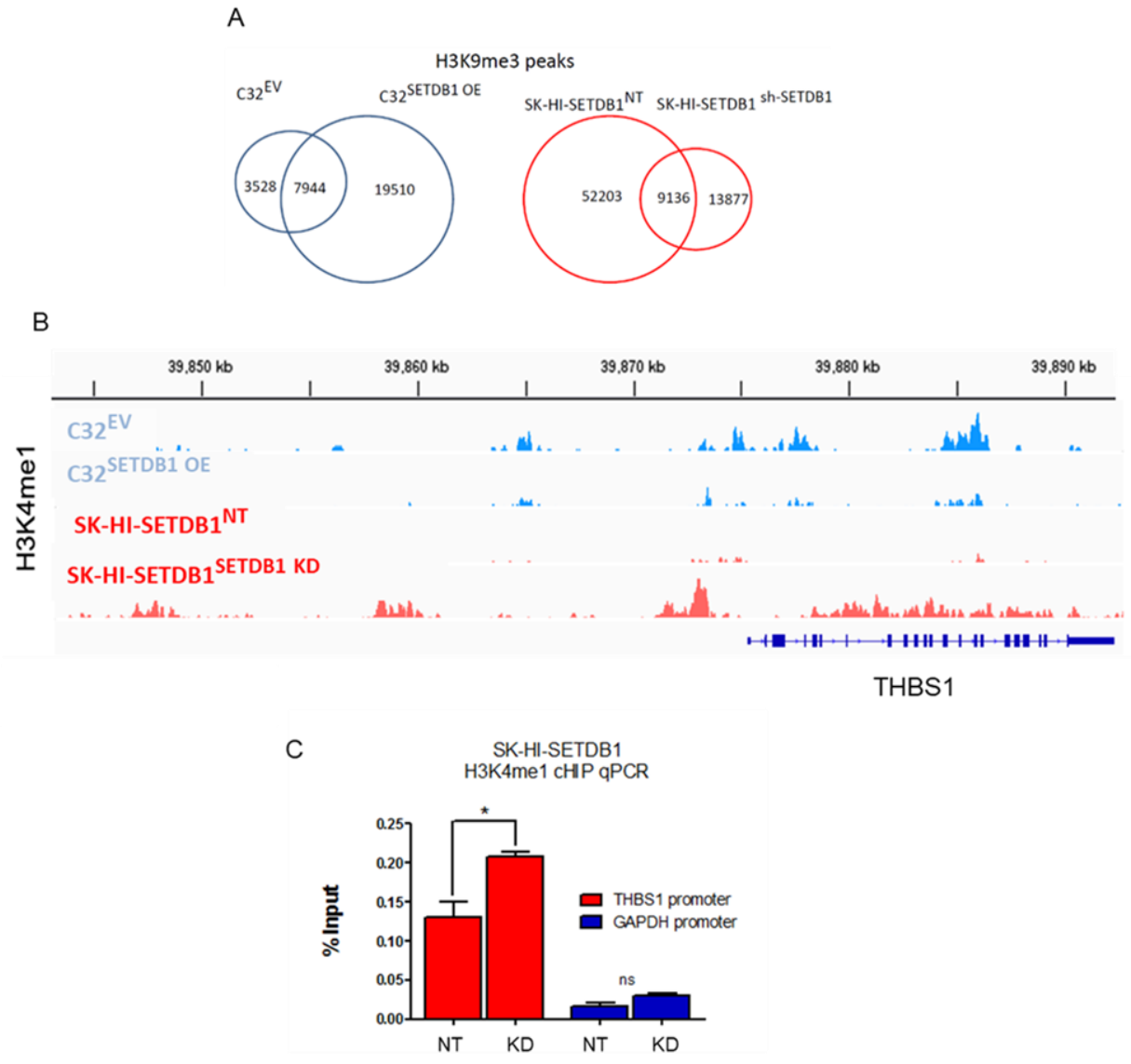

Figure 15: Identification of epigenetic traits altered by SETDB1 deregulation.A) Venn diagrams showing the number H3K9me3-related peaks detected with ChIP-seq performed with EV /SETDB1 OE

(C32) cells and NT/SETDB1 KD (SK-HI-SETDB1) cells. Indicated values refer to the quantity of genomic sites where H3K9me3 exclusively binds in each condition, while the diagrams' intersection regions are related to the common peaks. Upon SETDB1 induction, the percentage of H3K9me3 enriched regions drastically increased, while SETDB1 KD led to a pronounced loss of genome-wide H3K9me3 distribution. B) IGV visualization of H3K4me1 distribution profiles at the *THBS1* locus. SETDB1 overexpression led to a low levels of trimethylated H3K4 at genomic regions corresponding to THBS1 gene, while SETDB1 silencing resulted in the increase of H3K4me1 distribution and enrichment at *THBS1* regulatory sites. C) Real-time quantitative PCR of H3K4me1 ChIP DNA. Primers annealing with the THBS1- and GAPDH-(control) promoter were used to quantify H3K4me1 enrichment at those particular genomic sites in immunoprecipitated chromatin, compared with input samples. Quantifications were performed using the percent input method.

4.8 Mithramycin A treatment reduces SETDB1 levels and melanoma cell viability

From the results of my study, one can conclude that SETDB1 might play an important role during melanoma progression. For this reason, the next aim of this project was to establish a drug-based approach able to target SETDB1 expression in order to abrogate its melanoma promoting effect. Although a selective SETDB1 inhibitor has not been identified yet, SETDB1 expression could efficiently be blocked by the antitumoral drugs paclitaxel (Noh et al, 2014) or by unspecific histone methyltransferase inhibitors, like DZnep (Lee & Kim, 2013) and mithramycin A (Ryu et al, 2006) (Karanth et al, 2017). Within the scope of this study, mithramycin A (mit) was chosen for blocking SETDB1. Mit is an antitumor antibiotic widely used in clinical trials (Phase 2) for the treatment of several cancer types (ClinicalTrials.gov Identifier: NCT01624090).Functionally, mit is a DNA-binding factor that represses SETDB1 expression by competing with the transcription factor SP-1 for binding sites within the SETDB1 promoter region (Choi et al, 2014). I tested the mit capacity to specifically inhibit SETDB1 in melanoma cells by exposing melanoma cells with high SETDB1 expression levels (A375, SK-HI-SETDB1) to different mit concentrations (1 nM - 2 µM range) for 24 and 48h. Both cell lines showed high sensitivity to the treatment (mean IC_{50} values for A375: 866.8 nM after 24h of treatment, 38.45 nM after 48h of observation; IC_{50} SK-HI-SETDB1: 473.8 and 41.99 nM after 24 and 48h, respectively) (**Figure 16A**). Human dermal fibroblasts and

SETDB1 KD melanoma cells did not respond to the treatment (**Figure 16B and 16C**), suggesting that mit affects melanoma cells by blocking SETDB1. To further ascertain whether mit-mediated reduction of melanoma cell viability was related to SETDB1 inhibition, the SETDB1 expression levels in response to increasing concentrations of mit were assessed. After 24h of treatment, the SETDB1 RNA and protein level decreased gradually in accordance with the increment of mit doses. Following 24h of treatment with 300 nM mit, SETDB1 was almost totally silenced (for qPCR analysis, One-way ANOVA test was applied; p-value <0.0001) (**Figure 17A and 17B**). No further reduction of SETDB1 expression was observed with higher mit dosages. 24h exposure to 300 nM mit was established as the standard mit treatment for all the subsequent drug response experiments.

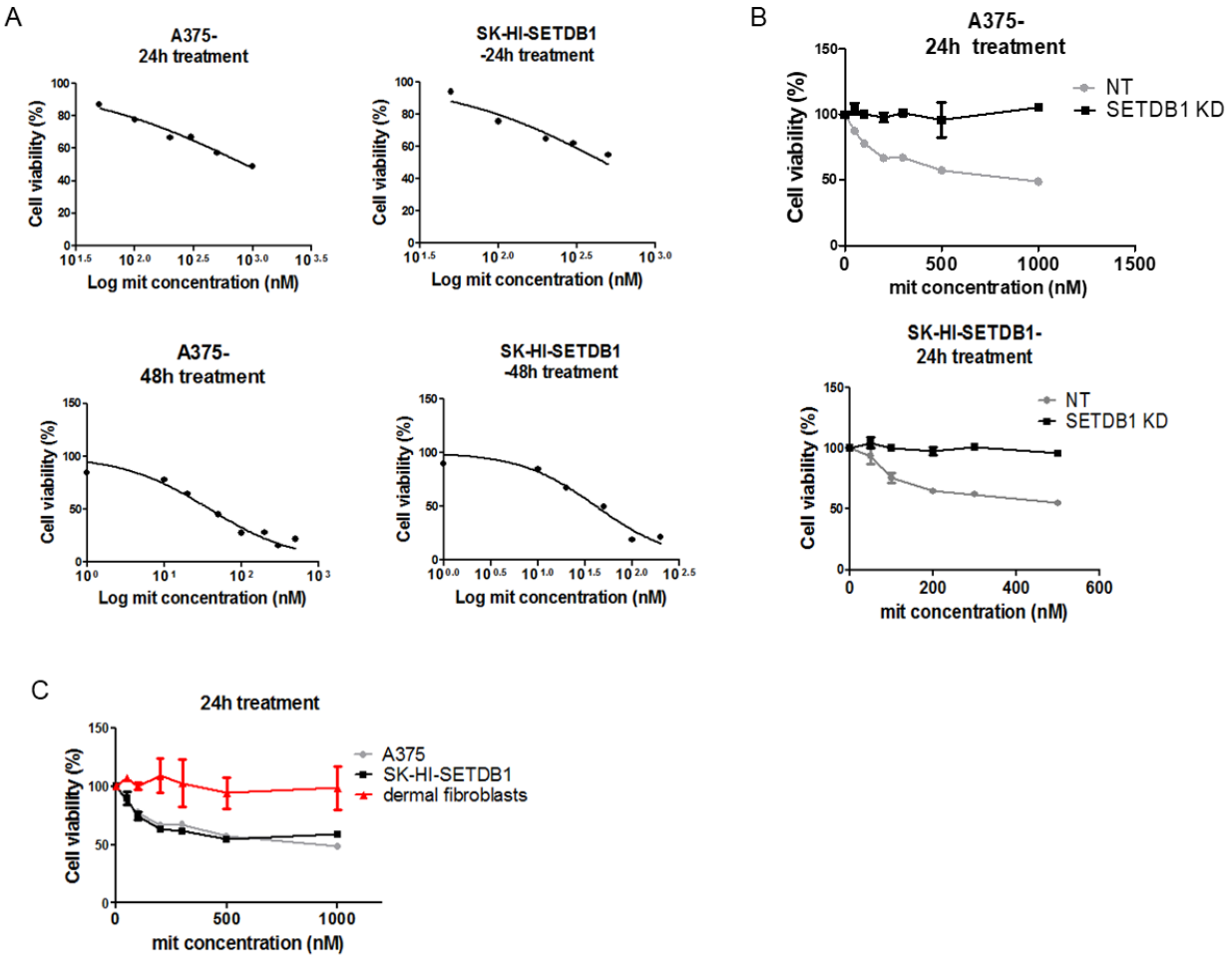

Figure 16: Melanoma cells showed great sensitivity to mithramycin A.A) Dose response curves of A375 and SK-HI-SETDB1 cells treated with increasing concentrations (nM) of mit for 24 and 48h. The viability of the cells treated with the vehicle control (DMSO) was set as 100%. B) Alamarblue assay to determine the viability of SETDB1 KD melanoma cells compared with the NT control upon 24h of mit exposure. C) Viability assay performed with dermal fibroblasts and two different melanoma cell lines treated with different mit concentrations for 24h.

In addition to an impairment of cell growth capacity, drastic changes in melanoma cell morphology were noted. Parental A375 cells appear like small and epithelioid cells, while SK-HI-SETDB1 cells (derived from the cell line SKMEL28) are bigger in size and possess dendritic structures. Upon mit exposure, both cell lines showed an altered morphology, with increased size, larger nuclei, reduction of cell-cytoplasm ratio and, for SK-HI-SETDB1 cells, less dendritic structures (**Figure 18**). From my data, one can conclude that mit reduced melanoma cell viability and altered their morphology via inhibiting SETDB1, which is specifically targeted by mit in a dose-dependent fashion.

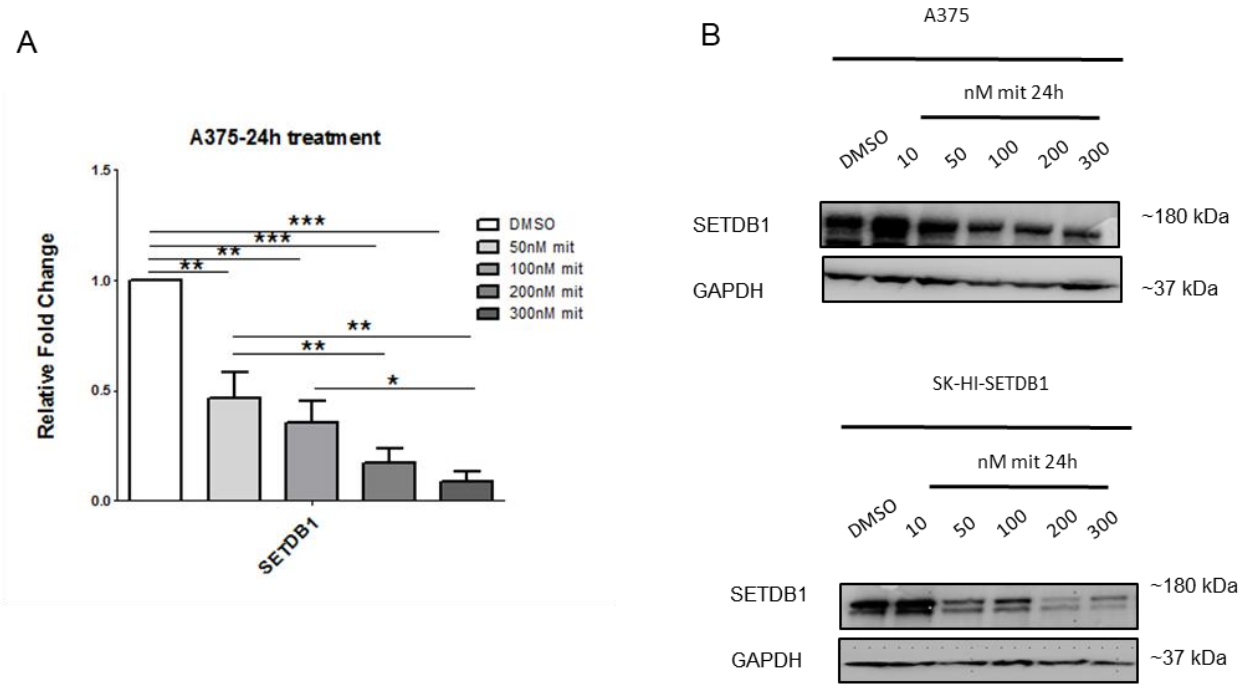

Figure 17: Mithramycin A completely abolished SETDB1 expression in melanoma cells.A) qPCR analysis of SETDB1 expression in A375 cells exposed to DMSO (control) and to increasing doses of mit for 24h. SETDB1 transcript levels decreased with increasing concentration of mit. B) Western blot detection of SETDB1 in A375 and SK-HI-SETDB1 cells showed a mit dose-dependent inhibition of SETDB1 expression

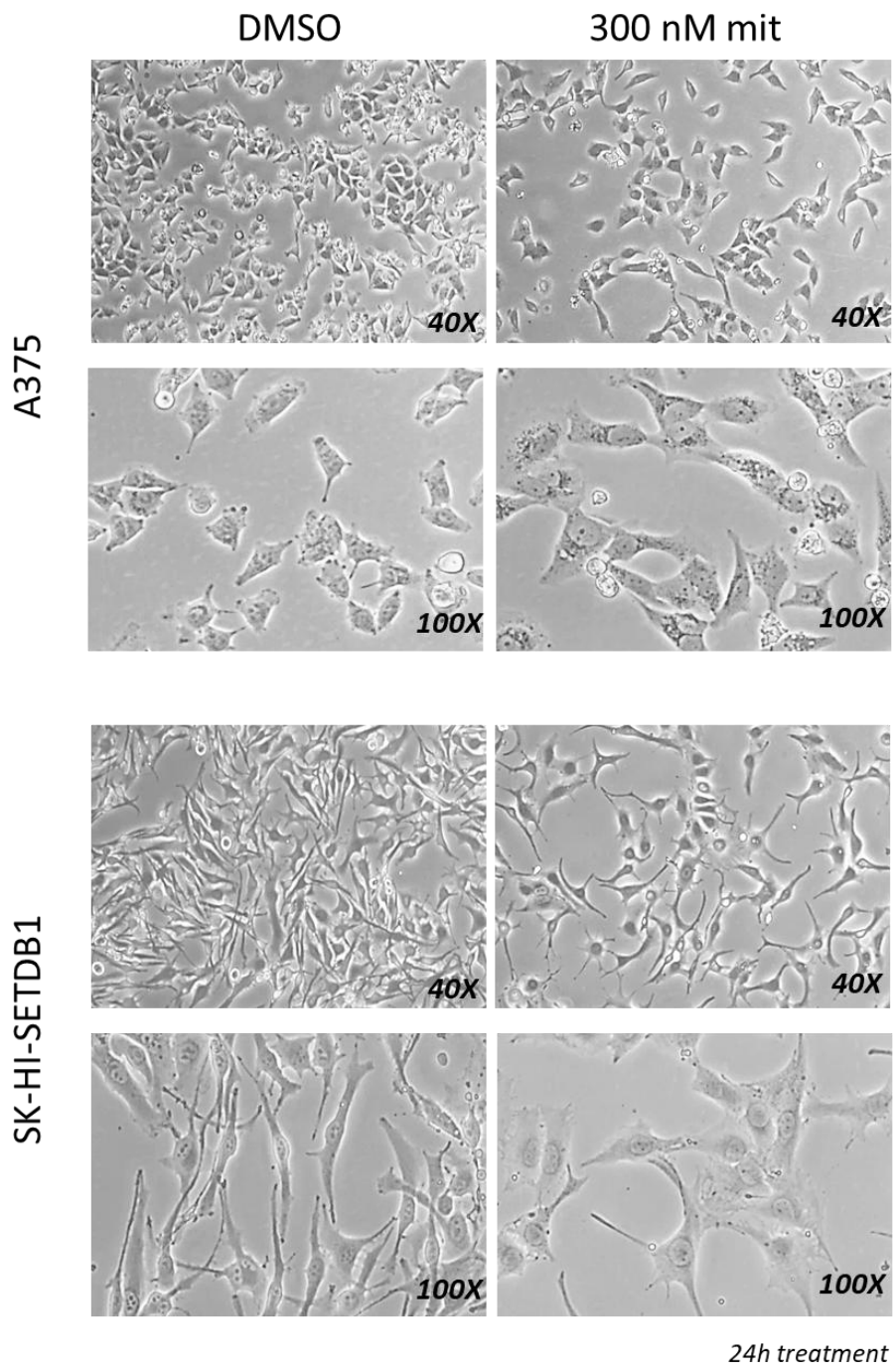

Figure 18: Mithamycin A treatment induced distinct morphological changes in melanoma cells. Following 300 nM mit-exposure for 24h, A375 and SK-HI-SETDB1 cells exhibited changes of cell size, shape and microscopic structures. Cells were magnified 40x and 100x with a light microscope.

4.9 Mithramycin A inhibition reverts the regulatory effect of SETDB1 on the expression of its downstream effectors

The consequences of mit-mediated SETDB1 inhibition were further analysed by evaluating variations in the regulatory network of SETDB1. A375 and SK-HI-SETDB1 cells were treated with 300 nM mit for 24h and afterwards the expression of SETDB1 downstream factors was assessed. It could be shown that the expression of pro-tumorigenic genes like *THBS1, SCG2, MMP3, IL6*, and *CCL2* was impaired. On the other hand, factors that were previously identified as "anti-metastatic", such as *DCT, TYRP1, ALDOC* and *APOE* displayed a strong induction (**Figure 19A and 19B**). These data further confirmed that several factors involved in cancer progression were regulated by SETDB1 and that SETDB1 inhibition led to the dysregulation of SETDB1-driven regulatory mechanisms. I also examined the H3K4me1 alterations related to SETDB1 expression in A375 cells following mit treatment. Focusing on the previously identified H3K4me1-binding region at the THBS1 promoter, it was possible to observe an enrichment of this histone mark upon drug treatment, mimicking the same epigenetic effect observed in SETDB1 KD cells (**Figure 19C**). I exploited the drug-based SETDB1-silencing approach to investigate the SETDB1-mediated DCT regulation. Although chromatin studies performed in this work did not reveal any alterations of chromatin state in the regulatory regions of the *DCT* gene, my data still indicate that SETDB1 impacts DCT expression on the transcriptional level. To test this hypothesis, the TRP2-lenti gene reporter plasmid was generated. TRP2-lenti is constituted of about 900 bp of the DCT promoter region containing melanocyte-specific *cis*-elements (Yokoyama et al, 1994) placed in front of the ORF of GFP. This construct was transduced in A375 and SK-HI-SETDB1 cells, which exhibit high endogenous SETDB1 and very low endogenous DCT expression. Consequently, transfected cells emitted no or only a very faint green fluorescence signal. However, following mit exposure, a general increase of the GFP signal was detected (**Figure 19D**). These data suggest that high SETDB1 expression suppresses DCT expression at the molecular level and, once SETDB1 was silenced, DCT was actively transcribed.

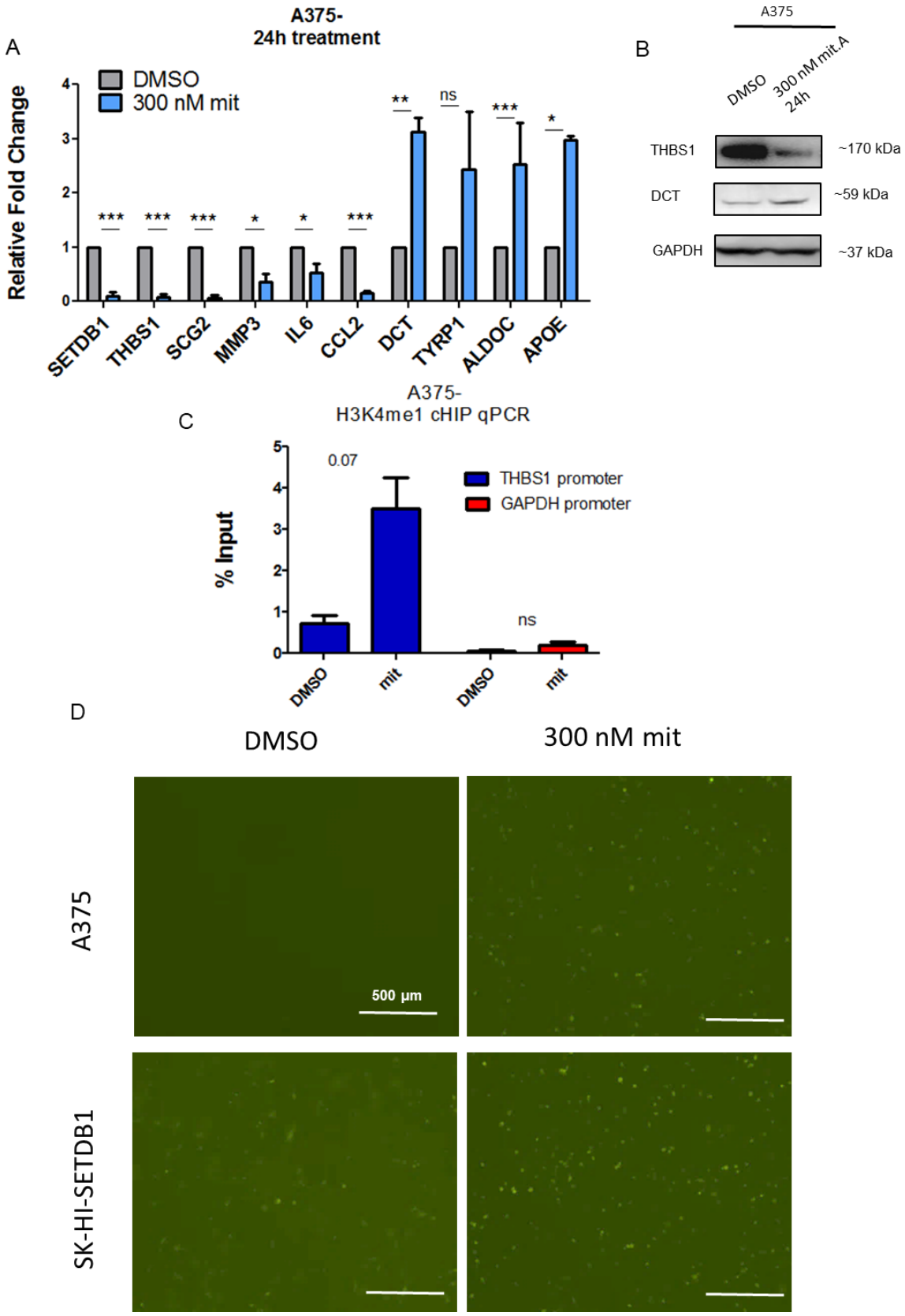
A
A375-
24h treatment
DMSO
300 nM mit
Relative Fold Change
SETDB1
THBS1
SCG2
MMP3
IL6
CCL2
DCT
TYRP1
ALDOC
APOE
B
A375
DMSO
300 nM mit.A
24h
THBS1
~170 kDa
DCT
~59 kDa
GAPDH
~37 kDa
C
A375-
H3K4me1 cHIP qPCR
% Input
0.07
THBS1 promoter
GAPDH promoter
ns
DMSO
mit
DMSO
mit
D
DMSO
300 nM mit
A375
SK-HI-SETDB1
500 µm

Figure 19: Gene expression analysis of melanoma cells following Mithramycin A-mediated SETDB1 inhibition.A) qPCR analysis of SETDB1 candidate downstream targets in A375 treated either with DMSO or with 300 nM mit. B) Immunoblotting for THBS1, DCT and GAPDH in the lysate of A375 cells treated with either DMSO- or mit. C) H3K4me1 ChIP-qPCR analysis of the THBS1 promoter region was performed in A375 cells cultured in the presence or absence of mit for 24h. Amplification of the GAPDH promoter served as a negative control. Plot represented the percentage of chromatin immunoprecipitated with a H3K4me1-specific antibody versus the total chromatin (input). D) Detection of GFP signals in A375 and SK-HI-SETDB1 melanoma cells, transduced with the TRP2-lenti construct and treated with 300 nM mit or DMSO by using fluorescence microscopy.

SETDB1-mediated secretory mechanisms may be affected by mit treatment. For this reason, proteome profiling of treated vs untreated cells was performed. Of note, mit-treated A375 cells showed a significant reduction of MMP8, IL8 and CCL2 secretion, while THBS1 secretion was not altered (**Figure 20**). Mit-mediated SETDB1 inhibition affected molecular mechanisms in melanoma, contributing to a drastic shift from an aggressive tumor cell-like behaviour towards a more differentiated phenotype.

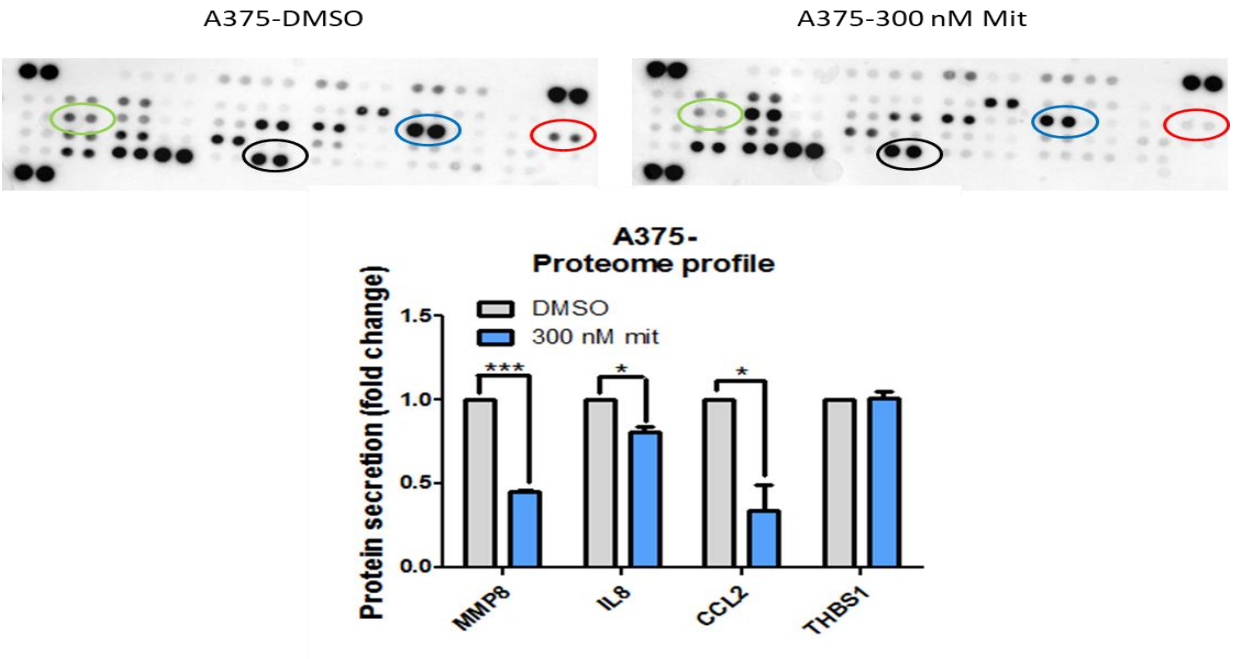

Figure 20: Downregulation of SETDB1 expression resulted in a decreased secretion of MMP8, IL8 and CCL2. Secretome analysis of A375 cells cultured for 1 day in the presence or absence of 300 nM mit performed with the Proteome profiler assay. Upper panel shows the mean pixel density of 55 different secreted proteins detected in the supernatant of cultured cells; MMP8 (blue circles), IL8 (green), CCL2 (red) and THBS1 (black) signals are highlighted. Lower panel displays the reduction of secretion of MMP8, IL8, CCL2 and THBS1 from cells exposed to mit, compared with the ones treated with DMSO.

4.10 Functional characterization of mithramycin A-treated melanoma cells

Knowing that mit treatment altered the expression of SETDB1 and its downstream targets in melanoma, I started examining the functional implications of this drug-induced process. As previously shown, SETDB1 knockdown or inactivation of its catalytic domain led to an impairment of the biological features mostly associated with aggressive tumor development and metastases formation, like cell motility, migration and invasion. I performed cell-based functional assays to ascertain whether mit treatment affects the migratory and invasive capacities of melanoma cells. Scratch wound healing and transwell invasion assays confirmed that mit-induced SETDB1 deprivation resulted in important reduction of cell motility, together with a drastically decreased invasion capacity (**Figure 21A and 21B**). To further investigate melanoma cell behaviour under the influence of the tumor microenvironment, a 2D invasion model was established. This system consists of a co-culture of melanoma cells and dermal fibroblasts. Previously, both cell types were fluorescently labelled by transduction with a lentiviral reporter constructs for fluorescence (GFP was constitutively expressed by melanoma cells, while fibroblasts expressed Tomato red fluorescent protein) to subsequently track them during the co-culture experiments. Initially, the two cell types were separated by a wound gap, allowing the cells to migrate towards each other. When the gap was fully closed, tumor invasive cells started to interact with fibroblasts and to invade the fibroblast layer that is composed of cells and extracellular matrix components released by fibroblasts. At this specific time point, mit was added (**Figure 22A**). Comparing the amount of invasive cells exposed to mit or DMSO (control) after 24 h showed significantly less mit-treated tumor cells scattered across the fibroblast layer compared with the control (**Figure 22B**). This indicated that the mithramycin A not only impaired the intrinsic migratory properties of the tumor cells, but also their capacity to interact with components of the tumor microenvironment. The impairment of the migratory and invasive properties of melanoma cells might be due to the deregulation of migration- and invasion-related proteins upon mit-mediated SETDB1 inhibition. Taken together, mit treatment led to a less aggressive melanoma cells phenotype characterized by reduced cell motility and invasive capacity.

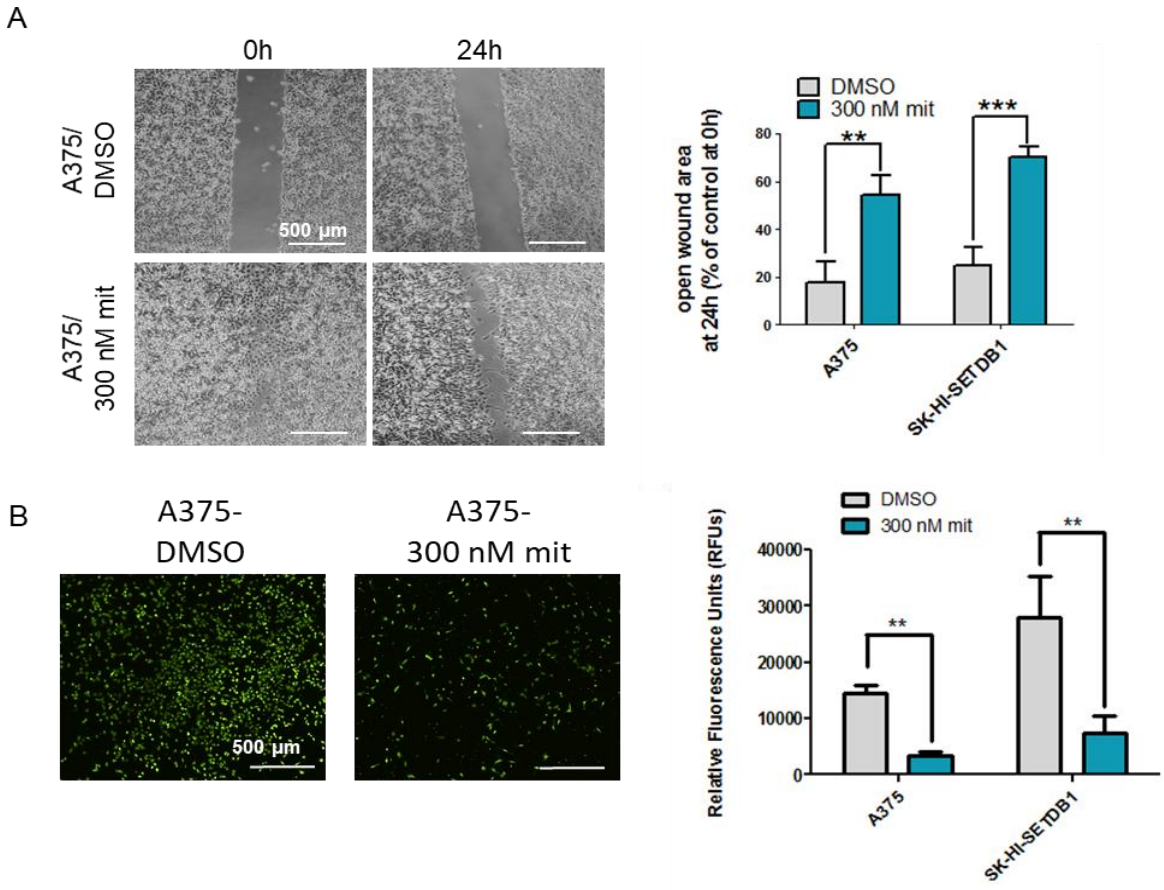

Figure 21: Migration and invasion analysis of melanoma cells exposed to mithramycin A.A) Quantification of the migration capacity of melanoma cells treated with DMSO or mit. On the left panel, representative images of scratch assays with A375 cells. On the right side, quantification of open gap area on scratched A375 and SK-HI-SETDB1 cell layers after 24h of stimulation. B) Transwell assay showing a strong reduction of invasion capacity of mit-treated melanoma cells. On the left side, microscopic images of invading fluorescent cells after DMSO- or mit-treatment. On the right side, quantification of the invasion rate for A375 and SK-HI-SETDB1 cells following mit exposure, measured as the relative fluorescence units (RFUs) released from these cells in comparison to DMSO-treated invading cells.

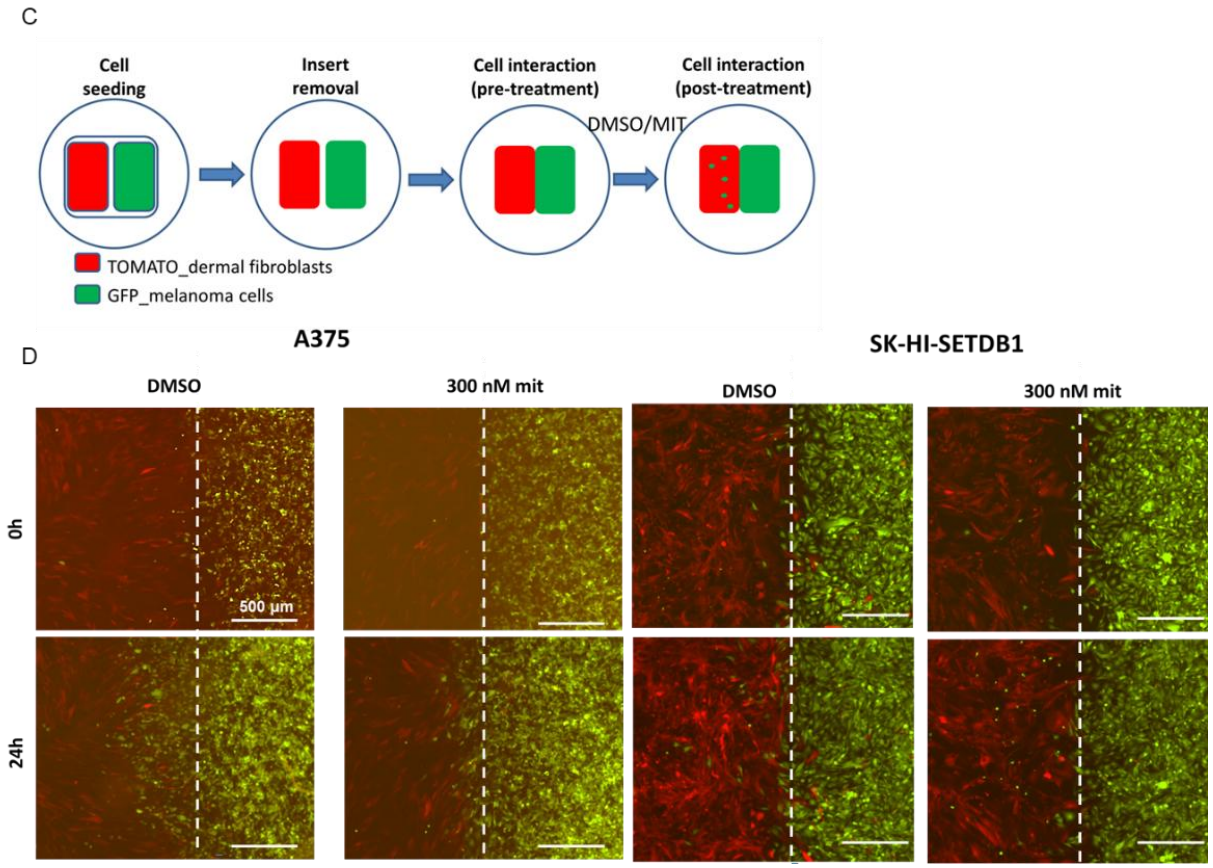

Figure 22: Mithramycin A limited the interactions of melanoma cells with dermal fibroblasts.A) Schematic overview of the 2D invasion system. B) Fluorescent images of 2D invasion assays. Melanoma cells and fibroblasts were co-cultured and subsequently exposed to 300 nM mit (or DMSO). After 24h, the number of tumor cells that have invaded the fibroblast layer was evaluated. A375 cells showed a massive invasive behavior, impaired by mit treatment. SK-HI-SETDB1 cells were able to disseminate within the fibroblast layer- Also in this case, mit totally inhibited the invasive capacity of SK-HI-SETDB1 cells (green dots observed at the front of the fibroblast layer were mostly non-viable tumor cells).

4.11 Combinatorial treatment of melanoma cells with mithramycin A and vemurafenib/trametinib enhanced the efficacy of targeted therapy

In order to find out if the application of mithramycin A might be a reasonable option for the treatment of melanoma, it was tested in combination with well-established targeted therapy compounds used in melanoma therapy. A375 and SK-HI-SETDB1 cells are known to be BRAF-mutated cell lines harbouring the V600E mutation in the BRAF protein. Due to this mutation the cells are sensitive towards the BRAF- and MEK-

inhibitors vemurafenib and trametinib, respectively. By treating melanoma cells with mithramycin A alone or in combination with vemurafenib or trametinib, I wanted to determine whether SETDB1-inhibition could increase the treatment efficacy. Cell viability assays with melanoma cells exposed to increasing concentrations of mit for 24h in combination with either 3 μM vemurafenib (mit+vem treatment) or 3 μM trametinib (mit+tra) showed that the combinatorial drug treatment induced more cell death than single drug-treatments (**Figure 23A and 23B**). A functional characterization of A375 and SK-HI-SETDB1 cells treated with SETDB1 inhibitor, BRAF/MEK inhibitors, and with a combination of all of them was done. Vem- and tra-treated cells showed a modest impairment of migratory and invasive capacity compared with the untreated ones, while the presence of mit for 24h triggered a functional regression of tumor cells (**Figure 23C and 23D**). As a conclusion, mithramycin A severely diminished the viability of melanoma cells expressing high amounts of SETDB1 and reduced their migrative and invasive capacity. Targeted therapies with MAPK inhibitors (vemurafenib and trametinib) in combination with mit showed an increased efficacy suggesting putative synergistic and multi-targeting mechanisms of action.

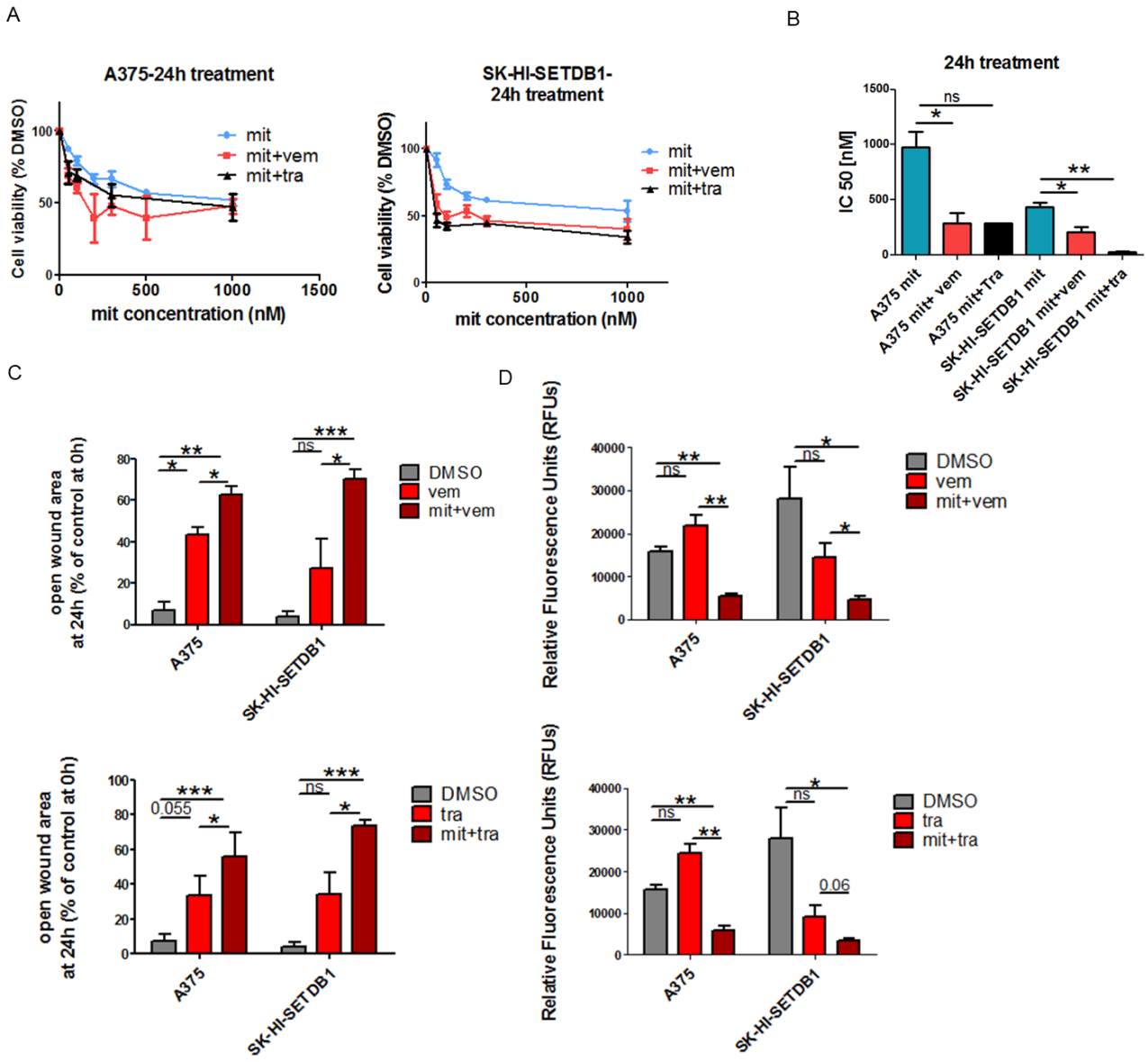

Figure 23: Treatment with mithramycin A in combination with BRAF-/MEK-inhibitors, strongly contributed to melanoma cell death and to an impairment of tumor cell features. A) Viability assay of A375 and SK-HI-SETDB1 melanoma cells treated with increasing doses of mit alone or in combination with sub lethal concentrations of vemurafenib (3 µM) or trametinib (3 µM). Cells showed a greater sensibility to the combined therapies after 24h. Viability of DMSO-treated (control) cells was set as 100%. B) A375 and SK-HI-SETDB1 mit IC_{50} (nM) related to the single treatment and in combination with vem and tra, for 24 hours. C) Quantification of the migration rate of melanoma cells. Cells were initially stimulated according to the established drug treatment conditions. After 8h, cells were scratched. Another 16h later the percentages of open gap area were defined. D) Transwell invasion assay performed with A375 and SK-HI-SETDB1 cells showing that the addition of 300 nM mit greatly reduced the invasive capacity of BRAF-mutated cell lines that were simultaneously treated with vemurafenib (mit+vem) or trametinib (mit+tra), compared to the same cells treated with the respective BRAF-inhibitor only.

5 Discussion

The incidence and mortality rates of malignant melanoma have dramatically increased over the past decade. Well-established and FDA-approved melanoma treatments based on immunotherapies and targeted therapies achieved good clinical responses. Nonetheless, these therapeutic approaches are still limited by the presence of adverse effects related to poor drug specificity, lack of efficacy and development of resistance mechanisms. Therefore, identification of innovative treatment strategies represents the biggest challenge in this field. Melanomas exhibit high levels of complexity and intratumoral heterogeneity (Andor et al, 2016). Tumor initiation, progression and metastasis are all the result of multiple, concomitant molecular events leading to the alteration of numerous cell signaling pathways. A better understanding of novel cancer-promoting mechanisms is essential to improve melanoma treatment options. Recently, some studies shed light on the contribution of epigenetic processes to melanomagenesis. In particular, the histone methyltransferase SETDB1 seems to play a pivotal role during melanoma progression. However, the precise mechanisms of action of SETDB1 are still unclear.

In this study, I elucidated the functional role of SETDB1 in melanoma, showing that: i) SETDB1 acted as master regulator of an oncogenic transcriptional network, ii) SETDB1 expression was associated with drastic changes of the epigenetic profile of melanoma cells, and iii) mithramycin A reduced cancer cell-specific features and induced death of melanoma cells by specifically targeting SETDB1.

5.1 SETDB1 promotes melanoma progression by modulating the expression of specific downstream effectors

Previous studies indicated an oncogenic role for SETDB1 in melanoma suggesting that this factor might be involved in cancer-related molecular processes. The first set of analyses examined the contribution of SETDB1 to inducing transcriptomic changes during melanoma tumorigenesis. Transcriptional profiling identified differentially

expressed genes following ectopic overexpression of SETDB1 in HT144 melanoma cells. Functional annotation revealed that many genes upregulated in SETDB1-overexpressing cell lines were part of gene sets related to regulation of cell proliferation, cell motility and EMT. These genes have been found to be more strongly expressed in melanoma and other tumor cells, such as breast and prostate cancer (Schartl et al, 2012) (Smit et al, 2016) (Yuan et al, 2015) (Ahmed et al, 2018). *In silico* interpretation of transcriptomic data suggested that high levels of SETDB1 induced the upregulation of multiple pro-tumorigenic factors in melanoma cells.

The analysis of putative SETDB1 target genes was extended to a group of secreted oncoproteins, whose expression was induced by SETDB1. Alterations of the tumor cell secretome heavily contribute to tumorigenic processes and, for this reason, represent a hallmark of carcinogenesis (Paltridge et al, 2013). Differential expression analysis indicated that SETDB1 upregulation increased the expression of genes encoding secreted proteins. Deregulated factors included the matricellular protein THBS1, the granule protein SCG2, the cytokine IL6, matrix metalloproteases (MMP1 and MMP3) and chemokines (CCL2 and CXCL8). SCG2 is a member of the granin family. Peitsch et al. demonstrated that SCG2 is highly expressed in primary and metastatic melanoma and that it is implicated in a cellular mechanism promoting melanoma cell migration (Peitsch et al, 2014). The role of IL6, matrix metalloproteases and chemokines in melanoma progression has been extensively studied by several groups (Hoejberg et al, 2012) (Moro et al, 2014) (Payne & Cornelius, 2002). In this work, I focused on the role of thrombospondin 1 (THBS1) as a putative downstream target of SETDB1. *THBS1* encodes for a multidomain glycoprotein belonging to the thrombospondin family. The THBS1 protein drives variegated effects in a wide range of tumors (Huang et al, 2017). In melanoma, THBS1 is expressed in mesenchymal-like cells and metastatic tumor biopsies. In this context, THBS1 enhances EMT, angiogenesis, pro-migratory, pro-invasive and pro-metastatic activities (Jayachandran et al, 2014) (Borsotti et al, 2015). Moreover, THBS1 needs to bind to the CD47 receptor to promote melanoma metastasis dissemination (Jeanne et al, 2016). While the oncogenic functions of THBS1 have been elucidated widely, little is known about THBS1 regulation. SETDB1 gain- and loss-of-function experiments showed that SETDB1 induced THBS1 expression in melanoma

cells, while SETDB1-knockdown resulted in decreased THBS1 levels. In addition to this, THBS1-knockdown in SETDB1-overexpressing melanoma cells impaired the migration capacity distinctly, supporting the hypothesis that THBS1 plays a role in establishing the SETDB1-induced migratory phenotype. This newly identified SETDB1-THBS1 axis was next examined in primary and metastatic melanoma tumor biopsies. Immunohistochemistry combined with tissue microarray analysis represents a powerful tool which allows to efficiently evaluate and compare the expression patterns of putative candidate factors in a large cohort of patients-derived samples, providing meaningful insights into the identification of predictive and prognostic tumor markers (Jawhar, 2009) (Schmidt et al, 2009). SETDB1 is frequently overexpressed in clinical melanoma samples (Ceol et al, 2011) (Miura et al, 2014). Patients included in this study were classified based on their SETDB1 IHC score. In line with previous works (Jayachandran et al, 2014) (Borsotti et al, 2015), THBS1 was found to be highly expressed in most of the analyzed melanoma tissues. Intense THBS1 signals were predominantly detected in cancer specimens with high SETDB1 expression, while patients characterized by low levels of SETDB1 expression also exhibited weak THBS1 signals. Hence, the co-expression of SETDB1 and THBS1 in tumor biopsies strongly corroborated their close connection. By further exploring SETDB1 and THBS1 expression patterns in primary melanoma tumor tissues, I could observe that both factors are heterogeneously distributed within the same lesion, showing more pronounced signals in outer regions corresponding to the invasive front of a tumor (Bryne et al, 1998). Several studies showed that accumulation and activation of tumorigenic factors in the tumor invasive area is an important indication of an aggressive phenotype of a tumor (Hofmann et al, 2003) (Mitsui et al, 2014) (Staub et al, 2007). In light of this, SETDB1 and THBS1, both identified as promoters of cell invasion, localize at the invasive fronts of melanomas. The colocalization of SETDB1 and THBS1 might represent a valid prognostic marker for advanced melanomas.

By analyzing differentially expressed genes in SETDB1 OE cell lines I identified several genes, whose expression seems to be negatively affected by SETDB1. These factors can be functionally classified into two different groups: melanocyte differentiation markers and metabolic enzymes. Pro-differentiation factors found downregulated

following overexpression of SETDB1 in melanoma cells included tyrosinase (TYR), tyrosinase-related protein 1 (TYRP1), dopachrome tautomerase (DCT, TRP2) and the premelanosome (PMEL17, gp100) proteins. These proteins are known as regulators of melanocyte development and functions (Guyonneau et al, 2004) (Raposo & Marks, 2007). In melanoma, the role of melanocytic markers is still under debate: while several studies report a loss of DCT, TYR and TYRP1 during melanoma progression (Lenggenhager et al, 2014) (Lee et al, 2018a) (Fang et al, 2002), others report that melanoma subpopulations can express these factors (Aris et al, 2012) (Pak et al, 2004). However, the expression of pro-differentiation markers positively correlates with a favorable clinical outcome in patients with metastatic melanoma (Takeuchi et al, 2003). In this study, the SETDB1-dependent expression of DCT in melanoma cells was examined. In SETDB1 OE melanoma cells, characterized by a more proliferative and aggressive behavior, DCT expression was strongly reduced, whereas high levels of DCT were observed in melanoma cell lines with low endogenous SETDB1 expression. This negative correlation suggests that SETDB1-positive cell populations possess might be less differentiated. The metabolic factors aldolase C (ALDOC) and apolipoprotein E (APOE) were also silenced upon SETDB1 induction. ALDOC and APOE mediate anti-tumorigenic effects: ALDOC expression negatively correlates with migration and invasion properties of oral squamous cell carcinoma (OSCC) cells (Li et al, 2016) and it is recruited as an effector by the metastasis suppressor NME1 in melanoma (Pamidimukkala et al, 2018). APOE acts as anti-angiogenic and anti-metastatic factor inducing melanoma regression (Pencheva et al, 2012). Hence, the findings of this study suggest that SETDB1 induced drastic transcriptomic changes characterized by the concomitant activation of a genes associated with augmented tumorigenesis and tumor progression and, on the other side, the repression of pro-differentiation/ anti-tumorigenic factors.

Knowing about SETDB1-mediated gene regulatory effects, further experiments were performed with the purpose to identify mechanisms of action of SETDB1 in greater detail. In particular, the aim was to ascertain if SETDB1 functions were related to its catalytic SET domain, which modulates the HMT activity of SETDB1. Moreover, the SET domain is directly involved in protein-protein interactions (Yeates, 2002). In order to

study the role of the SET domain, additional experiments were performed with a SETDB1-variant lacking the HMT activity due to two amino acid exchanges. Point mutations in the SET domain may lead to a complete inactivation of SETDB1, either by directly changing the catalytically active amino acid residues or by altering the structural conformation of the whole protein. Several somatic mutations of the SET domain of SETDB1 have been previously identified in patients. These mutations include missense alterations (G869E, C911F, S947C) and an in-frame deletion (F1250del). G869E resulted in a complete inactive protein (Kang et al, 2016). Ceol et al. described the effects of two amino acid substitutions (H1224K and C1226A) in a melanoma zebrafish model: mutated SETDB1 did not completely lose the methylation activity, since it was still recruited by other H3K9 HMTs, forming a multimeric complex (Ceol et al, 2011). However, this study showed that the H1224K/C1226K substitutions in the SET domain heavily impacted the effects of SETDB1 on human melanoma. First, a severe reduction of total H3K9me3 levels was observed in melanoma cells expressing the mutated SETDB1 variant, in comparison to cells expressing wild-type SETDB1. Moreover, whole-transcriptome analysis revealed that genes deregulated upon expression of SETDB1 where not deregulated in response to the expression of HC/KA SETDB1. HC/KA SETDB1 OE cells exhibited reduced THBS1 and increased DCT expression. This finding strongly confirmed that THBS1 and DCT served as SETDB1 target genes, and moreover suggested that the SET domain is responsible for THBS1 and DCT regulation. Integration of gene expression data with functional annotations unveiled the deregulation of biological processes related to cancer development and invasiveness, showing a negative correlation with the expression of the mutated SETDB1 variant. On the other hand, inactivation of the catalytic activity of SETDB1 abolished the repression of pro-differentiation genes by wild type SETDB1. Functional experiments validated these observations. Scratch migration and transwell invasion assays constitute effective and reliable *in vitro* approaches to assess the motile properties of tumor cells (Kramer et al, 2013). HC/KA SETDB1 OE cells exhibited limited migratory and invasive capacities compared with cells overexpressing the wild type SETDB1. Therefore, SET domain disruption led to an impairment of melanoma cell aggressiveness. Surprisingly, analysis of the proliferative rate of tumor cells did not reveal significant discrepancies in relation

to the mutational status of SETDB1. The lack of an anti-proliferative effect despite the concomitant reduction of cell migration and invasion may be the consequence of melanoma phenotype switching. In tumor cells, proliferation and invasion are uncoupled functions defined by different gene signatures (Hoek et al, 2008). Although SETDB1 expression has been linked to increased cell proliferation (Orouji, 2016), the data presented here suggest that the catalytic activity of the SET domain of SETDB1 mainly affects cell motility, while proliferative effects might be regulated by the other functional domains of SETDB1, such as MBD and tudors.

5.2 Analysis of epigenetic alterations in melanoma cells following SETDB1 dysregulation

Epigenetic regulators are often involved in cancer progression, either directly acting as transcription factors or through the modulation of epigenetic marks, providing the substrate for the transcriptional machinery. SETDB1 mediates the trimethylation of lysine residue number 9 (K9) on histone H3. H3K9me3 is typically known as a repressive chromatin mark. Nonetheless, SETDB1 was shown to promote the expression and secretion of pro-tumorigenic proteins. In order to address these apparently contradictory facts, the next set of analyses aimed at detecting and characterizing SETDB1-induced epigenetic alterations in cancer cells. ChIP sequencing was performed to investigate the whole-genome chromatin structure in melanoma cells. ChIP-seq analyses have greatly contributed to the identification of novel key factors deregulated in different cancer types (Zhang et al, 2014) (Raj et al, 2017). This study mainly focused on the detection of histone marks related to regulatory processes. As expected, ChIP-seq analysis of H3K9 trimethylation in melanoma cells proved that SETDB1 was the major regulator of genome-wide H3K9me3 distribution: increased SETDB1 levels resulted in an enrichment of chromatin sites marked by H3K9me3. This was in accordance with H3K9me3 protein levels detected in SETDB1 OE cells. Increased global H3K9me3 levels correlate with malignant transformation, dedifferentiation, pro-invasive behavior, drug tolerance and poor clinical outcome in

several cancer types, such as colorectal cancer, liposarcoma, melanoma and salivary adenoid cystic carcinoma (Yokoyama et al, 2013) (Keung et al, 2015) (Al Emran et al, 2018) (Xia et al, 2013). Conversely, SETDB1 knockdown strongly impaired the genome-wide abundance of H3K9me3 marks. It has been previously reported that tumor cells with reduced H3K9me3 levels acquire a differentiated phenotype or undergo apoptosis (Lee et al, 2018b) (Lu et al, 2018). Taken together, the abundance of the H3K9me3 mark could serve as an important prognostic factor in cancer.

While SETDB1 expression showed a positive correlation with H3K9me3 in melanoma cells, an opposite trend was observed for the levels of monomethylated lysine 4 on histone H3 (H3K4me1) at the *THBS1* promoter: increased H3K4me1 marks were observed upon SETDB1-silencing. The H3K4me1 mark is preferentially located at promoter and enhancer regions of active genes. H3K4 mono– and trimethylated forms are normally mutually exclusive and show differential distribution patterns in regulatory regions: while H3K4me3 marks are restricted to areas proximal to transcription start sites (TSS), H3K4me1 shows a widespread distribution on the entire promoter region and beyond the TSS (Cheng et al, 2014). H3K4me3-enriched active promoters show reduced levels of H3K4me1. Moreover, promoter-associated H3K4me1 marks modulate gene repression (Heintzman et al, 2007) (Cheng et al, 2014). A recent work conducted by Perner et al. exploited computational approaches to predict interactions between histone modifiers and chromatin marks. The data showed that a negative correlation exists between SETDB1 and H3K4me1, indicating that either SETDB1-chromatin association fails in the presence of H3K4me1 or, alternatively, H3K4me1-genome enrichment is reduced by SETDB1 expression (Perner et al, 2014). In light of this, H3K4me3 ChIP-seq data suggest that SETDB1 regulated the expression of its target genes via the modulation of H3K4me1 epigenetic marks at crucial regulatory sites.

The mechanism behind the SETDB1-mediated alteration of H3K4me1 still remains poorly understood. Epigenetic effects induced by SETDB1 might be directly carried out by other chromatin regulators, which would act as SETDB1 interaction partners. The H3K4me1-enriched region at the *THBS1* promoter represents a CTCF binding motif frequently occupied by the transcriptional repressor CTCF in a large number of cell

types (source: UCSC, https://genome.ucsc.edu/). CCCTC-binding factor (CTCF) is a zinc finger protein involved in numerous molecular processes related to maintenance of chromatin architecture and regulation of gene expression (Kim et al, 2015). Several histone modifications, including H3K4me1, localize in CTCF genomic sites and are involved in CTCF-mediated genomic mechanisms, such as chromatin looping and condensation (Barski et al, 2007) (Weth et al, 2014) (Oti et al, 2016). Interestingly, Jiang et al. reported that SETDB1 is essential for maintaining the correct 3D genome structure in mouse and human neuronal cells. SETDB1-silencing causes disruption of topologically associated domains (TADs), large genomic structures crucial for chromatin conformations (Dixon et al, 2016) and, strikingly, transcriptomic dysregulation of TAD-associated genes. Mechanistically, it was observed that TAD alterations caused by *SETDB1* ablation were accompanied by aberrant CTCF genomic binding (Jiang et al, 2017). Based on these observations, it is quite possible that CTCF may be implicated in epigenetic alterations induced by SETDB1 in melanoma.

5.3 Effects of the SETDB1 inhibitor mithramycin A on melanoma cells

Development of novel strategies for targeted therapy represents a growing area of cancer research. Over the past few years, considerable research efforts have been devoted to the identification and characterization of key factors that could serve as therapeutic targets.

Given its relevant oncogenic role, targeting SETDB1 may represent a promising therapeutic option for melanoma treatment. The DNA-binding antibiotic mithramycin A (mit) suppresses SETDB1 expression by modulating SP-1 protein activity. Mit exhibits potent antitumor effects in several types of cancer (Ream et al, 1968) (Dutcher et al, 1997) (Choi et al, 2014). Moreover, mit was included in a phase II clinical trial for the treatment of lung cancer, esophageal cancer, breast cancer, mesothelioma and gastrointestinal neoplasms (NCT01624090). Lung cancer cells treated with mit show reduced proliferation and decreased levels of SETDB1. Notably, mit treatment is only

effective against lung cancer cell lines with high SETDB1 gene amplification and expression levels (Rodriguez-Paredes et al, 2014). In this study, mit was tested on melanoma cell lines. Cell viability assays demonstrated that melanoma cells with extra *SETDB1* gene copies (SK-HI-SETDB1) and elevated levels of SETDB1 expression (A375) were particularly sensitive to mit treatment, whereas non-malignant cells, like dermal fibroblasts, as well as SETDB1-silenced melanoma cells were not affected by mit exposure. Furthermore, mit treatment abrogated SETDB1 expression in melanoma cells in a dose-dependent manner. These findings completely confirmed the inhibitory effects of mit observed in lung cancer cell lines.

Tumor cells exposed to anticancer drugs display deep alterations in morphology and function. Mit treatment led to drastic morphological changes of melanoma cells, exhibiting larger nuclei and less-pronounced membrane protrusions. Previous experiments revealed that ectopic expression of SETDB1 induced melanoma cells to acquire a more elongated, spindle-shaped morphology (Orouji, 2016). It has been reported that such morphological changes are predictive of an enhanced aggressive tumor cell behavior (Friedl & Alexander, 2011). Mit treatment seemed to revert this morphology. Changes of the shape of mouse and human melanoma cell were observed also upon treatment with doxorubicin and MAPKi (Mariani & Supino, 1990) (Powell et al, 2016).

In melanoma, $BRAF^{V600E}$-targeting therapy changes the transcriptome (Wongchenko et al, 2017) and secretome (Obenauf et al, 2015) of tumor cells. In a similar way, mit induced alterations of gene expression and protein secretion in melanoma cells. The pharmacological downregulation of SETDB1 with mit confirmed the downregulation of pro-tumorigenic and pro-invasive factors and increased levels of pro-differentiation and metabolic markers observed in SETDB1 knockdown or HC/KA SETDB1 OE cells. Once again, SETDB1 deregulation resulted in a bivalent gene expression pattern affecting melanoma cell properties and behavior.

In this study, the secretome of melanoma cells was analyzed with regard to SETDB1 expression levels. Profiling of the secretomes indicated that SETDB1 inhibition limited the release of several oncoproteins. Amongst the factors whose secretion was impaired

by mit treatment I could detect CCL2, a major driver of melanoma progression and metastasis (Payne & Cornelius, 2002), IL8, an inducer of angiogenesis found highly expressed in melanoma metastasis (Singh & Varney, 2000), and MMP8, which has been found to be frequently mutated and overexpressed in melanoma (Giambernardi et al, 2001) (Palavalli et al, 2009). Contrary to expectations, the level of secreted THBS1 was not affected by SETDB1 inhibition. This observation could be attributed to the multifunctional nature of the THBS1 protein due to its multimodular structure, which allows THBS1 to participate in different intra- and extracellular signaling pathways (Sid et al, 2004) (Resovi et al, 2014). In light of this, I speculated that endogenous THBS1 intracellular interactions are involved in melanoma progression.

THBS1 repression in mit-treated melanoma cells was shown to correlate with increased H3K4me1 at its promoter. Hence, mit also contributes to epigenetic effects. The impact of mit on epigenetic mechanisms has been previously reported by Banerjee et al., who observed that mit directly interacts with histone proteins and modulates histone modifications related to gene transcription, such as H3K18 acetylation (Banerjee et al, 2014).

As opposed to THBS1, DCT expression was strongly enhanced by mit exposure. DCT expression and DCT gene promoter activity are increased upon mit treatment, proving that SETDB1-mediated *DCT* regulation occurs at the transcriptomic level. This finding suggests that SETDB1-silencing induced melanoma tumor regression and the activation of a transcriptional program related to differentiation. ChIP-seq data analysis did not reveal any epigenetic alterations in the regulatory region of the *DCT* gene. I conclude that alternative genetic or epigenetic mechanisms, influenced by SETDB1, modulate DCT expression.

The investigation of the effect of SETDB1-inhibition on the functional properties of melanoma cells showed that mit treatment strongly suppressed their migration and invasion capacity. Mit modulate similar effects in several cancers: in glioma mit represses the expression of migration-related factors, impairing the glioma cell migratory

capacities; in salivary adenoid cystic carcinoma, mit limits cell invasion and EMT, while mit treatment reduces invasive and metastatic potential in lung cancer cells (Seznec et al, 2011) (Li et al, 2017) (Lin et al, 2007). In addition to wound healing and transwell assays, a 2D invasion model was used to better characterize melanoma cell motility. *In vitro* 2D invasion systems aim at simulating the conditions found in solid-tumor microenvironment, like the interaction with stromal cells (fibroblasts) and soluble factors released by fibroblasts (Nnetu et al, 2012). Melanoma cells activate fibroblasts which in turn sustain tumor cell growth, malignant transformation and drug resistance (Flach et al, 2011). In the presence of mit, however, melanoma cells which were in direct contact with fibroblasts still failed to migrate and invade the fibroblast layer.

Lastly, I evaluated the anti-tumorigenic effect of SETDB1-inbition in combination with established inhibitors of components of the MAPK pathway that is frequently deregulated in melanoma. BRAF- and MEK-inhibitors lead to melanoma cell death and tumor regression, resulting in positive clinical responses and improved outcomes. However, treatment with these inhibitors shows limited efficacy due to acquired mechanisms of drug resistance. Development and establishment of combinatorial/multi-targeted therapeutic strategies able to circumvent drug resistance represents the current challenge in melanoma research. Drug-response experiments revealed that mit, in combination with vemurafenib or trametinib, cooperatively promoted anti-proliferative, anti-migratory and anti-invasive effects. Furthermore, targeting SETDB1 mostly enhanced anti-tumorigenic effects in combinatorial treatments, whereas treatment with single MAPK inhibitors did not show any strong impairment of the migration and invasion capacity of melanoma cells. Taken together, my data suggests that combinatorial treatment of melanoma cells with mithramycin A and vemurafenib or trametinib could be a much more potent and more effective therapeutic option compared to single treatment with BRAF-inhibitors alone.

6 Conclusions

The present work aimed at providing a better understanding of the role and the functions of the histone methyltransferase SETDB1 in melanoma. Previous studies indicated that SETDB1 acts as major driver of melanoma progression. Melanoma cell lines and clinical tumor biopsies exhibit aberrant *SETDB1* amplification and expression, and high levels of SETDB1 correlate with an aggressive phenotype of melanoma cells. Nevertheless, the mechanistic role of SETDB1 in the context of melanoma was largely unknown.

Here, I present data indicating that SETDB1 exerts its oncogenic functions during melanoma progression through regulating the transcription of downstream targets and altering epigenetic mechanisms (**Figure 24A**). On the basis of my findings one can propose a model where SETDB1 exerts relevant transcriptomic effects in melanoma, in particular as activator of pro-tumorigenic factors, such as THBS1, and as a repressor of melanocyte-specific genes related to differentiation, like DCT. I conclude that the pro-tumorigenic effects mediated by SETDB1 during melanoma progression are the consequences of the activation of the newly identified SETDB1-centered regulatory network. Abolishment of the catalytic activity of SETDB1 totally abrogated the SETDB1-mediated oncogenic effects in melanoma cells.

This project also investigated the variations in the epigenetic landscape in melanoma cells. Findings of this work demonstrated that SETDB1 drove drastic epigenetic changes. SETDB1 dysregulation resulted in alterations of global H3K9me3 and local H3K4me1 mark distribution. In particular, differential H3K4me1 enrichment patterns modulate the expression of the SETDB1 target gene *THBS1.*

Exposure of melanoma cells to the SETDB1 inhibitor mithramycin A (mit) indicates that they are sensitive to this potent antitumor drug widely used in clinical studies on cancer treatment. Mit effectively suppressed the expression of SETDB1 and induced changes at the transcriptomic, epigenetic, morphological and functional level. To conclude, SETDB1 inhibition enhanced the efficacy of established MAPKi therapies against melanoma (**Figure 24B**). In conclusion, this work supports the central role of SETDB1

as a key regulator of melanoma progression and as a promising candidate target for treating advanced melanoma. The development of novel therapeutic strategies aiming at selectively targeting SETDB1 expression and functions may result in significant clinical benefits.

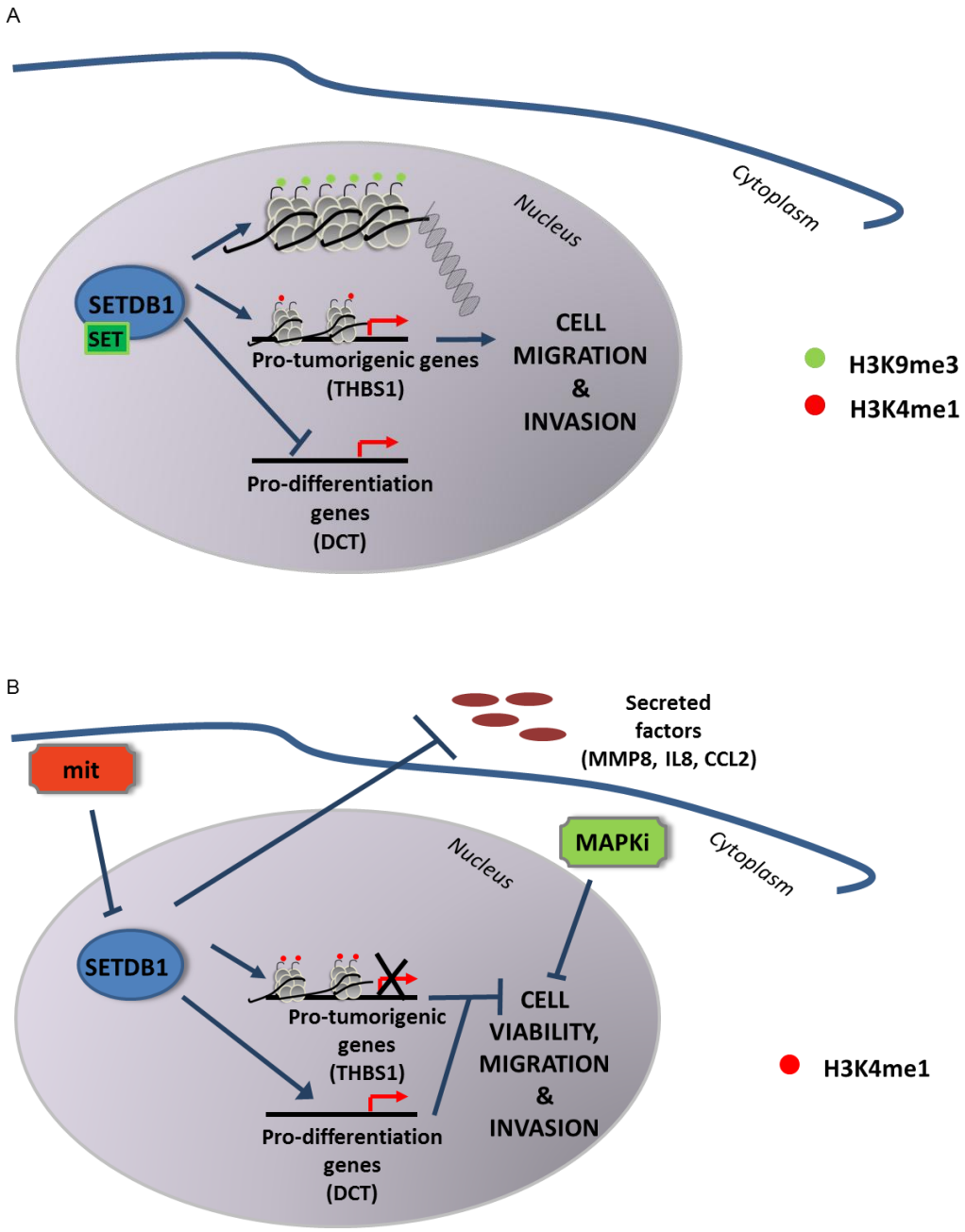

Figure 24: Schematic overview of the mechanistic role of SETDB1 in melanoma cells.A) SETDB1 expression induces drastic transcriptomic, epigenetic and functional effects. SETDB1 induces the

expression of oncogenic factors, such as THBS1, while it limits the expression of anti-metastatic and pro-differentiation genes, like DCT. The levels of the histone methyltransferase SETDB1 positively correlate with the global enrichment of its histone modification target, H3K9me3. SETDB1 expression strongly affects the monomethylated H3K4 distribution at *THBS1* regulatory sites, determining in this way the transcriptional regulation of THSB1. The activation of SETDB1-centered regulatory network in melanoma cells results in the acquisition of tumor aggressive properties, like cell migration and invasion. The oncogenic role of SETDB1 in melanoma is dependent by the activity of its catalytic SET domain. B) The antitumor antibiotic mithramycin A selectively inhibits SETDB1 expression in melanoma cells, reverting in this way all the SETDB1-mediated pro-tumorigenic effects: melanoma cells under mit treatments exhibit low expression of SETDB1 target oncogenes and high levels of genes downregulated by SETDB1 and involved in cell differentiation or cell metabolism mechanisms. THBS1 downregulation in SETDB1 high-expressing cells is accompanied by increased levels of H3K4me1 surrounding *THBS1* promoter region. SETDB1 inhibition results in a reduction of MMP8, IL8 and CCL2 protein secretion. Melanoma cells treated with mit show reduced cell viability, migration and invasion. Mit effects are increased in combinatorial treatments with MAPK inhibitors vemurafenib and trametinib.

7 References

(2015) A targeted therapy-driven tumor secretome underlies drug resistance. Cancer discovery 5**:** OF8

Abildgaard C, Guldberg P (2015) Molecular drivers of cellular metabolic reprogramming in melanoma. Trends in molecular medicine 21**:** 164-171

Aguissa-Toure AH, Li G (2012) Genetic alterations of PTEN in human melanoma. Cellular and molecular life sciences : CMLS 69**:** 1475-1491

Ahmed M, Lai TH, Zada S, Hwang JS, Pham TM, Yun M, Kim DR (2018) Functional Linkage of RKIP to the Epithelial to Mesenchymal Transition and Autophagy during the Development of Prostate Cancer. Cancers 10

Al Emran A, Marzese DM, Menon DR, Stark MS, Torrano J, Hammerlindl H, Zhang G, Brafford P, Salomon MP, Nelson N et al (2018) Distinct histone modifications denote early stress-induced drug tolerance in cancer. Oncotarget 9**:** 8206-8222

Alcazar O, Achberger S, Aldrich W, Hu Z, Negrotto S, Saunthararajah Y, Triozzi P (2012) Epigenetic regulation by decitabine of melanoma differentiation in vitro and in vivo. International journal of cancer 131**:** 18-29

Andor N, Graham TA, Jansen M, Xia LC, Aktipis CA, Petritsch C, Ji HP, Maley CC (2016) Pan-cancer analysis of the extent and consequences of intratumor heterogeneity. Nature medicine 22**:** 105-113

Aris M, Zubieta MR, Colombo M, Arriaga JM, Bianchini M, Alperovich M, Bravo AI, Barrio MM, Mordoh J (2012) MART-1- and gp100-expressing and -non-expressing melanoma cells are equally proliferative in tumors and clonogenic in vitro. The Journal of investigative dermatology 132**:** 365-374

Ascierto PA, Kirkwood JM, Grob JJ, Simeone E, Grimaldi AM, Maio M, Palmieri G, Testori A, Marincola FM, Mozzillo N (2012) The role of BRAF V600 mutation in melanoma. Journal of translational medicine 10**:** 85

Ashida A, Takata M, Murata H, Kido K, Saida T (2009) Pathological activation of KIT in metastatic tumors of acral and mucosal melanomas. International journal of cancer 124**:** 862-868

Bandarchi B, Jabbari CA, Vedadi A, Navab R (2013) Molecular biology of normal melanocytes and melanoma cells. Journal of clinical pathology 66**:** 644-648

Banerjee A, Sanyal S, Kulkarni KK, Jana K, Roy S, Das C, Dasgupta D (2014) Anticancer drug mithramycin interacts with core histones: An additional mode of action of the DNA groove binder. FEBS open bio 4**:** 987-995

Bannister AJ, Kouzarides T (2011) Regulation of chromatin by histone modifications. Cell research 21**:** 381-395

Barski A, Cuddapah S, Cui K, Roh TY, Schones DE, Wang Z, Wei G, Chepelev I, Zhao K (2007) High-resolution profiling of histone methylations in the human genome. Cell 129**:** 823-837

Basavapathruni A, Gureasko J, Porter Scott M, Hermans W, Godbole A, Leland PA, Boriack-Sjodin PA, Wigle TJ, Copeland RA, Riera TV (2016) Characterization of the Enzymatic Activity of SETDB1 and Its 1:1 Complex with ATF7IP. Biochemistry 55**:** 1645-1651

Bermudez Y (2014) Ultraviolet involvement in melanocyte transformation to melanoma. The British journal of dermatology 171**:** 1289

Bernardi R, Pandolfi PP (2003) Role of PML and the PML-nuclear body in the control of programmed cell death. Oncogene 22**:** 9048-9057

Bilodeau S, Kagey MH, Frampton GM, Rahl PB, Young RA (2009) SetDB1 contributes to repression of genes encoding developmental regulators and maintenance of ES cell state. Genes & development 23**:** 2484-2489

Binda O, LeRoy G, Bua DJ, Garcia BA, Gozani O, Richard S (2010) Trimethylation of histone H3 lysine 4 impairs methylation of histone H3 lysine 9: regulation of lysine methyltransferases by physical interaction with their substrates. Epigenetics 5**:** 767-775

Bird A (2001) Molecular biology. Methylation talk between histones and DNA. Science (New York, NY) 294**:** 2113-2115

Borsotti P, Ghilardi C, Ostano P, Silini A, Dossi R, Pinessi D, Foglieni C, Scatolini M, Lacal PM, Ferrari R et al (2015) Thrombospondin-1 is part of a Slug-independent motility and metastatic program in cutaneous melanoma, in association with VEGFR-1 and FGF-2. Pigment cell & melanoma research 28**:** 73-81

Bray F, Ferlay J, Soerjomataram I, Siegel RL, Torre LA, Jemal A (2018) Global cancer statistics 2018: GLOBOCAN estimates of incidence and mortality worldwide for 36 cancers in 185 countries. CA: a cancer journal for clinicians 68**:** 394-424

Bryne M, Boysen M, Alfsen CG, Abeler VM, Sudbo J, Nesland JM, Kristensen GB, Piffko J, Bankfalvi A (1998) The invasive front of carcinomas. The most important area for tumour prognosis? Anticancer research 18**:** 4757-4764

Cao J, Yan Q (2012) Histone ubiquitination and deubiquitination in transcription, DNA damage response, and cancer. Frontiers in oncology 2**:** 26

Carlino MS, Todd JR, Rizos H (2014) Resistance to c-Kit inhibitors in melanoma: insights for future therapies. Oncoscience 1**:** 423-426

Castonguay E, White SA, Kagansky A, St-Cyr DJ, Castillo AG, Brugger C, White R, Bonilla C, Spitzer M, Earnshaw WC et al (2015) Panspecies small-molecule disruptors of heterochromatin-mediated transcriptional gene silencing. Molecular and cellular biology 35**:** 662-674

Ceol CJ, Houvras Y, Jane-Valbuena J, Bilodeau S, Orlando DA, Battisti V, Fritsch L, Lin WM, Hollmann TJ, Ferre F et al (2011) The histone methyltransferase SETDB1 is recurrently amplified in melanoma and accelerates its onset. Nature 471**:** 513-517

Chang Y, Zhang X, Horton JR, Upadhyay AK, Spannhoff A, Liu J, Snyder JP, Bedford MT, Cheng X (2009) Structural basis for G9a-like protein lysine methyltransferase inhibition by BIX-01294. Nature structural & molecular biology 16**:** 312-317

Chen Y, Jie W, Yan W, Zhou K, Xiao Y (2012) Lysine-specific histone demethylase 1 (LSD1): A potential molecular target for tumor therapy. Critical reviews in eukaryotic gene expression 22**:** 53-59

Cheng J, Blum R, Bowman C, Hu D, Shilatifard A, Shen S, Dynlacht BD (2014) A role for H3K4 monomethylation in gene repression and partitioning of chromatin readers. Molecular cell 53**:** 979-992

Cheung P, Tanner KG, Cheung WL, Sassone-Corsi P, Denu JM, Allis CD (2000) Synergistic coupling of histone H3 phosphorylation and acetylation in response to epidermal growth factor stimulation. Molecular cell 5**:** 905-915

Chiba T, Saito T, Yuki K, Zen Y, Koide S, Kanogawa N, Motoyama T, Ogasawara S, Suzuki E, Ooka Y et al (2015) Histone lysine methyltransferase SUV39H1 is a potent target for epigenetic therapy of hepatocellular carcinoma. International journal of cancer 136**:** 289-298

Cho S, Park JS, Kang YK (2014) AGO2 and SETDB1 cooperate in promoter-targeted transcriptional silencing of the androgen receptor gene. Nucleic acids research 42: 13545-13556

Cho S, Park JS, Kwon S, Kang YK (2012) Dynamics of Setdb1 expression in early mouse development. Gene expression patterns : GEP 12: 213-218

Choi ES, Nam JS, Jung JY, Cho NP, Cho SD (2014) Modulation of specificity protein 1 by mithramycin A as a novel therapeutic strategy for cervical cancer. Scientific reports 4: 7162

Cichorek M, Wachulska M, Stasiewicz A, Tyminska A (2013) Skin melanocytes: biology and development. Postepy dermatologii i alergologii 30: 30-41

Cuellar TL, Herzner AM, Zhang X, Goyal Y, Watanabe C, Friedman BA, Janakiraman V, Durinck S, Stinson J, Arnott D et al (2017) Silencing of retrotransposons by SETDB1 inhibits the interferon response in acute myeloid leukemia. The Journal of cell biology 216: 3535-3549

Diaz-Nunez M, Diez-Torre A, De Wever O, Andrade R, Arluzea J, Silio M, Arechaga J (2016) Histone deacetylase inhibitors induce invasion of human melanoma cells in vitro via differential regulation of N-cadherin expression and RhoA activity. BMC cancer 16: 667

Dillon SC, Zhang X, Trievel RC, Cheng X (2005) The SET-domain protein superfamily: protein lysine methyltransferases. Genome biology 6: 227

Dixon JR, Gorkin DU, Ren B (2016) Chromatin Domains: The Unit of Chromosome Organization. Molecular cell 62: 668-680

Dong X, Weng Z (2013) The correlation between histone modifications and gene expression. Epigenomics 5: 113-116

Du J, Miller AJ, Widlund HR, Horstmann MA, Ramaswamy S, Fisher DE (2003) MLANA/MART1 and SILV/PMEL17/GP100 are transcriptionally regulated by MITF in melanocytes and melanoma. The American journal of pathology 163: 333-343

Dudley ME, Yang JC, Sherry R, Hughes MS, Royal R, Kammula U, Robbins PF, Huang J, Citrin DE, Leitman SF et al (2008) Adoptive cell therapy for patients with metastatic melanoma: evaluation of intensive myeloablative chemoradiation preparative regimens. Journal of clinical oncology : official journal of the American Society of Clinical Oncology 26: 5233-5239

Dutcher JP, Coletti D, Paietta E, Wiernik PH (1997) A pilot study of alpha-interferon and plicamycin for accelerated phase of chronic myeloid leukemia. Leukemia research 21**:** 375-380

Eggermont AM, Suciu S, Santinami M, Testori A, Kruit WH, Marsden J, Punt CJ, Sales F, Gore M, Mackie R et al (2008) Adjuvant therapy with pegylated interferon alfa-2b versus observation alone in resected stage III melanoma: final results of EORTC 18991, a randomised phase III trial. Lancet (London, England) 372**:** 117-126

Fang D, Tsuji Y, Setaluri V (2002) Selective down-regulation of tyrosinase family gene TYRP1 by inhibition of the activity of melanocyte transcription factor, MITF. Nucleic acids research 30**:** 3096-3106

Fang Y, Xue JL, Shen Q, Chen J, Tian L (2012) MicroRNA-7 inhibits tumor growth and metastasis by targeting the phosphoinositide 3-kinase/Akt pathway in hepatocellular carcinoma. Hepatology (Baltimore, Md) 55**:** 1852-1862

Fei Q, Shang K, Zhang J, Chuai S, Kong D, Zhou T, Fu S, Liang Y, Li C, Chen Z et al (2015) Histone methyltransferase SETDB1 regulates liver cancer cell growth through methylation of p53. Nature communications 6**:** 8651

Ferguson B, Handoko HY, Mukhopadhyay P, Chitsazan A, Balmer L, Morahan G, Walker GJ (2019) Different genetic mechanisms mediate spontaneous versus UVR-induced malignant melanoma. eLife 8

Flach EH, Rebecca VW, Herlyn M, Smalley KS, Anderson AR (2011) Fibroblasts contribute to melanoma tumor growth and drug resistance. Molecular pharmaceutics 8**:** 2039-2049

Freedberg DE, Rigas SH, Russak J, Gai W, Kaplow M, Osman I, Turner F, Randerson-Moor JA, Houghton A, Busam K et al (2008) Frequent p16-independent inactivation of p14ARF in human melanoma. Journal of the National Cancer Institute 100**:** 784-795

Friedl P, Alexander S (2011) Cancer invasion and the microenvironment: plasticity and reciprocity. Cell 147**:** 992-1009

Galli SJ, Tsai M, Wershil BK (1993) The c-kit receptor, stem cell factor, and mast cells. What each is teaching us about the others. The American journal of pathology 142**:** 965-974

Gao Y, Geng J, Hong X, Qi J, Teng Y, Yang Y, Qu D, Chen G (2014) Expression of p300 and CBP is associated with poor prognosis in small cell lung cancer. International journal of clinical and experimental pathology 7**:** 760-767

Gazze G (2018) Combination therapy for metastatic melanoma: a pharmacist's role, drug interactions & complementary alternative therapies. Melanoma management 5**:** MMT07

Giambernardi TA, Sakaguchi AY, Gluhak J, Pavlin D, Troyer DA, Das G, Rodeck U, Klebe RJ (2001) Neutrophil collagenase (MMP-8) is expressed during early development in neural crest cells as well as in adult melanoma cells. Matrix biology : journal of the International Society for Matrix Biology 20**:** 577-587

Gillette TG, Hill JA (2015) Readers, writers, and erasers: chromatin as the whiteboard of heart disease. Circulation research 116**:** 1245-1253

Giotopoulos G, Chan WI, Horton SJ, Ruau D, Gallipoli P, Fowler A, Crawley C, Papaemmanuil E, Campbell PJ, Gottgens B et al (2016) The epigenetic regulators CBP and p300 facilitate leukemogenesis and represent therapeutic targets in acute myeloid leukemia. Oncogene 35**:** 279-289

Gloster HM, Jr., Neal K (2006) Skin cancer in skin of color. Journal of the American Academy of Dermatology 55**:** 741-760; quiz 761-744

Goding CR (2000) Mitf from neural crest to melanoma: signal transduction and transcription in the melanocyte lineage. Genes & development 14**:** 1712-1728

Goldstein AM (2004) Familial melanoma, pancreatic cancer and germline CDKN2A mutations. Human mutation 23**:** 630

Greene MH, Clark WH, Jr., Tucker MA, Kraemer KH, Elder DE, Fraser MC (1985) High risk of malignant melanoma in melanoma-prone families with dysplastic nevi. Annals of internal medicine 102**:** 458-465

Greer EL, Shi Y (2012) Histone methylation: a dynamic mark in health, disease and inheritance. Nature reviews Genetics 13**:** 343-357

Grosso JF, Jure-Kunkel MN (2013) CTLA-4 blockade in tumor models: an overview of preclinical and translational research. Cancer immunity 13**:** 5

Guenther MG, Jenner RG, Chevalier B, Nakamura T, Croce CM, Canaani E, Young RA (2005) Global and Hox-specific roles for the MLL1 methyltransferase. Proceedings of the National Academy of Sciences of the United States of America 102**:** 8603-8608

Guyonneau L, Murisier F, Rossier A, Moulin A, Beermann F (2004) Melanocytes and pigmentation are affected in dopachrome tautomerase knockout mice. Molecular and cellular biology 24**:** 3396-3403

Hammond EM, Mandell DJ, Salim A, Krieg AJ, Johnson TM, Shirazi HA, Attardi LD, Giaccia AJ (2006) Genome-wide analysis of p53 under hypoxic conditions. Molecular and cellular biology 26**:** 3492-3504

Heintzman ND, Stuart RK, Hon G, Fu Y, Ching CW, Hawkins RD, Barrera LO, Van Calcar S, Qu C, Ching KA et al (2007) Distinct and predictive chromatin signatures of transcriptional promoters and enhancers in the human genome. Nature genetics 39**:** 311-318

Herviou L, Cavalli G, Cartron G, Klein B, Moreaux J (2016) EZH2 in normal hematopoiesis and hematological malignancies. Oncotarget 7**:** 2284-2296

Hodi FS, O'Day SJ, McDermott DF, Weber RW, Sosman JA, Haanen JB, Gonzalez R, Robert C, Schadendorf D, Hassel JC et al (2010) Improved survival with ipilimumab in patients with metastatic melanoma. The New England journal of medicine 363**:** 711-723

Hodis E, Watson IR, Kryukov GV, Arold ST, Imielinski M, Theurillat JP, Nickerson E, Auclair D, Li L, Place C et al (2012) A landscape of driver mutations in melanoma. Cell 150**:** 251-263

Hoejberg L, Bastholt L, Schmidt H (2012) Interleukin-6 and melanoma. Melanoma research 22**:** 327-333

Hoek KS, Eichhoff OM, Schlegel NC, Dobbeling U, Kobert N, Schaerer L, Hemmi S, Dummer R (2008) In vivo switching of human melanoma cells between proliferative and invasive states. Cancer research 68**:** 650-656

Hoek KS, Goding CR (2010) Cancer stem cells versus phenotype-switching in melanoma. Pigment cell & melanoma research 23**:** 746-759

Hofmann UB, Eggert AA, Blass K, Brocker EB, Becker JC (2003) Expression of matrix metalloproteinases in the microenvironment of spontaneous and experimental melanoma metastases reflects the requirements for tumor formation. Cancer research 63**:** 8221-8225

Hornig E, Heppt MV, Graf SA, Ruzicka T, Berking C (2016) Inhibition of histone deacetylases in melanoma-a perspective from bench to bedside. Experimental dermatology 25**:** 831-838

Huang T, Sun L, Yuan X, Qiu H (2017) Thrombospondin-1 is a multifaceted player in tumor progression. Oncotarget 8**:** 84546-84558

Ibrahim N, Buchbinder EI, Granter SR, Rodig SJ, Giobbie-Hurder A, Becerra C, Tsiaras A, Gjini E, Fisher DE, Hodi FS (2016) A phase I trial of panobinostat (LBH589) in patients with metastatic melanoma. Cancer medicine 5**:** 3041-3050

Jakob JA, Bassett RL, Jr., Ng CS, Curry JL, Joseph RW, Alvarado GC, Rohlfs ML, Richard J, Gershenwald JE, Kim KB et al (2012) NRAS mutation status is an independent prognostic factor in metastatic melanoma. Cancer 118**:** 4014-4023

Jawhar NM (2009) Tissue Microarray: A rapidly evolving diagnostic and research tool. Annals of Saudi medicine 29**:** 123-127

Jayachandran A, Anaka M, Prithviraj P, Hudson C, McKeown SJ, Lo PH, Vella LJ, Goding CR, Cebon J, Behren A (2014) Thrombospondin 1 promotes an aggressive phenotype through epithelial-to-mesenchymal transition in human melanoma. Oncotarget 5**:** 5782-5797

Jazirehi AR, Arle D (2013) Epigenetic regulation of the TRAIL/Apo2L apoptotic pathway by histone deacetylase inhibitors: an attractive approach to bypass melanoma immunotherapy resistance. American journal of clinical and experimental immunology 2**:** 55-74

Jazirehi AR, Lim A, Dinh T (2016) PD-1 inhibition and treatment of advanced melanoma-role of pembrolizumab. American journal of cancer research 6**:** 2117-2128

Jeanne A, Boulagnon-Rombi C, Devy J, Theret L, Fichel C, Bouland N, Diebold MD, Martiny L, Schneider C, Dedieu S (2016) Matricellular TSP-1 as a target of interest for impeding melanoma spreading: towards a therapeutic use for TAX2 peptide. Clinical & experimental metastasis 33**:** 637-649

Jiang Y, Loh YE, Rajarajan P, Hirayama T, Liao W, Kassim BS, Javidfar B, Hartley BJ, Kleofas L, Park RB et al (2017) The methyltransferase SETDB1 regulates a large neuron-specific topological chromatin domain. Nature genetics 49**:** 1239-1250

Josling GA, Selvarajah SA, Petter M, Duffy MF (2012) The role of bromodomain proteins in regulating gene expression. Genes 3**:** 320-343

Jurkowska RZ, Qin S, Kungulovski G, Tempel W, Liu Y, Bashtrykov P, Stiefelmaier J, Jurkowski TP, Kudithipudi S, Weirich S et al (2017) H3K14ac is linked to methylation of H3K9 by the triple Tudor domain of SETDB1. Nature communications 8**:** 2057

Kalal BS, Upadhya D, Pai VR (2017) Chemotherapy Resistance Mechanisms in Advanced Skin Cancer. Oncology reviews 11**:** 326

Kang HC, Kim HK, Lee S, Mendez P, Kim JW, Woodard G, Yoon JH, Jen KY, Fang LT, Jones K et al (2016) Whole exome and targeted deep sequencing identify genome-wide allelic loss and frequent SETDB1 mutations in malignant pleural mesotheliomas. Oncotarget 7**:** 8321-8331

Kang YK (2015) SETDB1 in Early Embryos and Embryonic Stem Cells. Current issues in molecular biology 17: 1-10

Kanzler H, Barrat FJ, Hessel EM, Coffman RL (2007) Therapeutic targeting of innate immunity with Toll-like receptor agonists and antagonists. Nature medicine 13: 552-559

Karanth AV, Maniswami RR, Prashanth S, Govindaraj H, Padmavathy R, Jegatheesan SK, Mullangi R, Rajagopal S (2017) Emerging role of SETDB1 as a therapeutic target. Expert opinion on therapeutic targets 21: 319-331

Keung EZ, Akdemir KC, Al Sannaa GA, Garnett J, Lev D, Torres KE, Lazar AJ, Rai K, Chin L (2015) Increased H3K9me3 drives dedifferentiated phenotype via KLF6 repression in liposarcoma. The Journal of clinical investigation 125: 2965-2978

Kim KH, Roberts CW (2016) Targeting EZH2 in cancer. Nature medicine 22: 128-134

Kim S, Yu NK, Kaang BK (2015) CTCF as a multifunctional protein in genome regulation and gene expression. Experimental & molecular medicine 47: e166

Kirkwood JM, Ibrahim JG, Sosman JA, Sondak VK, Agarwala SS, Ernstoff MS, Rao U (2001) High-dose interferon alfa-2b significantly prolongs relapse-free and overall survival compared with the GM2-KLH/QS-21 vaccine in patients with resected stage IIB-III melanoma: results of intergroup trial E1694/S9512/C509801. Journal of clinical oncology : official journal of the American Society of Clinical Oncology 19: 2370-2380

Kiuru M, Busam KJ (2017) The NF1 gene in tumor syndromes and melanoma. Laboratory investigation; a journal of technical methods and pathology 97: 146-157

Kramer N, Walzl A, Unger C, Rosner M, Krupitza G, Hengstschlager M, Dolznig H (2013) In vitro cell migration and invasion assays. Mutation research 752: 10-24

Krieg C, Letourneau S, Pantaleo G, Boyman O (2010) Improved IL-2 immunotherapy by selective stimulation of IL-2 receptors on lymphocytes and endothelial cells. Proceedings of the National Academy of Sciences of the United States of America 107: 11906-11911

Lanitis E, Dangaj D, Irving M, Coukos G (2017) Mechanisms regulating T-cell infiltration and activity in solid tumors. Ann Oncol 28: xii18-xii32

Lee DH, Ahn SS, Kim JB, Lim Y, Lee YH, Shin SY (2018) Downregulation of alpha-Melanocyte-Stimulating Hormone-Induced Activation of the Pax3-MITF-Tyrosinase Axis by Sorghum Ethanolic Extract in B16F10 Melanoma Cells. International journal of molecular sciences 2018 Jun; 19(6): 1640.

Lee E, Wang J, Jung Y, Cackowski FC, Taichman RS (2018b) Reduction of two histone marks, H3k9me3 and H3k27me3 by epidrug induces neuroendocrine differentiation in prostate cancer. Journal of cellular biochemistry 119**:** 3697-3705

Lee JH, Choi JW, Kim YS (2011) Frequencies of BRAF and NRAS mutations are different in histological types and sites of origin of cutaneous melanoma: a meta-analysis. The British journal of dermatology 164**:** 776-784

Lee JK, Kim KC (2013) DZNep, inhibitor of S-adenosylhomocysteine hydrolase, down-regulates expression of SETDB1 H3K9me3 HMTase in human lung cancer cells. Biochemical and biophysical research communications 438**:** 647-652

Lee JS, Smith E, Shilatifard A (2010) The language of histone crosstalk. Cell 142**:** 682-685

Leiter U, Eigentler T, Garbe C (2014) Epidemiology of skin cancer. Advances in experimental medicine and biology 810**:** 120-140

Lekmine F, Chang CK, Sethakorn N, Das Gupta TK, Salti GI (2007) Role of microphthalmia transcription factor (Mitf) in melanoma differentiation. Biochemical and biophysical research communications 354**:** 830-835

Lenggenhager D, Curioni-Fontecedro A, Storz M, Shakhova O, Sommer L, Widmer DS, Seifert B, Moch H, Dummer R, Mihic-Probst D (2014) An Aggressive Hypoxia Related Subpopulation of Melanoma Cells is TRP-2 Negative. Translational oncology 7**:** 206-212

Li H, Rauch T, Chen ZX, Szabo PE, Riggs AD, Pfeifer GP (2006) The histone methyltransferase SETDB1 and the DNA methyltransferase DNMT3A interact directly and localize to promoters silenced in cancer cells. The Journal of biological chemistry 281**:** 19489-19500

Li J, Gao H, Meng L, Yin L (2017) Mithramycin inhibits epithelial-to-mesenchymal transition and invasion by downregulating SP1 and SNAI1 in salivary adenoid cystic carcinoma. Tumour biology : the journal of the International Society for Oncodevelopmental Biology and Medicine 39**:** 1010428317708697

Li X, Wu D, Shen J, Zhou M, Lu Y (2013) Rapamycin induces autophagy in the melanoma cell line M14 via regulation of the expression levels of Bcl-2 and Bax. Oncology letters 5**:** 167-172

Li YJ, Huang TH, Hsiao M, Lin BR, Cheng SJ, Yang CN, Lai WT, Wu TS, Fan JR, Kuo MY et al (2016) Suppression of fructose-bisphosphate aldolase C expression as a predictor of advanced oral squamous cell carcinoma. Head & neck 38 Suppl 1**:** E1075-1085

Lienlafa M, Perez-Villarroela P, Knoxa T, Pabona M, Sahakiana E, Powersa J, Woana KV, Leeb C, Chenga F, Denga S et al (2016) Essential role of HDAC6 in the regulation of PD-L1 in melanoma. Molecular oncology 10**:** 735-750

Lin RK, Hsu CH, Wang YC (2007) Mithramycin A inhibits DNA methyltransferase and metastasis potential of lung cancer cells. Anti-cancer drugs 18**:** 1157-1164

Livingstone E, Zimmer L, Vaubel J, Schadendorf D (2014) BRAF, MEK and KIT inhibitors for melanoma: adverse events and their management. Chinese clinical oncology 3**:** 29

Lu C, Yang D, Sabbatini ME, Colby AH, Grinstaff MW, Oberlies NH, Pearce C, Liu K (2018) Contrasting roles of H3K4me3 and H3K9me3 in regulation of apoptosis and gemcitabine resistance in human pancreatic cancer cells. BMC cancer 18**:** 149

Mahadevan A, Patel VL, Dagoglu N (2015) Radiation Therapy in the Management of Malignant Melanoma. Oncology (Williston Park, NY) 29**:** 743-751

Mariani M, Supino R (1990) Morphological alterations induced by doxorubicin in B16 melanoma cells. Cancer letters 51**:** 209-212

McGinty RK, Tan S (2015) Nucleosome structure and function. Chemical reviews 115**:** 2255-2273

Melling N, Thomsen E, Tsourlakis MC, Kluth M, Hube-Magg C, Minner S, Koop C, Graefen M, Heinzer H, Wittmer C et al (2015) Overexpression of enhancer of zeste homolog 2 (EZH2) characterizes an aggressive subset of prostate cancers and predicts patient prognosis independently from pre- and postoperatively assessed clinicopathological parameters. Carcinogenesis 36**:** 1333-1340

Ming M, Han W, Zhao B, Sundaresan NR, Deng CX, Gupta MP, He YY (2014) SIRT6 promotes COX-2 expression and acts as an oncogene in skin cancer. Cancer research 74**:** 5925-5933

Minkovsky A, Sahakyan A, Rankin-Gee E, Bonora G, Patel S, Plath K (2014) The Mbd1-Atf7ip-Setdb1 pathway contributes to the maintenance of X chromosome inactivation. Epigenetics & chromatin 7**:** 12

Mirmohammadsadegh A, Marini A, Nambiar S, Hassan M, Tannapfel A, Ruzicka T, Hengge UR (2006) Epigenetic silencing of the PTEN gene in melanoma. Cancer research 66: 6546-6552

Mitsui H, Suarez-Farinas M, Gulati N, Shah KR, Cannizzaro MV, Coats I, Felsen D, Krueger JG, Carucci JA (2014) Gene expression profiling of the leading edge of cutaneous squamous cell carcinoma: IL-24-driven MMP-7. The Journal of investigative dermatology 134: 1418-1427

Miura S, Maesawa C, Shibazaki M, Yasuhira S, Kasai S, Tsunoda K, Maeda F, Takahashi K, Akasaka T, Masuda T (2014) Immunohistochemistry for histone h3 lysine 9 methyltransferase and demethylase proteins in human melanomas. The American Journal of dermatopathology 36: 211-216

Mocellin S, Nitti D (2011) Cutaneous melanoma in situ: translational evidence from a large population-based study. The oncologist 16: 896-903

Moro N, Mauch C, Zigrino P (2014) Metalloproteinases in melanoma. European journal of cell biology 93: 23-29

Muntean AG, Hess JL (2009) Epigenetic dysregulation in cancer. The American journal of pathology 175: 1353-1361

Na HH, Noh HJ, Cheong HM, Kang Y, Kim KC (2016) SETDB1 mediated FosB expression increases the cell proliferation rate during anticancer drug therapy. BMB reports 49: 238-243

Newell-Price J, Clark AJ, King P (2000) DNA methylation and silencing of gene expression. Trends in endocrinology and metabolism: TEM 11: 142-148

Nnetu KD, Knorr M, Käs J, Zink M (2012) The impact of jamming on boundaries of collectively moving weak-interacting cells. New Journal of Physics 14: 115012

Noble D (2015) Conrad Waddington and the origin of epigenetics. The Journal of experimental biology 218: 816-818

Noh HJ, Kim KA, Kim KC (2014) p53 down-regulates SETDB1 gene expression during paclitaxel induced-cell death. Biochemical and biophysical research communications 446: 43-48

Obenauf AC, Zou Y, Ji AL, Vanharanta S, Shu W, Shi H, Kong X, Bosenberg MC, Wiesner T, Rosen N et al (2015) Therapy-induced tumour secretomes promote resistance and tumour progression. Nature 520: 368-372

Olcina MM, Leszczynska KB, Senra JM, Isa NF, Harada H, Hammond EM (2016) H3K9me3 facilitates hypoxia-induced p53-dependent apoptosis through repression of APAK. Oncogene 35**:** 793-799

Olsen EA, Kim YH, Kuzel TM, Pacheco TR, Foss FM, Parker S, Frankel SR, Chen C, Ricker JL, Arduino JM et al (2007) Phase IIb multicenter trial of vorinostat in patients with persistent, progressive, or treatment refractory cutaneous T-cell lymphoma. Journal of clinical oncology : official journal of the American Society of Clinical Oncology 25**:** 3109-3115

Orouji E (2016) Genetic and epigenetic regulations in malignant melanoma. In Clinical Cooperation Unit Dermato-oncology,

Department of Dermatology, Allergology and Venereology,

Mannheim Medical Faculty.

Oti M, Falck J, Huynen MA, Zhou H (2016) CTCF-mediated chromatin loops enclose inducible gene regulatory domains. BMC genomics 17**:** 252

Pak BJ, Lee J, Thai BL, Fuchs SY, Shaked Y, Ronai Z, Kerbel RS, Ben-David Y (2004) Radiation resistance of human melanoma analysed by retroviral insertional mutagenesis reveals a possible role for dopachrome tautomerase. Oncogene 23**:** 30-38

Palavalli LH, Prickett TD, Wunderlich JR, Wei X, Burrell AS, Porter-Gill P, Davis S, Wang C, Cronin JC, Agrawal NS et al (2009) Analysis of the matrix metalloproteinase family reveals that MMP8 is often mutated in melanoma. Nature genetics 41**:** 518-520

Paltridge JL, Belle L, Khew-Goodall Y (2013) The secretome in cancer progression. Biochimica et biophysica acta 1834**:** 2233-2241

Pamidimukkala NV, Leonard MK, Snyder D, McCorkle JR, Kaetzel DM (2018) Metastasis Suppressor NME1 Directly Activates Transcription of the ALDOC Gene in Melanoma Cells. Anticancer research 38**:** 6059-6068

Payne AS, Cornelius LA (2002) The role of chemokines in melanoma tumor growth and metastasis. The Journal of investigative dermatology 118**:** 915-922

Peitsch WK, Doerflinger Y, Fischer-Colbrie R, Huck V, Bauer AT, Utikal J, Goerdt S, Schneider SW (2014) Desmoglein 2 depletion leads to increased migration and upregulation of the chemoattractant secretoneurin in melanoma cells. PloS one 9**:** e89491

Pencheva N, Tran H, Buss C, Huh D, Drobnjak M, Busam K, Tavazoie SF (2012) Convergent multi-miRNA targeting of ApoE drives LRP1/LRP8-dependent melanoma metastasis and angiogenesis. Cell 151**:** 1068-1082

Perner J, Lasserre J, Kinkley S, Vingron M, Chung HR (2014) Inference of interactions between chromatin modifiers and histone modifications: from ChIP-Seq data to chromatin-signaling. Nucleic acids research 42**:** 13689-13695

Piekarz RL, Frye R, Prince HM, Kirschbaum MH, Zain J, Allen SL, Jaffe ES, Ling A, Turner M, Peer CJ et al (2011) Phase 2 trial of romidepsin in patients with peripheral T-cell lymphoma. Blood 117**:** 5827-5834

Pinner S, Jordan P, Sharrock K, Bazley L, Collinson L, Marais R, Bonvin E, Goding C, Sahai E (2009) Intravital imaging reveals transient changes in pigment production and Brn2 expression during metastatic melanoma dissemination. Cancer research 69**:** 7969-7977

Pol J, Kroemer G, Galluzzi L (2016) First oncolytic virus approved for melanoma immunotherapy. Oncoimmunology 5**:** e1115641

Pourakbar S, Pluard TJ, Accurso AD, Farassati F (2017) Ezh2, a novel target in detection and therapy of breast cancer. OncoTargets and therapy 10**:** 2685-2687

Powell MR, Sheehan DJ, Kleven DT (2016) Altered Morphology and Immunohistochemical Characteristics in Metastatic Malignant Melanoma After Therapy With Vemurafenib. The American Journal of dermatopathology 38**:** e137-139

Rafique I, Kirkwood JM, Tarhini AA (2015) Immune checkpoint blockade and interferon-alpha in melanoma. Seminars in oncology 42**:** 436-447

Raj U, Aier I, Semwal R, Varadwaj PK (2017) Identification of novel dysregulated key genes in Breast cancer through high throughput ChIP-Seq data analysis. Scientific reports 7**:** 3229

Raposo G, Marks MS (2007) Melanosomes--dark organelles enlighten endosomal membrane transport. Nature reviews Molecular cell biology 8**:** 786-797

Rea S, Eisenhaber F, O'Carroll D, Strahl BD, Sun ZW, Schmid M, Opravil S, Mechtler K, Ponting CP, Allis CD et al (2000) Regulation of chromatin structure by site-specific histone H3 methyltransferases. Nature 406**:** 593-599

Ream NW, Perlia CP, Wolter J, Taylor SG, 3rd (1968) Mithramycin therapy in disseminated germinal testicular cancer. Jama 204**:** 1030-1036

Regina C, Compagnone M, Peschiaroli A, Lena A, Annicchiarico-Petruzzelli M, Piro MC, Melino G, Candi E (2016) Setdb1, a novel interactor of DeltaNp63, is involved in breast tumorigenesis. Oncotarget 7**:** 28836-28848

Resovi A, Pinessi D, Chiorino G, Taraboletti G (2014) Current understanding of the thrombospondin-1 interactome. Matrix biology : journal of the International Society for Matrix Biology 37**:** 83-91

Rodriguez-Paredes M, Martinez de Paz A, Simo-Riudalbas L, Sayols S, Moutinho C, Moran S, Villanueva A, Vazquez-Cedeira M, Lazo PA, Carneiro F et al (2014) Gene amplification of the histone methyltransferase SETDB1 contributes to human lung tumorigenesis. Oncogene 33**:** 2807-2813

Rossetto D, Avvakumov N, Cote J (2012) Histone phosphorylation: a chromatin modification involved in diverse nuclear events. Epigenetics 7**:** 1098-1108

Ryu H, Lee J, Hagerty SW, Soh BY, McAlpin SE, Cormier KA, Smith KM, Ferrante RJ (2006) ESET/SETDB1 gene expression and histone H3 (K9) trimethylation in Huntington's disease. Proceedings of the National Academy of Sciences of the United States of America 103**:** 19176-19181

Saraon P, Cretu D, Musrap N, Karagiannis GS, Batruch I, Drabovich AP, van der Kwast T, Mizokami A, Morrissey C, Jarvi K et al (2013) Quantitative proteomics reveals that enzymes of the ketogenic pathway are associated with prostate cancer progression. Molecular & cellular proteomics : MCP 12**:** 1589-1601

Schartl M, Kneitz S, Wilde B, Wagner T, Henkel CV, Spaink HP, Meierjohann S (2012) Conserved expression signatures between medaka and human pigment cell tumors. PloS one 7**:** e37880

Schmidt LH, Biesterfeld S, Kummel A, Faldum A, Sebastian M, Taube C, Buhll R, Wiewrodt R (2009) Tissue microarrays are reliable tools for the clinicopathological characterization of lung cancer tissue. Anticancer research 29**:** 201-209

Schultz DC, Ayyanathan K, Negorev D, Maul GG, Rauscher FJ, 3rd (2002) SETDB1: a novel KAP-1-associated histone H3, lysine 9-specific methyltransferase that contributes to HP1-mediated silencing of euchromatic genes by KRAB zinc-finger proteins. Genes & development 16**:** 919-932

Segura MF, Fontanals-Cirera B, Gaziel-Sovran A, Guijarro MV, Hanniford D, Zhang G, Gonzalez-Gomez P, Morante M, Jubierre L, Zhang W et al (2013) BRD4 sustains melanoma proliferation and represents a new target for epigenetic therapy. Cancer research 73**:** 6264-6276

Seznec J, Silkenstedt B, Naumann U (2011) Therapeutic effects of the Sp1 inhibitor mithramycin A in glioblastoma. Journal of neuro-oncology 101**:** 365-377

Shi X, Tasdogan A, Huang F, Hu Z, Morrison SJ, DeBerardinis RJ (2017) The abundance of metabolites related to protein methylation correlates with the metastatic capacity of human melanoma xenografts. Science advances 3**:** eaao5268

Shtivelman E, Davies MQ, Hwu P, Yang J, Lotem M, Oren M, Flaherty KT, Fisher DE (2014) Pathways and therapeutic targets in melanoma. Oncotarget 5**:** 1701-1752

Sid B, Sartelet H, Bellon G, El Btaouri H, Rath G, Delorme N, Haye B, Martiny L (2004) Thrombospondin 1: a multifunctional protein implicated in the regulation of tumor growth. Critical reviews in oncology/hematology 49**:** 245-258

Singh RK, Varney ML (2000) IL-8 expression in malignant melanoma: implications in growth and metastasis. Histology and histopathology 15**:** 843-849

Sinnberg T, Menzel M, Ewerth D, Sauer B, Schwarz M, Schaller M, Garbe C, Schittek B (2011) beta-Catenin signaling increases during melanoma progression and promotes tumor cell survival and chemoresistance. PloS one 6**:** e23429

Smit L, Berns K, Spence K, Ryder WD, Zeps N, Madiredjo M, Beijersbergen R, Bernards R, Clarke RB (2016) An integrated genomic approach identifies that the PI3K/AKT/FOXO pathway is involved in breast cancer tumor initiation. Oncotarget 7**:** 2596-2610

Soura E, Eliades PJ, Shannon K, Stratigos AJ, Tsao H (2016) Hereditary melanoma: Update on syndromes and management: Genetics of familial atypical multiple mole melanoma syndrome. Journal of the American Academy of Dermatology 74**:** 395-407; quiz 408-310

Souroullas GP, Jeck WR, Parker JS, Simon JM, Liu JY, Paulk J, Xiong J, Clark KS, Fedoriw Y, Qi J et al (2016) An oncogenic Ezh2 mutation induces tumors through global redistribution of histone 3 lysine 27 trimethylation. Nature medicine 22**:** 632-640

Spandidos A, Wang X, Wang H, Dragnev S, Thurber T, Seed B (2008) A comprehensive collection of experimentally validated primers for Polymerase Chain Reaction quantitation of murine transcript abundance. BMC genomics 9**:** 633

Sripathy SP, Stevens J, Schultz DC (2006) The KAP1 corepressor functions to coordinate the assembly of de novo HP1-demarcated microenvironments of heterochromatin required for KRAB zinc finger protein-mediated transcriptional repression. Molecular and cellular biology 26**:** 8623-8638

Staub E, Groene J, Heinze M, Mennerich D, Roepcke S, Klaman I, Hinzmann B, Castanos-Velez E, Pilarsky C, Mann B et al (2007) Genome-wide expression patterns of invasion front, inner tumor mass and surrounding normal epithelium of colorectal tumors. Molecular cancer 6**:** 79

Stewart MD, Li J, Wong J (2005) Relationship between histone H3 lysine 9 methylation, transcription repression, and heterochromatin protein 1 recruitment. Molecular and cellular biology 25**:** 2525-2538

Subramanian A, Tamayo P, Mootha VK, Mukherjee S, Ebert BL, Gillette MA, Paulovich A, Pomeroy SL, Golub TR, Lander ES et al (2005) Gene set enrichment analysis: a knowledge-based approach for interpreting genome-wide expression profiles. Proceedings of the National Academy of Sciences of the United States of America 102**:** 15545-15550

Sun Q, Ding D, Liu X, Guo SW (2016) Tranylcypromine, a lysine-specific demethylase 1 (LSD1) inhibitor, suppresses lesion growth and improves generalized hyperalgesia in mouse with induced endometriosis. Reproductive biology and endocrinology : RB&E 14**:** 17

Sun QY, Ding LW, Xiao JF, Chien W, Lim SL, Hattori N, Goodglick L, Chia D, Mah V, Alavi M et al (2015) SETDB1 accelerates tumourigenesis by regulating the WNT signalling pathway. The Journal of pathology 235**:** 559-570

Tachibana K, Gotoh E, Kawamata N, Ishimoto K, Uchihara Y, Iwanari H, Sugiyama A, Kawamura T, Mochizuki Y, Tanaka T et al (2015) Analysis of the subcellular localization of the human histone methyltransferase SETDB1. Biochemical and biophysical research communications 465**:** 725-731

Takeuchi H, Kuo C, Morton DL, Wang HJ, Hoon DS (2003) Expression of differentiation melanoma-associated antigen genes is associated with favorable disease outcome in advanced-stage melanomas. Cancer research 63**:** 441-448

Taniguchi Y (2014) Hox transcription factors: modulators of cell-cell and cell-extracellular matrix adhesion. BioMed research international 2014**:** 591374

Tas F (2012) Metastatic behavior in melanoma: timing, pattern, survival, and influencing factors. Journal of oncology 2012**:** 647684

Tiffen JC, Gunatilake D, Gallagher SJ, Gowrishankar K, Heinemann A, Cullinane C, Dutton-Regester K, Pupo GM, Strbenac D, Yang JY et al (2015) Targeting activating mutations of EZH2 leads to potent cell

growth inhibition in human melanoma by derepression of tumor suppressor genes. Oncotarget 6**:** 27023-27036

Torre LA, Bray F, Siegel RL, Ferlay J, Lortet-Tieulent J, Jemal A (2015) Global cancer statistics, 2012. CA: a cancer journal for clinicians 65**:** 87-108

Tsai KK, Zarzoso I, Daud AI (2014) PD-1 and PD-L1 antibodies for melanoma. Human vaccines & immunotherapeutics 10**:** 3111-3116

Tschiersch B, Hofmann A, Krauss V, Dorn R, Korge G, Reuter G (1994) The protein encoded by the Drosophila position-effect variegation suppressor gene Su(var)3-9 combines domains of antagonistic regulators of homeotic gene complexes. The EMBO journal 13**:** 3822-3831

Verdone L, Caserta M, Di Mauro E (2005) Role of histone acetylation in the control of gene expression. Biochemistry and cell biology = Biochimie et biologie cellulaire 83**:** 344-353

Verfaillie A, Imrichova H, Atak ZK, Dewaele M, Rambow F, Hulselmans G, Christiaens V, Svetlichnyy D, Luciani F, Van den Mooter L et al (2015) Decoding the regulatory landscape of melanoma reveals TEADS as regulators of the invasive cell state. Nature communications 6**:** 6683

Villanueva J, Herlyn M (2008) Melanoma and the tumor microenvironment. Current oncology reports 10**:** 439-446

Wagner NB, Weide B, Reith M, Tarnanidis K, Kehrel C, Lichtenberger R, Pflugfelder A, Herpel E, Eubel J, Ikenberg K et al (2015) Diminished levels of the soluble form of RAGE are related to poor survival in malignant melanoma. International journal of cancer 137**:** 2607-2617

Watson M, Holman DM, Maguire-Eisen M (2016) Ultraviolet Radiation Exposure and Its Impact on Skin Cancer Risk. Seminars in oncology nursing 32**:** 241-254

Wellbrock C, Arozarena I (2015) Microphthalmia-associated transcription factor in melanoma development and MAP-kinase pathway targeted therapy. Pigment cell & melanoma research 28**:** 390-406

Weth O, Paprotka C, Gunther K, Schulte A, Baierl M, Leers J, Galjart N, Renkawitz R (2014) CTCF induces histone variant incorporation, erases the H3K27me3 histone mark and opens chromatin. Nucleic acids research 42**:** 11941-11951

Whiteman DC, Green AC, Olsen CM (2016) The Growing Burden of Invasive Melanoma: Projections of Incidence Rates and Numbers of New Cases in Six Susceptible Populations through 2031. The Journal of investigative dermatology 136**:** 1161-1171

Wilson MA, Schuchter LM (2016) Chemotherapy for Melanoma. Cancer treatment and research 167**:** 209-229

Wolchok JD, Neyns B, Linette G, Negrier S, Lutzky J, Thomas L, Waterfield W, Schadendorf D, Smylie M, Guthrie T, Jr. et al (2010) Ipilimumab monotherapy in patients with pretreated advanced melanoma: a randomised, double-blind, multicentre, phase 2, dose-ranging study. The Lancet Oncology 11**:** 155-164

Wong SL, Faries MB, Kennedy EB, Agarwala SS, Akhurst TJ, Ariyan C, Balch CM, Berman BS, Cochran A, Delman KA et al (2018) Sentinel Lymph Node Biopsy and Management of Regional Lymph Nodes in Melanoma: American Society of Clinical Oncology and Society of Surgical Oncology Clinical Practice Guideline Update. Journal of clinical oncology : official journal of the American Society of Clinical Oncology 36**:** 399-413

Wongchenko MJ, McArthur GA, Dreno B, Larkin J, Ascierto PA, Sosman J, Andries L, Kockx M, Hurst SD, Caro I et al (2017) Gene Expression Profiling in BRAF-Mutated Melanoma Reveals Patient Subgroups with Poor Outcomes to Vemurafenib That May Be Overcome by Cobimetinib Plus Vemurafenib. Clinical cancer research : an official journal of the American Association for Cancer Research 23**:** 5238-5245

Wu PC, Lu JW, Yang JY, Lin IH, Ou DL, Lin YH, Chou KH, Huang WF, Wang WP, Huang YL et al (2014) H3K9 histone methyltransferase, KMT1E/SETDB1, cooperates with the SMAD2/3 pathway to suppress lung cancer metastasis. Cancer research 74**:** 7333-7343

Xia R, Zhou R, Tian Z, Zhang C, Wang L, Hu Y, Han J, Li J (2013) High expression of H3K9me3 is a strong predictor of poor survival in patients with salivary adenoid cystic carcinoma. Archives of pathology & laboratory medicine 137**:** 1761-1769

Yang H, Salz T, Zajac-Kaye M, Liao D, Huang S, Qiu Y (2014) Overexpression of histone deacetylases in cancer cells is controlled by interplay of transcription factors and epigenetic modulators. FASEB journal : official publication of the Federation of American Societies for Experimental Biology 28**:** 4265-4279

Yang L, Mei Q, Zielinska-Kwiatkowska A, Matsui Y, Blackburn ML, Benedetti D, Krumm AA, Taborsky GJ, Jr., Chansky HA (2003) An ERG (ets-related gene)-associated histone methyltransferase interacts with histone deacetylases 1/2 and transcription co-repressors mSin3A/B. The Biochemical journal 369**:** 651-657

Yang L, Xia L, Wu DY, Wang H, Chansky HA, Schubach WH, Hickstein DD, Zhang Y (2002) Molecular cloning of ESET, a novel histone H3-specific methyltransferase that interacts with ERG transcription factor. Oncogene 21**:** 148-152

Yap KL, Zhou MM (2011) Structure and mechanisms of lysine methylation recognition by the chromodomain in gene transcription. Biochemistry 50**:** 1966-1980

Yeates TO (2002) Structures of SET domain proteins: protein lysine methyltransferases make their mark. Cell 111**:** 5-7

Yokoyama K, Yasumoto K, Suzuki H, Shibahara S (1994) Cloning of the human DOPAchrome tautomerase/tyrosinase-related protein 2 gene and identification of two regulatory regions required for its pigment cell-specific expression. The Journal of biological chemistry 269**:** 27080-27087

Yokoyama Y, Hieda M, Nishioka Y, Matsumoto A, Higashi S, Kimura H, Yamamoto H, Mori M, Matsuura S, Matsuura N (2013) Cancer-associated upregulation of histone H3 lysine 9 trimethylation promotes cell motility in vitro and drives tumor formation in vivo. Cancer science 104**:** 889-895

Yoo KH, Hennighausen L (2012) EZH2 methyltransferase and H3K27 methylation in breast cancer. International journal of biological sciences 8**:** 59-65

Yu H, Ma M, Yan J, Xu L, Yu J, Dai J, Xu T, Tang H, Wu X, Li S et al (2017) Identification of coexistence of BRAF V600E mutation and EZH2 gain specifically in melanoma as a promising target for combination therapy. Journal of translational medicine 15**:** 243

Yu L, Wang Z, Zhang Z, Ren X, Lu X, Ding K (2015) Small-molecule BET inhibitors in clinical and preclinical development and their therapeutic potential. Current topics in medicinal chemistry 15**:** 776-794

Yu Y, Schleich K, Yue B, Ji S, Lohneis P, Kemper K, Silvis MR, Qutob N, van Rooijen E, Werner-Klein M et al (2018) Targeting the Senescence-Overriding Cooperative Activity of Structurally Unrelated H3K9 Demethylases in Melanoma. Cancer cell 33**:** 322-336 e328

Yuan F, Zhou Y, Wang M, Yang J, Wu K, Lu C, Kong X, Cai YD (2015) Identifying New Candidate Genes and Chemicals Related to Prostate Cancer Using a Hybrid Network and Shortest Path Approach. Computational and mathematical methods in medicine 2015**:** 462363

Yuan J, Ku GY, Gallardo HF, Orlandi F, Manukian G, Rasalan TS, Xu Y, Li H, Vyas S, Mu Z et al (2009a) Safety and immunogenicity of a human and mouse gp100 DNA vaccine in a phase I trial of patients with melanoma. Cancer immunity 9**:** 5

Yuan P, Han J, Guo G, Orlov YL, Huss M, Loh YH, Yaw LP, Robson P, Lim B, Ng HH (2009b) Eset partners with Oct4 to restrict extraembryonic trophoblast lineage potential in embryonic stem cells. Genes & development 23**:** 2507-2520

Zhan T, Rindtorff N, Boutros M (2017) Wnt signaling in cancer. Oncogene 36**:** 1461-1473

Zhang Y, Huang Z, Zhu Z, Liu J, Zheng X, Zhang Y (2014) Network analysis of ChIP-Seq data reveals key genes in prostate cancer. European journal of medical research 19**:** 47

Table 1: IPA functional annotations of cancer-related biological functions predicted to be increased (positive z-score) in SETDB1 OE HT144 melanoma cell lines, compared with control (EV HT144) cells.

Diseases or Functions Annotation	Predicted Activation State	z-score	p-Value	Molecules
Growth of tumor	Increased	3,231	1,87E-11	ANXA2,AXL,BIRC2,CCL2,CD24,CEACAM1,CXCL8,CYGB,DCT,DKK1
Invasion of tumor	Increased	2,651	1,77E-10	ANXA2,APOE,CCL2,CD24,CEACAM1,HMOX1,HYAL1,IL6,KLF4, MMP1
Invasion of tumor cells	Increased	2,254	2,78E-08	CD24,CEACAM1,HMOX1,IL6,KLF4,MMP1,MMP3,NRP1,PTGS2, TGFA
Metastasis	Increased	3,138	0,000000257	APOE,AXL,CCL2,CD24,CPA4,CXCL8,DKK1,GYG2,HMOX1,IL6
Advanced malignant tumor	Increased	3,138	0,000000913	APOE,AXL,CCL2,CD24,CPA4,CXCL8,DKK1,GYG2,HMOX1,IL6
Metastatic solid tumor	Increased	2,153	0,000000956	AXL,CCL2,CD24,CPA4,CXCL8,DKK1,GYG2,HMOX1,IL6,MMP1
Advanced malignant solid tumor	Increased	2,153	0,00000264	AXL,CCL2,CD24,CPA4,CXCL8,DKK1,GYG2,HMOX1,IL6,KLF4
Progression of tumor	Increased	2,18	0,0000249	ANXA2,APOE,AXL,CXCL8,IL6,MMP1,NRP1,PTGS2,THBS1,TUBB4A
Metastasis of cells	Increased	2,01	0,0000256	CCL2,CD24,CXCL8,HMOX1,LAMA5,MMP1,MMP3,PTGS2,TGFA, THBS1
Metastasis of tumor cell lines	Increased	2,01	0,0000769	CCL2,CD24,CXCL8,HMOX1,LAMA5,MMP1,MMP3,PTGS2,THBS1
Invasion of tissue	Increased	2,606	0,000217	AXL,CCL2,CD24,CXCL8,EVL,MMP1,MMP3,NRP1

Table 2: Top-enriched DAVID biological terms related to downregulated genes in SETDB1 OE HT144 melanoma cell lines compared with control (EV HT144) cells.

Category	Term	p-Value	Genes
GOTERM_BP_DIRECT	GO:0042438: melanin biosynthetic process	1.03E-07	DCT, TYRP1, TYR, PMEL, CITED1
UP_KEYWORDS	Melanin biosynthesis	9.48E-07	DCT, TYRP1, TYR, PMEL
UP_SEQ_FEATURE	signal peptide	1.15E-05	TF, TYRP1, FXYD3, A2M, IL17RD, PCOLCE, DCT, IGSF11, TYR, APOE, BCHE, SERPINA5, SERPINA3, FGL2, CEACAM1, PLTP, PI15, MAG, HYAL1, RNASE1, PMEL, MGP, NBL1, LAMA5, FKBP14, FCRLA
UP_KEYWORDS	Secreted	1.57E-05	HAPLN1, HYAL1, TF, A2M, RNASE1, PMEL, TNFSF14, MGP, PCOLCE, NBL1, BCHE, LAMA5, APOE, SERPINA5, SERPINA3, FGL2, CEACAM1, PLTP, PI15
INTERPRO	IPR002227:Tyrosinase	3.18E-05	DCT, TYRP1, TYR
INTERPRO	IPR008922:Uncharacterised domain, di-copper centre	3.18E-05	DCT, TYRP1, TYR
UP_KEYWORDS	Signal	3.66E-05	TF, TYRP1, FXYD3, A2M, IL17RD, PCOLCE, DCT, IGSF11, TYR, APOE, BCHE, SERPINA5, SERPINA3, FGL2, CEACAM1, PLTP, PI15, MAG, HYAL1, RNASE1, PMEL, MGP, MSRB2, NBL1, LAMA5, FKBP14, QPRT, FCRLA
UP_SEQ_FEATURE	topological domain:Lumenal, melanosome	5.80E-05	DCT, TYRP1, TYR
GOTERM_CC_DIRECT	GO:0072562~blood microparticle	1.54E-04	TF, A2M, HSPA2, BCHE, APOE, SERPINA3
UP_KEYWORDS	Glycoprotein	1.85E-04	TF, TYRP1, A2M, TNFSF14, IL17RD, PCOLCE, DCT, IGSF11, TYR, ACSL1, TSPAN10, APOE, BCHE, SERPINA5, SERPINA3, FGL2, CEACAM1, PLTP, PI15, HAPLN1, MAG, HYAL1, RNASE1, PMEL, GYG2, P2RX7, LAMA5, FKBP14
GOTERM_CC_DIRECT	GO:0042470~melanosome	3.64E-04	DCT, TYRP1, TYR, PMEL, RAB17
GOTERM_CC_DIRECT	GO:0070062~extracellular exosome	5.62E-04	HYAL1, TF, A2M, FXYD3, RNASE1, MGP, PCOLCE, IGSF11, HSPA2, LAMA5, APOE, SERPINA5, RAB17, SERPINA3, AIF1L, QPRT, FGL2, CEACAM1, TUBB4A, GNG7, PI15
GOTERM_CC_DIRECT	GO:0033162~melanosome membrane	5.94E-04	DCT, TYRP1, TYR
GOTERM_CC_DIRECT	GO:0043025~neuronal cell body	6.35E-04	P2RX7, MYO10, APOE, RAB17, CYGB, PPARGC1A, TUBB4A

Table 3: IPA functional annotations of cell movement-related biological functions predicted to be decreased (negative z-score) in HC/KA SETDB1 OE HT144 melanoma cell lines, compared with control (SETDB1 OE HT144) cells.

Diseases or Functions Annotation	Predicted Activation State	p-Value	z-score	Molecules
Migration of cells	Decreased	1,8E-10	-2,204	A2M,ABCB4,ADA,ADAM19,AGT,AIM2,ALPP,ANXA2,AXL,BCAR3
Invasion of tumor cell lines	Decreased	2,12E-08	-2,107	A2M,AGT,AXL,BCAR3,CAV1,CCL2,CCND1,CD151,CD24,CSE1L
Cell movement of endothelial cells	Decreased	4,81E-08	-3,041	AGT,ANXA2,AXL,CAV1,CCL2,CD151,CXCL1,CXCL8,DKK1,EFNB2
Migration of tumor cells	Decreased	6,71E-08	-3,249	CAV1,CCL2,CD151,COL4A3BP,CSE1L,CSF2RA,CXCL1,CXCL8,FGFR4, GSN
Cell movement of tumor cell lines	Decreased	7,29E-08	-2,161	A2M,AGT,ANXA2,AXL,BCAR3,BRK1,CAV1,CCL2,CCND1,CD151
Migration of endothelial cells	Decreased	7,73E-08	-2,724	AGT,ANXA2,AXL,CAV1,CCL2,CD151,CXCL1,CXCL8,DKK1,EFNB2
Migration of tumor cell lines	Decreased	0,000000133	-2,036	A2M,AGT,ANXA2,AXL,BCAR3,BRK1,CAV1,CCL2,CCND1,CD151
Migration of cancer cells	Decreased	0,000000393	-2,944	CAV1,CCL2,CD151,COL4A3BP,CSE1L,CSF2RA,CXCL8,FGFR4,GSN, HRAS
Cell movement of prostate cancer cell lines	Decreased	0,00000271	-2,234	ANXA2,AXL,CAV1,CD151,CXCL8,GDF15,HMOX1,HRAS,ID1,IL6
Cell movement of tumor cells	Decreased	0,00000379	-2,621	CAV1,CCL2,COL4A3BP,CSF2RA,CXCL8,FGFR4,GSN,HRAS,IL6,LAMA5
Movement of vascular endothelial cells	Decreased	0,000035	-2,528	ANXA2,CD151,CXCL1,CXCL8,DKK1,EFNB2,F11R,ID1,IL24,LEP
Invasion of melanoma cell lines	Decreased	0,0000445	-2,156	CD151,CXCL8,LAMA5,MITF,MMP1,MX1,POU3F2,PTGS2,RND3
Cell movement of cancer cells	Decreased	0,0000555	-2,65	CAV1,CCL2,CSF2RA,CXCL8,GSN,HRAS,IL6,LAMA5,NRP1,THBS1
Chemotaxis	Decreased	0,000348	-2,531	A2M, AGT,ANXA2,AXL,CAV1,CCL2,CCND1,CD151,COL4A3BP, CSF2RA
Homing of cells	Decreased	0,000409	-2,667	A2M,AGT,ANXA2,AXL,CAV1,CCL2,CCND1,CD151,COL4A3BP, CSF2RA

8 Acknowledgements

At the end of every journey there comes the time to draw conclusions about what has been done and experienced. These four years spent in Germany to conduct my thesis work have been really intense and they strongly contributed to my professional and personal growth. I am extremely grateful for having had the opportunity to learn a lot and to get in touch with people from different educational background and cultures.

First, I would like to express my deepest gratitude to **Prof. Jochen Utikal** who gave me the unique chance to start and carry out a PhD project related to interesting research fields, such as melanoma biology and translational oncology. Moreover, I am really thankful for believing in my capabilities from the beginning and for continuously supporting me with insightful advices and fruitful discussions.

I would like to thank **Prof. Viktor Umansky** for contributing to the supervision of my project by making his knowledge and experience available and by giving meaningful suggestions and feedbacks.

I am very grateful to **Dr. Martin Sprick** for his support during my TAC meetings and to **Dr. Daniel Lipka** and **Oliver Mücke** for their precious help related to my ChIP-seq experiments. Special thanks to the HBIGS graduate school's members, **Dr. Rolf Lutz** and **Martina Galvan**, who kindly assisted me during my first period in Germany and during all the PhD period.

During this experience I have met brilliant scientists and, most importantly, amazing people, with which I had the great honour and pleasure to share the laboratory life.

Especially, I would like to thank **Elias** for getting me started in the laboratory and for mentoring me, even from miles away. Your support was indispensable and it will never be forgotten.

Thanks to **Daniel** for his great help in the laboratory and for contributing to establish a relaxed and cheerful environment in our group. I want to thank **Lio** for the many interesting scientific (and non-scientific) conversations we had in these years.

I would like to particularly thank my colleagues **Laura** and **Karol**; we started our PhD in the same period and this allowed us to attend together many scientific events and to share all the good and bad moments which characterize the PhD life. Thank you girls, soon all three of us will be on the other side!

Special thanks to **Jenny** for her kindness and for the essential work she makes in our lab.

I want to thank all the other past and current lab mates, especially **Sachindra, Huizi, Ke, Ze, Sunee, Marlene, Juliane, Tamara** and **James**; with all of you I have spent very nice and funny moments. I will always have good memories of each of you.

I also want to thank all my friends and my family, who are a big part of my life. Especially, I would like to thank my “German relative” **zia Milena** who, although we never met each other before, warmly welcomed me in Germany and gave me full support and assistance from the very first day in this country.

Special thanks to my parents and my sister for all the love, thoughtfulness and help they were able to send to me, despite the distance.

Last but not least, I want to thank **Antonella**, the one who more than any others was always there for me, for every challenge, delusions or successes I experienced; the one who decided to follow me in Germany and, lastly, the one who made me make the luckiest man in the world by becoming my wife.

My most sincere gratitude goes to each of you.